

Article

Optimized 4,5-Diarylimidazoles as Potent/Selective Inhibitors of Protein Kinase CK1 δ and Their Structural Relation to p38 α MAPK

Jakob Halekotte ^{1,†}, Lydia Witt ¹, Chiara Ianes ^{2,†}, Marc Krüger ², Mike Bührmann ³, Daniel Rauh ³, Christian Pichlo ⁴, Elena Brunstein ⁴, Andreas Luxenburger ⁵, Ulrich Baumann ⁴, Uwe Knippschild ², Joachim Bischof ^{2,*} and Christian Peifer ^{1,*}

¹ Institute of Pharmacy, Christian-Albrechts-University of Kiel, Gutenbergstraße 76, D-24118 Kiel, Germany; jhalekotte@pharmazie.uni-kiel.de (J.H.); lwitt@pharmazie.uni-kiel.de (L.W.)

² Department of General and Visceral Surgery, Ulm University Hospital, Albert-Einstein-Allee 23, D-89081 Ulm, Germany; chiara.ianes@uni-ulm.de (C.I.); marcm3012@googlemail.com (M.K.); uwe.knippschild@uniklinik-ulm.de (U.K.)

³ Institute of Chemical Biology, Dortmund University of Technology, Otto-Hahn-Straße 4a, D-44227 Dortmund, Germany; mike.buehrmann@googlemail.com (M.B.); daniel.rauh@tu-dortmund.de (D.R.)

⁴ Department for Chemistry, University of Cologne, Otto-Fischer-Straße 12-14, D-50674 Cologne, Germany; pichloc@uni-koeln.de (C.P.); Elena.Brunstein@uni-koeln.de (E.B.); ubaumann@uni-koeln.de (U.B.)

⁵ The Ferrier Research Institute, Victoria University of Wellington, Gracefield Research Centre, 69 Gracefield Road, Lower Hutt P.O. Box 33-436, New Zealand; Andreas.Luxenburger@vuw.ac.nz

* Correspondence: joachim.bischof@uniklinik-ulm.de (J.B.); cpeifer@pharmazie.uni-kiel.de (C.P.); Tel.: +49-731-500-53589 (J.B.); +49-431-880-1137 (C.P.)

† These authors contribute equally to this work.

‡ These two authors contribute equally to this work.

Academic Editors: Pierre Koch and Stefan Laufer

Received: 31 January 2017; Accepted: 20 March 2017; Published: 24 March 2017

Abstract: The involvement of protein kinase CK1 δ in the pathogenesis of severe disorders such as Alzheimer's disease, amyotrophic lateral sclerosis, familial advanced sleep phase syndrome, and cancer has dramatically increased interest in the development of effective small molecule inhibitors for both therapeutic application and basic research. Unfortunately, the design of CK1 isoform-specific compounds has proved to be highly complicated due to the existence of six evolutionarily conserved human CK1 members that possess similar, different, or even opposite physiological and pathophysiological implications. Consequently, only few potent and selective CK1 δ inhibitors have been reported so far and structurally divergent approaches are urgently needed in order to establish SAR that might enable complete discrimination of CK1 isoforms and related p38 α MAPK. In this study we report on design and characterization of optimized 4,5-diarylimidazoles as highly effective ATP-competitive inhibitors of CK1 δ with compounds **11b** (IC₅₀ CK1 δ = 4 nM, IC₅₀ CK1 ϵ = 25 nM), **12a** (IC₅₀ CK1 δ = 19 nM, IC₅₀ CK1 ϵ = 227 nM), and **16b** (IC₅₀ CK1 δ = 8 nM, IC₅₀ CK1 ϵ = 81 nM) being among the most potent CK1 δ -targeting agents published to date. Inhibitor compound **11b**, displaying potential as a pharmacological tool, has further been profiled over a panel of 321 protein kinases exhibiting high selectivity. Cellular efficacy has been evaluated in human pancreatic cancer cell lines Colo357 (EC₅₀ = 3.5 μ M) and Panc89 (EC₅₀ = 1.5 μ M). SAR is substantiated by X-ray crystallographic analysis of **16b** in CK1 δ and **11b** in p38 α .

Keywords: protein kinase CK1; formerly known as casein kinase 1; p38 MAPK; kinase inhibitors; 4,5-diaryl-imidazoles; Alzheimer's disease; amyotrophic lateral sclerosis; familial advanced sleep phase syndrome; cancer

1. Introduction

Protein kinase CK1 δ is a member of the ubiquitously expressed and constitutively active Ser/Thr-specific CK1 (formerly known as casein kinase 1) family which comprises the six human isoforms α , γ 1, γ 2, γ 3, δ , and ϵ , together with their closest relatives the tau tubulin kinases 1 and 2 (TTBK1/2) and vaccinia-related kinases 1-3 (VRK1-3) [1-3]. Despite CK1 being evolutionarily highly conserved within their catalytic domains, all isoforms differ significantly in the length and the primary structure of their regulatory N- and C-terminal regions. Among them, isoforms δ and ϵ display the highest consensus, with a 98% sequence identity within their catalytic domain and at least 40% homology within their autoregulatory C-terminal domains [2-5]. Pathophysiologically, identification of mutations within the coding region of CK1 δ as well as deregulation of CK1 δ expression and/or activity levels as important determinants in development and progression of severe human disorders such as Alzheimer's disease (AD) [2,6-8], amyotrophic lateral sclerosis (ALS) [9], familial advanced sleep phase syndrome (FASPS) [10], and cancer [2,5,11-19] has dramatically increased interest in the development of potent and selective small molecule kinase inhibitors for both therapeutic approaches and basic research. However, the existence of paralogous CK1 isoforms that possess similar, different, or even opposite physiological and pathophysiological implications render the design of suitable candidate molecules that target CK1 δ in an ideally isoform-dependent manner enormously difficult. The most extensively used and characterized CK1 inhibitor to date, IC261, moderately inhibits CK1 isoforms δ and ϵ (IC_{50} CK1 δ/ϵ = 1 μ M, IC_{50} CK1 α = 10 μ M) and proved valuable in diverse pharmacological studies [16,20-22]. Furthermore, IC261 even revealed therapeutic potential for the treatment of pancreatic cancer in a subcutaneous mouse xeno-transplantation model, despite the fact that the inhibitor is active against several other targets, including tubulin polymerization and ion channels [16,22-24]. In addition, few further compounds have been reported as CK1 inhibitors, mainly those which are commonly referred to as "linear" [25,26] and "tear-drop"-like binders [27] with respect to their three-dimensional structure. Among the latter, a promising 4,5-diarylimidazole-based inhibitor **1**, originally designed as an inhibitor of p38 α MAPK, was revealed in 2009 by Peifer et al. to inhibit CK1 δ/ϵ with IC_{50} values in the low nanomolar range (**1** IC_{50} CK1 δ = 5 nM, **1** IC_{50} CK1 ϵ = 73 nM) [28]. Interestingly, sulfoxidation of thioether **1** leading to sulfoxide **2** significantly enhanced discrimination of highly related isoforms δ and ϵ to at least 40-fold while preserving good potency for CK1 δ (**2** IC_{50} CK1 δ = 11 nM, **2** IC_{50} CK1 ϵ = 447 nM, Figure 1) [28]. Unfortunately, the reduced chemical stability of **1** and **2** in solution due to *E/Z*-isomerization and the presence of a *Michael* acceptor moiety in the cinnamic acid side chain are responsible for their limited usability in vitro and in vivo.

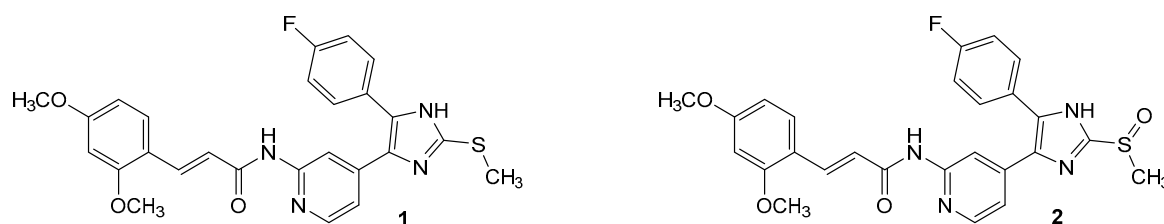
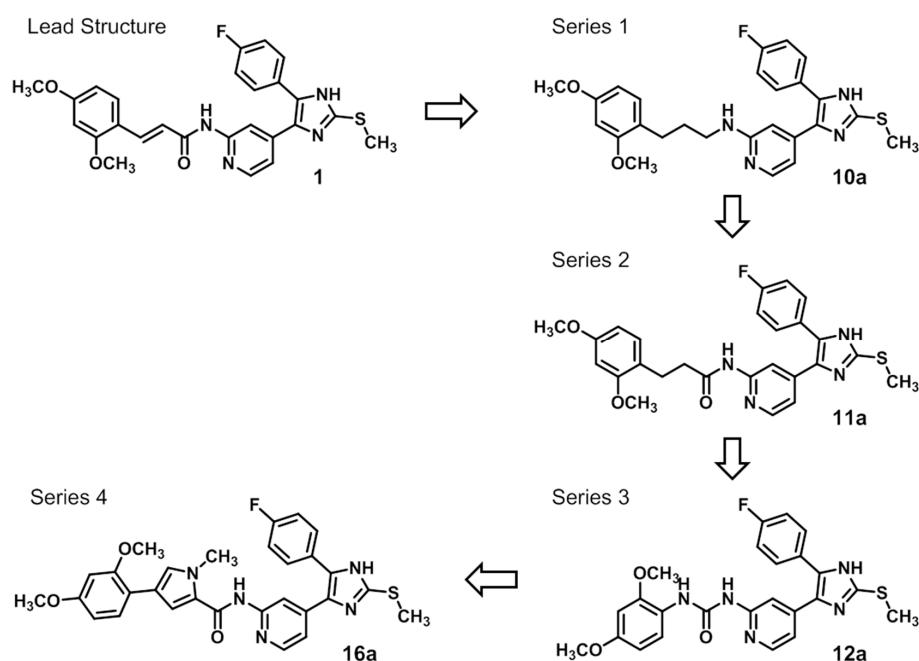


Figure 1. ATP-competitive dual specific inhibitors **1** and **2** of CK1 δ/ϵ and p38 α MAPK.

The present follow-up [28] study reports on the optimization of lead structures **1** and **2**, respectively, leading to stable novel inhibitors of CK1 δ/ϵ with IC_{50} values in the low nanomolar range. The optimization strategy followed a well-established procedure in medicinal chemistry including in silico design, hit synthesis, and in vitro biological evaluation [29,30].

Furthermore, core catalytic residues Lys38 and Asp149 [13,31] coordinate a structural water within the catalytic cleft which donates another hydrogen bond towards an imidazole nitrogen of the respective inhibitor. Gatekeeper residue Met82 is rotated by 180° towards Pro66 [13,31], thereby permitting access to the hydrophobic pocket I (*selectivity pocket, HPI*) [2,34] which is ideally occupied by the 4-fluorophenyl moiety [31,35]. Molecular modeling further suggests five-membered heterocycles to dictate an ideal angle for positioning of the vicinal aryl moieties within the ATP-binding pocket of CK1δ [36]. The (*E*)-configured cinnamic acid side chain of **1** and **2** extends into the spacious solvent-exposed hydrophobic region II (*affinity pocket, HRII*) [2,34]. Modeling calculations further considered different di- or trimethoxyphenyl substitution pattern optimal within this region as they enable flexible occupation of hydrophobic surfaces and shielding deeper cavities of the ATP-binding pocket from surrounding water, thus entailing increased enthalpic contribution of buried hydrogen bonds. Analogous binding poses have been achieved regarding p38α with the bidentate hinge-binding moiety addressing Met109 and the imidazole-*N* accepting a hydrogen bond from Lys53. Rotation of the smaller gatekeeper residue Thr106, however, does not seem necessary in order to occupy *HPI*.

The binding modes described above are based on (*E*)-configured cinnamic moieties of **1** and **2**, respectively. In contrast, molecular modeling of the respective (*Z*)-configurations did not result in plausible binding modes (not shown). Accordingly, computational analysis assume these (*Z*)-stereoisomers to be less bioactive. Furthermore, the acrylamide *Michael* acceptor moiety of the cinnamic acid side chain was considered responsible for the observed chemical instability of **1** and **2** in solution. In line with this notion, within a short period of time after preparing a solution of **1** and **2** in DMSO a HPLC analysis showed an increasing number of not identifiable degradation products. Consequently, our primary goal towards an optimized inhibitor was to gain chemical stability. Thus, having identified the cinnamic side chain to be responsible for the chemical instability issue we aimed towards stable side chains attached at the validated 2-aminopyridine core moiety. By these modifications we set out to explore the respective hydrophobic region II formerly occupied by the cinnamic acid moiety. At the same time, both potency and selectivity for CK1δ were taken into account. Therefore, in our systematic approach four structurally divergent series of inhibitors with variable side chains (Scheme 1) have been designed based on the following considerations.



Scheme 1. Structural considerations based on molecular modeling leading to lead structure **1** derivatives **10a** (series 1), **11a** (series 2), **12a** (series 3), and **16a** (series 4).

First, removal of both the planar (sp^2) π -bond and carbonyl group in **1** and **2** led to respective sp^3 hybridized 3-(2,4-dimethoxyphenyl)propanamine **10a** and derivatives (series 1). However, at this position of the ligand, additional degrees of freedom and enhanced conformational flexibility are typically accompanied by losses of both potency and selectivity; Second, maintaining the amide function but formally reducing the π -bond resulted in presumably stable and potent 3-(2,4-dimethoxyphenyl)propionic amide derivatives (e.g., **11a**, series 2). Third, a carbamide moiety in **12a** and derivatives (series 3) might enable an additional hydrogen bond towards hinge Leu85 and therefore could account for enthalpic binding energy gains. The additional fixation was further suggested to exploit different folding of related CK1 δ , CK1 ϵ , and p38 α within range of the hinge region and thus to be a key parameter for triggering inhibitor selectivity. And fourth, fixing the (*E*)-configuration of cinnamic amides **1** and **2** within five-membered heterocycles led to 4-(2,4-dimethoxyphenyl)-1-methyl-1*H*-pyrrole-2-carboxylic amide (**16a**, series 4). Taken together, by our compound design concept in the side chain *Michael* acceptor characteristics and inactive (*Z*)-isomers were eliminated while potentially conserving beneficial impacts regarding potency and selectivity.

Based on the inhibitor categories described above we generated a virtual set of compounds being subsequently processed in a LigPrep/Glide docking campaign using CK1 δ (pdb 3UZP [31]) and p38 α (pdb 1BMK [33]) protein structures. Thereby we focused on variation of side chains addressing the *HR11* while maintaining the fixed 4,5-diaryl-imidazole pharmacophore. This included different sets of substituted lipophilic and mainly sterically demanding moieties in order to exploit this region. As methoxy-substituents were assumed most favorable in this context, efforts have been devoted to methoxy-screenings investigating different substitution patterns.

2.2. Synthesis

In order to effectively synthesize the designed and top ranked hits from docking, a straightforward five-step procedure towards the building blocks 2-fluoro-4-(5-(4-fluorophenyl)-2-(methylthio)-1*H*-imidazol-4-yl)pyridine (**6**) and 4-(5-(4-fluorophenyl)-2-(methylthio)-1*H*-imidazol-4-yl)pyridine-2-amine (**7**) was established in accordance to literature protocols [37,38]. In the final step, by substitution of key compounds **6** and **7**, variations of side chains were introduced and thus four compound series were prepared (Scheme 2).

Slightly deviating from the procedure depicted in Scheme 2, pyridine-2-amine **10a** has been synthesized by a S_N2 reaction of single Boc-protected 2-amino-4-methylpyridine and 1-(3-bromopropyl)-2,4-dimethoxybenzene (**9**) followed by subsequent formation of the 4,5-diaryl-imidazole scaffold using the procedure developed for synthesis of **6**. Alkyl halide **9** was synthesized from 3-(2,4-dimethoxyphenyl)propionic acid by reduction [39] followed by an Appel reaction using triphenylphosphine and *N*-bromosuccinimide (Scheme 3) [40]. Detailed information about the synthesis of **10a** is presented in the Supporting Information.

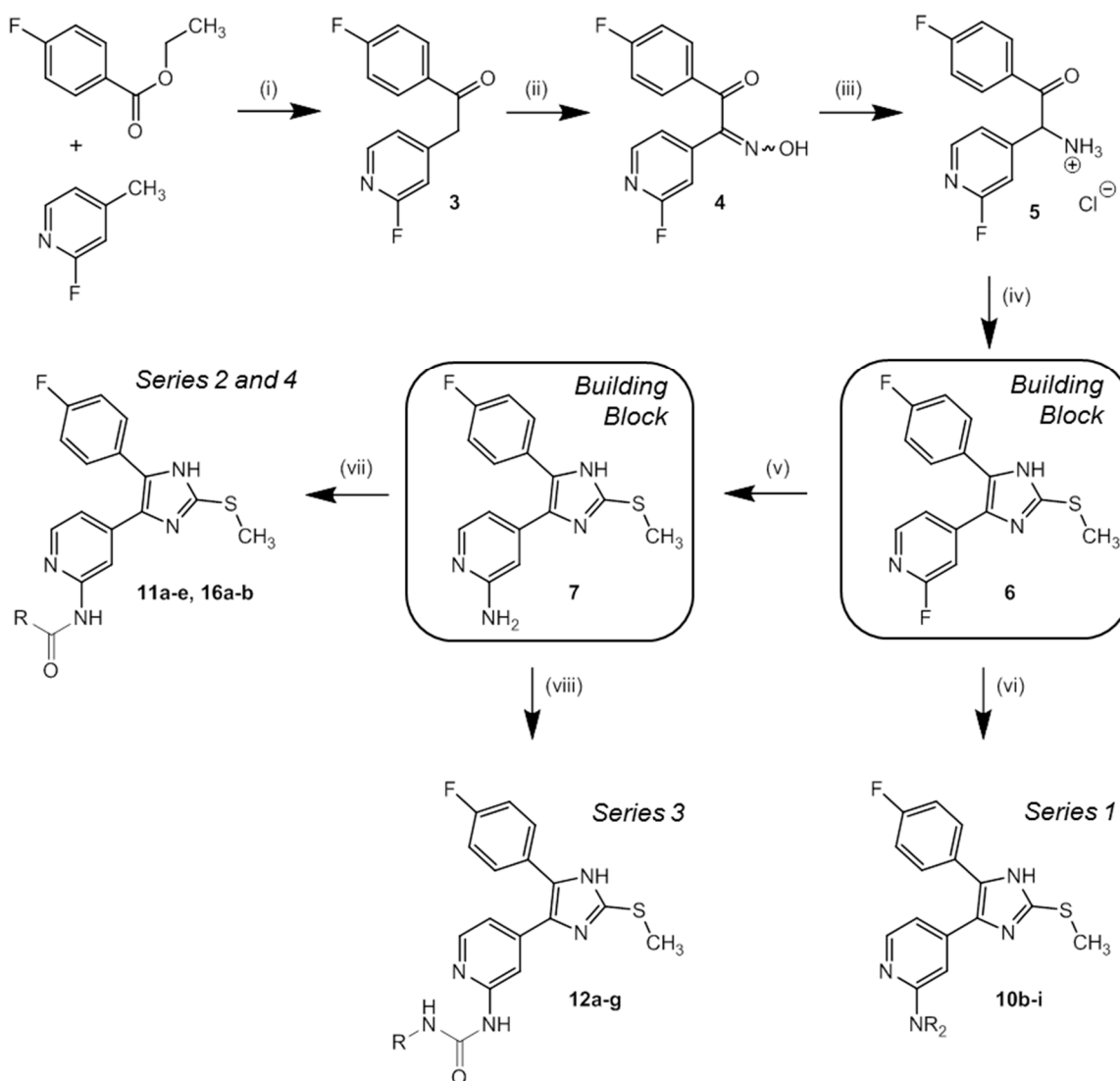
Series 1 pyridine-2-amines **10b–f** and piperazines **10g–i** were prepared by a Tschitschibabin-like nucleophilic substitution [32,38]. Therefore, 2-fluoropyridine **6** was dissolved or suspended in an excess of the appropriate amine or piperazine and heated to 160 °C (Scheme 2). In general, in this reaction primary amines accounted for better yields.

Syntheses of series 2 included the reaction of building block **7** with CDI-activated differently di- or trimethoxy-substituted 3-phenylpropionic acids to afford amides **11a–e**. The poor nucleophilic character of **7**, however, required heating to 110 °C in order to achieve suitable reactivity (Scheme 2) [28].

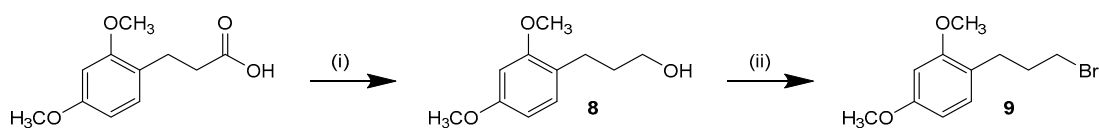
In contrast, highly reactive isocyanates readily acylated **7** at room temperature in terms of a Wöhler-like synthesis leading to series 3 carbamide derivatives **12a–g** (Scheme 2) [41]. Noteworthy, addition of Hünig's base led to increased yields and reactions had to be performed under protective gas atmosphere in order to prevent formation of carbamide dimers.

Series 4 precursor 4-(2,4-dimethoxy-phenyl)pyrrole-2-carboxylic acid was prepared in a three step synthesis starting from ethyl 4-bromo-1*H*-pyrrole-2-carboxylate [42]. Methylation of the pyrrole

nitrogen using methyl iodide was followed by Suzuki cross-coupling with (2,4-dimethoxyphenyl) boronic acid and subsequent simple ester hydrolysis in diluted alkali. The 2,5-dimethoxyphenyl side chain derivative **15b** has been synthesized analogously. Finally, **16a–b** were obtained by PyBOP-supported amide coupling with building block **7** under elevated temperature (Scheme 4).

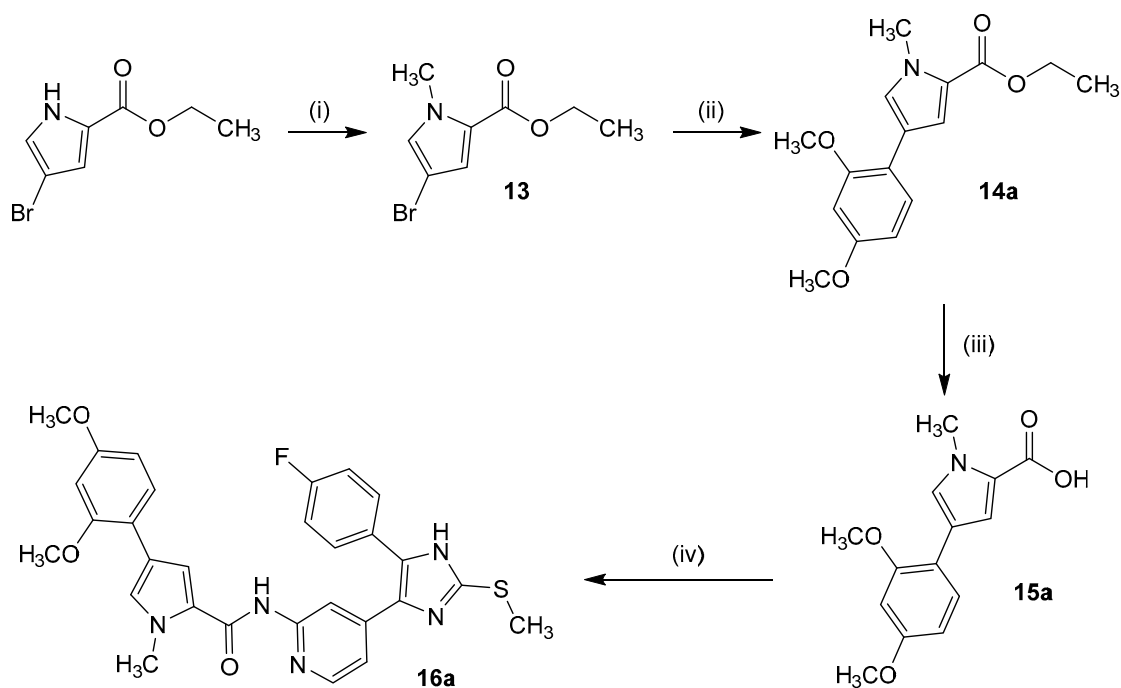


Scheme 2. Synthesis of key building blocks **6** and **7** as well as inhibitors **10b–i** (series 1), **11a–e** (series 2), **12a–g** (series 3), and **16a–b** (series 4). *Reagents and Conditions:* (i) NaHMDS, THF, 2 h 0 °C, 1 h r.t.; (ii) CH_3CHOOH , NaNO_2 , 1 h 0 °C, 3.5 h r.t.; (iii) H_2 , Pd/C, HCl-saturated 2-propanol, 12 h r.t.; (iv) methyl thiocyanate, DMF, 45 min reflux, 45 min r.t.; (v) NH_3 , 20–30 bar, 18 h 180 °C; (vi) HNR_2 , 12 h 160 °C; (vii) carboxylic acid, CDI or PyBOP/DIPEA, DMF, 12 h 110 °C; (viii) isocyanate, DIPEA, DMF, 12 h r.t.

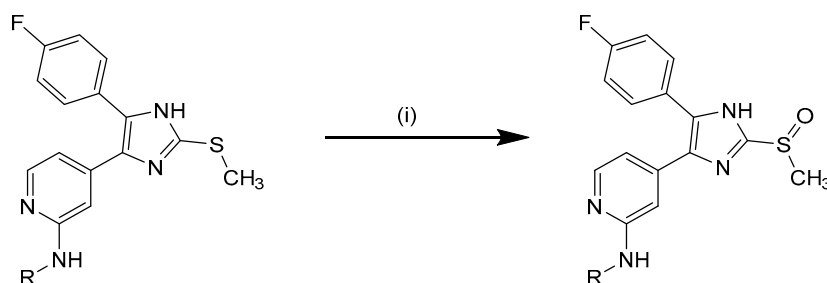


Scheme 3. Synthesis of 1-(3-bromopropyl)-2,4-dimethoxybenzene (**9**). *Reagents and Conditions:* (i) LiAlH_4 , THF, 1 h r.t.; (ii) NBS, PPh_3 , DCM, 2 h r.t.

As mentioned above, the respective sulfoxides might possess interesting potential regarding selectivity. Therefore, oxidation of selected compounds was performed in accordance to literature using Oxone[®] at 0 °C or at ambient temperature (Scheme 5). During thioether oxidation it was essential to strictly monitor reaction progress for quenching at the sulfoxide level [28]. Accordingly, sulfoxidation was performed for compounds **10c–d**, **11a–b**, **12a**, **12c–g**, and **16a** leading to **10j–k** (series 1), **11f–g** (series 2), **12h–m** (series 3), and **16c** (series 4). It has to be noted that sulfoxides are chiral compounds and we are always referring to the racemate. However, docking analysis did not reveal differences between the enantiomers. In the literature the racemate is reported for this inhibitor class with only one exception, where the *R*-configuration was observed to possess increased affinity for p38 α MAPK [43].



Scheme 4. Synthesis of 4-(2,4-dimethoxyphenyl)-1-methyl-1H-pyrrole-2-carboxylic acid (**15a**). *Reagents and Conditions:* (i) NaH, DMF, 20 min 0 °C, CH₃I, 15 min 0 °C, 2.5 h r.t.; (ii) 2,4-dimethoxyphenyl boronic acid, Pd(PPh₃)₄, aq. NaHCO₃, DMF, 4 h reflux, 12 h r.t.; (iii) aq. NaOH, THF/methanol, 5 h 50 °C, 12 h r.t., (iv) DIPEA, DMF, 30 min r.t., 7, 12 h 110 °C.



Scheme 5. Synthesis of sulfoxides. *Reagents and Conditions:* (i) Oxone[®] (potassium peroxomonosulfate), THF/H₂O, 30 min–2 h 0 °C.

All synthesized target compounds **10a–k**, **11a–g**, **12a–m**, **16a–c** are listed in Table 1. They were stable in DMSO solution at room temperature without detectable degradation over a period of 72 h by HPLC analysis.

Table 1. Synthesized test compounds of series 1, 2, 3, and 4. R refers to the side chains indicated in Scheme 5. Only a limited selection of thioether compounds has been oxidized leading to sulfoxide compounds (12h–12m, 16c). Abbreviation: # compound number.

Thioether #	Sulfoxide #	R	Thioether #	Sulfoxide #	R
10a			11c		
10b			11d		
10c	10j		12a	12h	
10d	10k		12b		
10e			12c	12i	
10f			12d	12j	
10g			12e	12k	
10h			12f	12l	
10i			12g	12m	
11a	11f		16a	16c	
11b	11g		16b		

2.3. Kinase Assays and IC₅₀ Determination

Compounds **10a–k** (series 1), **11a–g** (series 2), **12a–m** (series 3), and **16a–c** (series 4) have initially been screened for their ability to inhibit the activity of CK1 δ and CK1 ϵ in an in vitro kinase assay at a concentration of 10 μ M. Inhibitors exhibiting promising effects were further subjected to IC₅₀ value determination (Table 2). In addition, IC₅₀ values regarding inhibition of CK1 δ and p38 α MAPK have commercially been obtained from ProQinase GmbH (Freiburg, Germany) for **11b**, **12a**, and **16b** as these were the most potent representatives of their respective series (Table 3). In comparison to our data, IC₅₀ values measured by ProQinase appear slightly lower due to the different assay setup

such as the ATP concentration used (compare Experimental Section/Supporting Information and www.proqinase.com).

Table 2. IC₅₀ values of promising inhibitors for CK1δ and CK1ε. All compounds have initially been screened in an in vitro assay against CK1δ and CK1ε at a concentration of 10 μM. The most promising agents were subjected to IC₅₀ value determination. Results are presented as mean ± SD from experiments performed in triplicate (*n* = 3). Abbreviation: # compound number.

Compound #	CK1δ IC ₅₀ (nM)	CK1ε IC ₅₀ (nM)
10a	386 ± 86	6731 ± 2680
10d	644 ± 274	3323 ± 1297
10e	344 ± 104	1753 ± 738
11a	20 ± 2	129 ± 22
11b	4 ± 1	25 ± 4
11c	14 ± 2	91 ± 12
11d	20 ± 4	233 ± 38
11e	27 ± 3	204 ± 32
11f	93 ± 12	499 ± 70
11g	87 ± 2	573 ± 104
12a	19 ± 3	227 ± 37
12b	31 ± 3	186 ± 28
12d	47 ± 6	272 ± 52
12e	35 ± 10	203 ± 67
12f	196 ± 22	498 ± 124
12h	153 ± 24	910 ± 18
12j	160 ± 26	804 ± 160
12k	115 ± 18	764 ± 207
12l	88 ± 14	623 ± 139
12m	48 ± 8	182 ± 39
16a	9 ± 1	45 ± 7
16b	8 ± 1	81 ± 15
16c	32 ± 4	181 ± 32

Table 3. IC₅₀ values of key inhibitors for CK1δ and p38α MAPK. IC₅₀ values of the most promising agents of series 2 (**11b**), series 3 (**12a**), and series 4 (**16b**) have commercially been obtained from ProQinase GmbH (Freiburg, Germany). Single experiments have been performed (*n* = 1). Abbreviation: # compound number.

Compound #	CK1δ IC ₅₀ (nM)	p38α IC ₅₀ (nM)
11b	<3	10
12a	10	28
16b	<3	10

Fortunately, potent CK1δ inhibition and appropriate SAR correlated with the calculated binding modes for the majority of compounds. Especially **11b**, **16a**, and **16b** exhibited excellent efficacy with IC₅₀ values in the single-digit nanomolar range in standardized kinase assays and are therefore among the most potent CK1δ inhibitors reported to date. In general, loss of potency for series 1 inhibitors when compared to lead structure **1** has been observed in vitro: while **1** has an IC₅₀ for CK1δ of 5 nM [28] a side chain without both carbonyl group and π-bond resulted in considerably decreased inhibition (e.g., series 1, **10a** IC₅₀ CK1δ = 386 nM). In contrast, compounds possessing the carbonyl group but without π-bond afforded chemically stable series 2 (e.g., **11a** IC₅₀ CK1δ = 20 nM, IC₅₀ CK1ε = 129 nM) and thereby restored potency almost to the level reported for lead **1** (IC₅₀ CK1δ = 5 nM, IC₅₀ CK1ε = 73 nM). Isoform selectivity regarding CK1ε, however, seemed to be slightly decreased. Consequently, the π-bond of lead **1** can be identified to be responsible for compound instability, while the carbonyl depicts an important determinant concerning potency. In addition, series 3 and 4 both provided potent inhibitors of CK1δ with IC₅₀ values in the low nanomolar range. However, the aimed impact on CK1δ/ε isoform selectivity by rigidification of the double bond in

the (*E*)-configuration has not been fully achieved. Unfortunately, tridentate hinge binding carbamide derivatives **12a–m** (series 3) were actually limited by their poor solubility in vitro.

Oxidation of the exocyclic sulfur at the imidazole-2-position of thioether **1** to afford sulfoxide **2** reflects in vivo metabolization by phase I enzymes [44]. Interestingly, this sulfoxidation increased CK1 δ / ϵ isoform selectivity in one reported previously study [28]. In our hands, however, this effect could not be confirmed for the newly designed and synthesized set of inhibitors as oxidation only slightly altered potency, though without significantly affecting isoform selectivity. Nevertheless, sulfoxidized compounds remained potent inhibitors of CK1 δ with IC₅₀ values in the low nanomolar range. This indicates that these agents will retain activity despite metabolization.

2.4. X-ray Analysis of Binding Modes in CK1 δ and p38 α

In order to verify modeled binding modes and to obtain further insights regarding ligand-protein interactions determining selectivity we set out to co-crystallize potent inhibitors of series 2, 3, and 4 (**11b**, **12a**, and **16b**) in CK1 δ . In line with this notion, a ligand-protein structure of **16b** could be co-crystallized with a C-terminally truncated CK1 δ construct and the complex structure was determined at 2.0 Å resolution. Unfortunately, co-crystallization of **11b** and **12a** failed experimentally.

Additionally, overall most active agent **11b** has been co-crystallized with p38 α MAPK at 1.9 Å resolution. In fact, crystallographic data largely confirmed the calculated binding pose of **16b** within the active site of CK1 δ (Figure 3). As determined by X-ray analysis the 4-fluorophenyl moiety deeply penetrates into *HPI*, enabled by rotation of gatekeeper Met82 towards Pro66. The bidentate hinge-binding 2-aminopyridine motif forms two hydrogen bonds towards Leu85. Furthermore, Lys38 and Asp149 coordinate a water molecule which donates another hydrogen bond accepted by an imidazole nitrogen of **16b**. *HRII*, however, is addressed by bulky 4-(2,5-dimethoxyphenyl)-1-methyl-1*H*-pyrrole-2-carboxamide, probably displacing energetically unfavorable water molecules and shielding deeper hydrophobic cavities of the binding pocket. Although the 2,5-dimethoxyphenyl moiety herein mainly interacts with Pro87 by π -aliphatic-stacking, electron density has also been observed within range of Phe95 which can be interpreted by different conformers of **16b**, thus indicating additional interaction. The complex of **11b** in p38 α MAPK predominantly confirmed the expected 4,5-diaryl-imidazole core fitting, similar to CK1 δ , with gatekeeper Thr106-lined *HPI* occupied by the 4-fluorophenyl moiety and the 2-aminopyridine acting as bidentate hinge binder addressing Met109. The ATP-binding pocket in this structure does not contain structural water molecules and Lys53 directly interacts with **11b** imidazole nitrogen by formation of a hydrogen bond. Interestingly, DFG-motif Phe169 is coordinated between **11b** imidazole-*N* and Lys53 by π - π - and, most likely, π -cation-stacking, respectively, thereby interrupting the hydrophobic spine consisting of Leu75, Leu86, Phe169, and His148 [45–47]. This pose is stabilizing the kinase in an intermediate conformation between DFG-in and DFG-out (*DFG-in-between*) [48], thereby showing several characteristics similar to type-I $\frac{1}{2}$ -like inhibition of p38 α MAPK [49,50], although molecular alignment studies may suggest the DFG-in state most likely to be inhibited by **11b** as well. However, the DFG-out conformation can be assumed to be sterically prohibited (Figure 4, left). Interestingly, the 3-(2,5-dimethoxyphenyl)propionic amide side chain of **11b** addressing *HRII* has not been definitely resolvable by X-ray analysis in terms of electron density (Figure 4, right). In fact, this is in agreement with our hypothesis postulating high flexibility of this ligand part within *HRII*. In line with this notion, we originally designed bulky inhibitor side chains to suboptimal fit into less extensive hydrophobic region II of p38 α MAPK, in turn allowing higher affinity for CK1 δ . Thus, in that way paying enthalpic and entropic penalty should result in decreased affinity for p38 α MAPK when compared to the situation in CK1 δ [51]. However, in contrast to our hypothesis inhibitors actually showing the bulky side chain, e.g., **11b**, **12a**, and **16b**, were determined to be nanomolar inhibitors of p38 α MAPK as well as of CK1 δ . This finding suggests that—despite bulky side chains—the core 4,5-diaryl-imidazole scaffold addressing both ATP sites of CK1 δ and p38 α is able to determine high affinity for these kinases.

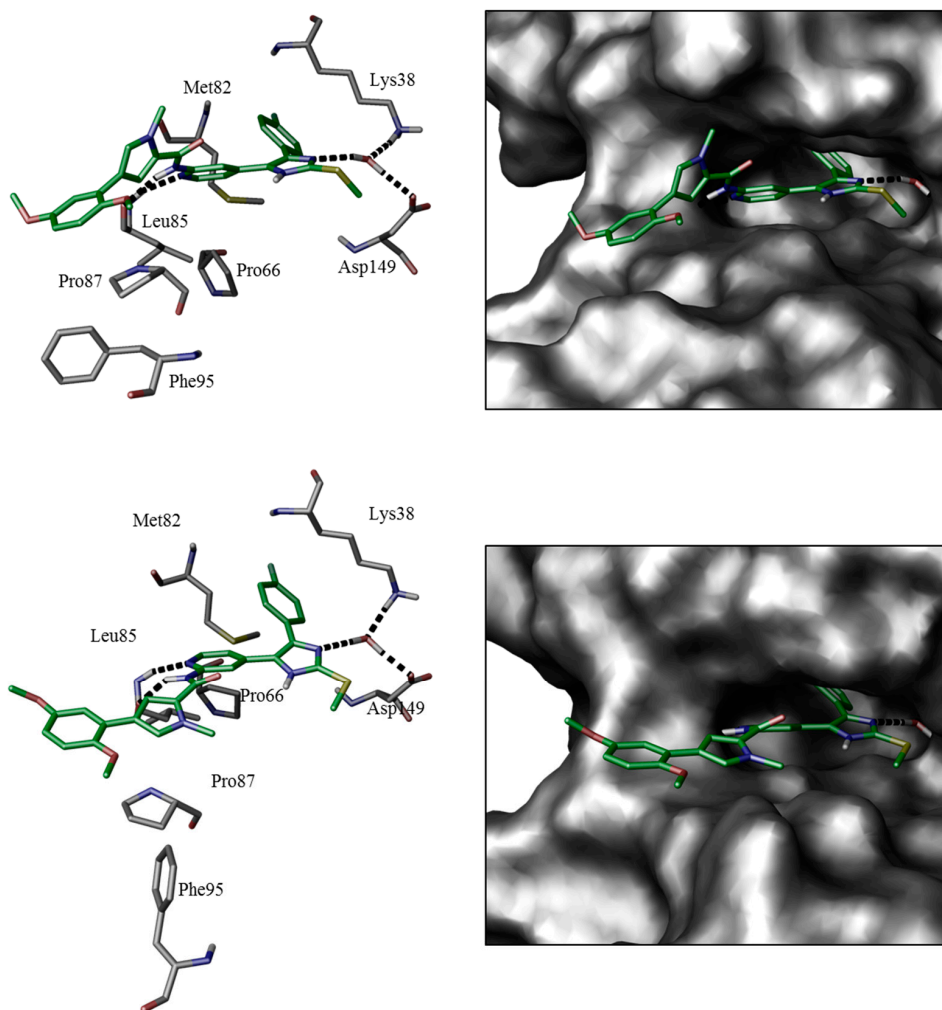


Figure 3. Similar binding modes of 16b in CK1 δ have been gained by co-crystallization (**top**, pdb 5MQV) and molecular modeling (**bottom**, pdb 3UZP [31]). The poses are presented by key residues and hydrogen bond interactions (**left**) and Connolly molecular surface (**right**).

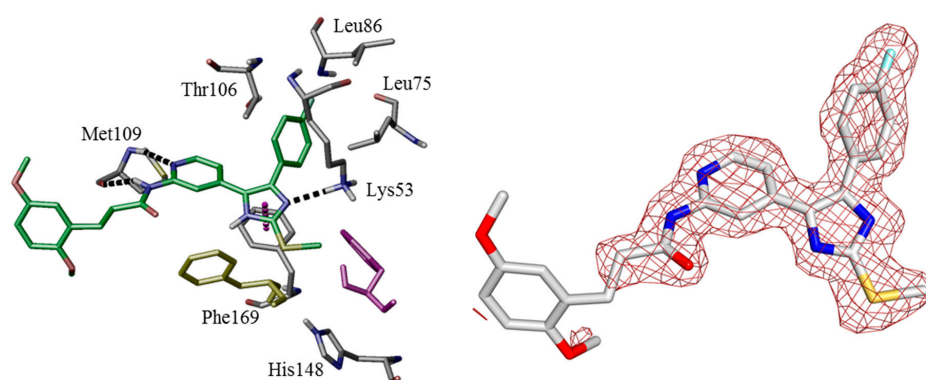


Figure 4. Co-crystallization of 11b in p38 α MAPK (pdb 5ML5). The binding mode is presented by key residues and hydrogen bond interactions as well as π - π -stacking (**left**). DFG Phe169 is stabilized in an intermediate state between active DFG-in (purple, pdb 1BMK [33]) and inactive DFG-out (yellow, pdb 1WBT [52]) conformation. DFG-in/out states were represented by structure alignment using Schrödinger software. The inhibitor side chain addressing *HRII* has not been definitely resolvable in terms of electron density (**right**, generated with PyMOL).

2.5. Selectivity Profiling of **11b**

In order to further characterize potent inhibitor **11b** selectivity profiling has been performed at a concentration of 100 nM in a panel of 321 protein kinases (ProQinase GmbH). These data revealed high selectivity of **11b** for CK1 δ hitting only six additional kinases with residual activities less than 50% apart from CK1 δ (residual activity = 3%) and CK1 ϵ (residual activity = 7%, CK1 isoforms γ 1–3 remained unaffected). Among these, CK1 α (residual activity = 26%) and p38 α MAPK (residual activity = 22%) were found as prominent targets. Also the highly related kinases JNK2 (residual activity = 21%), JNK3 (residual activity = 37%), and RIPK2 (residual activity = 45%) were identified as additional hits. Furthermore, Tyr-specific kinase LCK (residual activity = 26%) was inhibited (Figure 5 and Supporting Information). Consequently, **11b** represents an agent highly selective for CK1 δ within the range of its IC₅₀ value of 4 nM with an overall selectivity score S(50) of 0.027. The S-Score(50) has been calculated in accordance to Karaman et al. [53] describing the portion of kinases with a residual activity >50% in relation to all tested kinases included in this project.

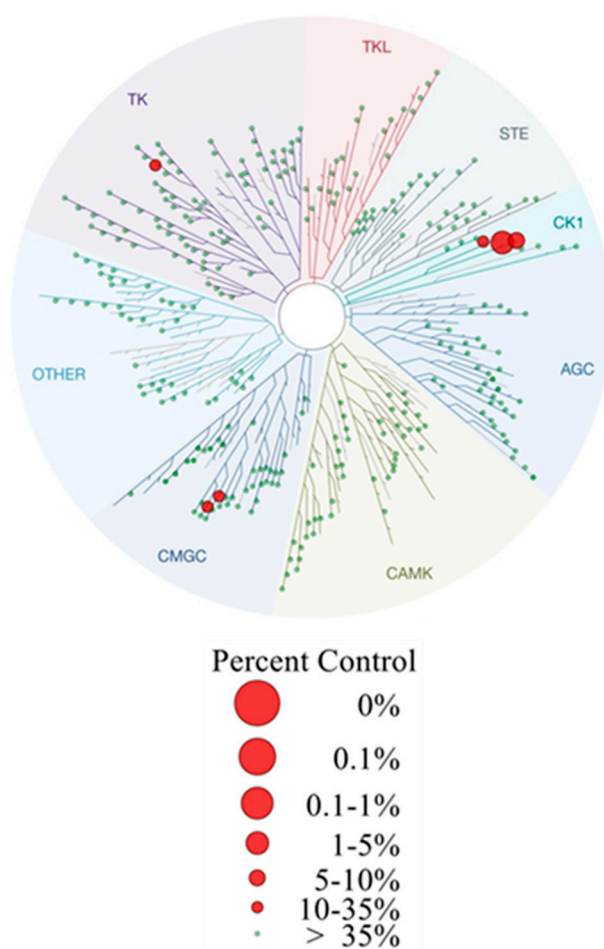


Figure 5. Dendrogram representation of selectivity profiling of **11b** screened over 321 protein kinases at a concentration of 100 nM (ProQinase GmbH, Freiburg, Germany). Residual activity was determined compared to DMSO control. The S-Score(50) of **11b** is 0.027. The dendrogram was generated utilizing TREEspot Software Tool, DISCOVERX CORPORATION 2010. Corresponding raw data are given in Supplementary Table S5.

2.6. Cellular Assays and EC₅₀ Determination

Synthesized compounds have further been evaluated regarding their efficacy in cellular systems in MTT viability assays using colorectal HT-29 or pancreatic Colo357, Panc89, Panc-1, and MiaPaCa-2

carcinoma cell lines. The cell lines were chosen as they are reportedly overexpressing CK1 δ and CK1 ϵ and exhibit resistance against a variety of chemotherapeutic agents [12,15,16]. In general, amines **10a–k** (series 1) were rather ineffective, even at an elevated concentration of 20 μ M with **10e** being most active exhibiting an EC₅₀ value of 9.3 μ M in HT-29 cells (data can be found in Supporting Information). For the subsequently designed compound series EC₅₀ data were only obtained for compounds which showed the most promising inhibition of CK1 δ in vitro. Inhibitors from series 2 (**11a–e**) showed significant increases of potency, presumably referable to the amide carbonyl group which has already been reported to beneficially affect metabolic stability [44]. As expected, **16a–b** (series 4) were only slightly less active. In contrast, carbamides **12a–k** (series 3) were only moderately active, presumably suffering from poor solubility. Among all series, **11b** again proved the most effective agent with EC₅₀ values of 3.5 μ M and 1.5 μ M in Colo357 and Panc89 cells, respectively (determined EC₅₀ values can be found in Table 4).

Table 4. EC₅₀ values of selected inhibitor compounds as determined for Colo357, Panc89, Panc-1, and MiaPaCa-2 cell lines. Results are presented as mean \pm SD from experiments performed in triplicate ($n = 3$). Abbreviations: # compound number; n.d., not determined.

Compound #	EC ₅₀ Values (μ M)			
	Colo357	Panc89	MiaPaCa-2	Panc-1
11a	4.1 \pm 1.7	2.5 \pm 1	4.9 \pm 0.8	7.0 \pm 0.7
11b	3.5 \pm 0.3	1.5 \pm 0.4	n.d.	n.d.
11c	1.9 \pm 0.6	6.1 \pm 3.0	n.d.	n.d.
11d	5.9 \pm 2.4	7.8 \pm 0.4	n.d.	n.d.
11e	4.5 \pm 1.3	8.3 \pm 2.2	n.d.	n.d.
12a	17.4 \pm 0.04	19.6 \pm 3.8	15.22 \pm 0.04	16.1 \pm 5.6
12b	15.5 \pm 1.6	n.d.	11.6 \pm 1.1	15.2 \pm 2.6
12e	14.9 \pm 2.6	7.5 \pm 3.0	n.d.	n.d.
16a	n.d.	n.d.	2.4 \pm 0.7	5.1 \pm 1.6
16b	5.7 \pm 2.2	7.3 \pm 1.9	2.3 \pm 0.2	5.4 \pm 1.5
16c	16.7 \pm 5.6	n.d.	7.7 \pm 2.5	10.2 \pm 3.2

If the EC₅₀ values determined in cell-based assays are compared with in vitro determined IC₅₀ data, massive differences can be observed and compounds which appeared to be extremely potent are apparently less efficient in the treatment of living cells. This difference is compound and cell line dependent, can be due to different reasons, and has already been documented in previous reports [26,54]. Firstly, limited cell permeability of small molecule inhibitors may limit their cellular uptake resulting in lower potency; Secondly, once compounds successfully crossed the cell membrane, ATP-competitive inhibitors must compete with high intracellular ATP levels leading to a discrepancy between IC₅₀ values determined by enzymatic versus cellular assays. Additionally, time of binding in the ATP pocket and drug export systems can reduce the inhibitory effect. Therefore, cell-based assays are essential in order to validate the inhibitory effects of newly identified small molecule inhibitors.

3. Materials and Methods

3.1. Molecular Modeling

Molecular modeling was performed on a DELL Precision T5500 eight core workstation. For visualization Maestro, version 10.6, 2016 (Schrödinger LLC, New York, NY, USA) was used. Protein crystal structures were prepared prior to docking by the Protein Preparation Wizard [55] synchronizing the following modules: Epik, version 3.6, 2016 [56]; Impact, version 7.1, 2016; Prime, version 4.4, 2016 [57]. In order to achieve high Enrichment-factors, the common refinement protocol by Sastry et al. [55] has been adjusted: the process involved assignment of bond orders, addition of hydrogen atoms, identification of disulfide bonds, and the conversion of artificial selenomethionines to

methionines (default settings). Missing side chains were filled in using Prime. Missing loops have not been detected. Water molecules beyond 5 Å from hetero atoms have been deleted automatically. H-bond optimization was performed in a standard sampling, the Root-mean-square deviation for atomic positions cutoff for heavy atoms in subsequent protein minimization was set to 0.3 Å

Ligands were prepared to generate energetically minimized three-dimensional coordinates with an extended cutoff by MacroModel, version 11.2, 2016 (Schrödinger LLC). Ionization and tautomeric states were estimated at pH 7 ± 2 by LigPrep, version 3.8, 2016 (Schrödinger LLC) [55], utilizing Hammett and Taft methodology-based Epik [56]. Additionally, Epik state penalties ($\text{kcal}\cdot\text{mol}^{-1}$) were calculated for each ligand to quantify the energetic cost for state transition in solution [55]. In order to indicate ligand flexibility, up to 50 bioactive conformers per ligand were identified and prioritized utilizing the conformational search module in the fast mode (ConfGen, version 3.6, 2016, Schrödinger LLC) [58]. Receptor grid generation was generated with Glide, version 7.1, 2016 (Schrödinger LLC) [59]. For ligand docking and screening the Glide XP workflow was used [59]. Energetically minimized ligand conformations were docked into the active site of the protein; possible binding poses were determined and subsequently ranked based on their calculated binding affinities.

3.2. Chemistry

Infrared spectra were recorded on an IRAffinity-1S FTIR-spectrometer (Shimadzu Europa GmbH, Hannover, Germany). NMR spectra were recorded on an Avance III 300 spectrometer, tempered at 298 K: ^1H (300 MHz), ^{13}C -NMR (75 MHz) (Bruker Daltonik GmbH, Bremen, Germany). The data is reported as follows: chemical shift in ppm from tetramethylsilane (TMS) as external standard, multiplicity and coupling constant J (Hz). Spectra were either referenced to TMS or internal DMSO- d_6 (^1H -NMR δ 2.50) and internal DMSO- d_6 (^{13}C -NMR δ 39.52) or internal CHCl_3 (^1H -NMR δ 7.26) and internal CDCl_3 (^{13}C -NMR δ 77.00). The following NMR abbreviations have been used: b (broad), s (singlet), d (doublet), t (triplet), m (unresolved multiplet). Several target compounds show spectra of at least two isomers in DMSO- d_6 with a maximal ratio of 1:3. These are due to atropisomers and tautomers as already reported for similar 4,5-diaryl-imidazoles [32]. Although such effects have not been observed whenever CDCl_3 was used, DMSO- d_6 was the most frequented solvent with respect to its favorable solubility-mediating properties. For reasons of clarity, signals are only given for the main isomer. The labelling scheme of structures to correlate NMR signals can be found in Supporting Information. LC-MS was performed with an 1100 HPLC system (Agilent Technologies, Santa Clara, CA, USA) over an Agilent Eclipse XDB-C8 column (150×4.6 mm, $5 \mu\text{m}$) using a 0.1% acetic acid/acetonitrile gradient for mobile phase (flow rate = $1 \text{ mL}\cdot\text{min}^{-1}$). Mass spectra with nominal solution were recorded on a Bruker Esquire \sim LC ion trap mass spectrometer with electron spray ionization (ESI) operating in the positive ion mode, with the following parameters: drying gas nitrogen $8 \text{ L}\cdot\text{min}^{-1}$, nebulizer 35 psi, drying temperature $350 \text{ }^\circ\text{C}$. HRMS spectra were recorded on an AccuTOFTM GCv 4G electron ionization (EI)/field desorption (FD) mass spectrometer (JEOL Germany, Freising, Germany). For clarity, only the highest measured peak is given for mass spectra. Melting points/decomposition temperatures were determined on a SMP3 Melting Point Apparatus (Stuart Scientific, Keison Products, Chelmsford, Essex, UK) and are uncorrected. Column chromatography was performed using a LaFlash system (VWR International GmbH, Darmstadt, Germany). The crude product was loaded on silica gel 60 (63–200 μm) (Macherey-Nagel, Düren, Germany) or PuriFlash IR-50 C18 modified silica gel (50 μm) (Interchim Deutschland GmbH, Mannheim, Germany) and packed in Interchim PuriFlash-DLE/12G dry-load precolumns. Pre-packed Interchim PuriFlash-30SIHP silica gel columns (30 μm , 40 g) and Interchim PuriFlash-15C18HP modified silica gel columns (15 μm , 55 g) were used for separation with flow rates usually adjusted to $30 \text{ mL}\cdot\text{min}^{-1}$ or $20.5 \text{ mL}\cdot\text{min}^{-1}$. Progress of reactions was monitored by thin-layer chromatography (TLC) performed with Macherey-Nagel 0.2 mm Polygram[®] SIL G/UV₂₅₄ pre-coated silica gel polyester sheets and Silicagel 60 RP-18 F₂₅₄ modified silica gel aluminum plates (Merck Millipore, Darmstadt, Germany). Where necessary, reactions were carried out in a nitrogen atmosphere using 4 Å molecular

sieves. All reagents and solvents were obtained from commercial sources (abcr GmbH, Karlsruhe, Germany; Sigma-Aldrich Chemie GmbH, Munich, Germany; Merck Group, Munich, Germany; Merck Millipore; Acros Organics Thermo Fisher Scientific, Geel, Belgium; VWR International GmbH, Hannover, Germany and used as received: THF was used after distillation over Na/benzophenone. HPLC analysis was performed on a Hewlett Packard HP 1050 Series using either a ZORBAX® Eclipse XDB-C8 (150 mm × 4.6 mm, 5 μm) or a Kinetex® C8 (150 × 4.6 mm, 5 μm) column (mobile phase flow 1.5 mL·min⁻¹, gradient KH₂PO₄ buffer 10 mM, pH 2.3/methanol, UV-detection 254 nm). All key compounds submitted to biological assays were proven by this method to show ≥98% purity. Syntheses under elevated pressure were performed in Berghof highpreactor™ BR-25 with corresponding heating block on a MR Hei-Standard laboratory heating plate (Heidolph, Schwabach, Germany). Microwave syntheses were performed in a CEM Discover Microwave Synthesizer (CEM GmbH, Kamp-Lintfort, Germany) under air cooling and high stirring with a maximal power of 100 W.

3.2.1. Syntheses of Key Building Blocks 3–7

1-(4-Fluorophenyl)-2-(2-fluoropyridin-4-yl)-ethan-1-one (3). NaHMDS (66.7 mL 2 M solution in THF, 133 mmol) was slowly added to a stirred solution of 2-fluoro-4-methylpyridine (10.6 mL, 103 mmol) and ethyl 4-fluorobenzoate (18.1 mL, 123 mmol) in 40 mL anhyd. THF at 0 °C under a nitrogen atmosphere. After stirring at 0 °C for 2 h the reaction was allowed to reach rt and stirring continued for 1 h. The mixture was diluted with ethyl acetate and washed twice with 10% aq. HCl. The organic layer was dried over anhyd. Na₂SO₄ and solvent was removed under reduced pressure. Recrystallization from ethyl acetate afforded **3** as colorless solid. Yield 23.9 g (quant.); C₁₃H₉F₂NO (M_r 233.22); m.p. 102 °C; ¹H-NMR (DMSO-*d*₆): δ = 4.59 (s, 2H, CH₂), 7.10 (s, 1H, C₃H, Pyr), 7.25–7.27 (m, 1H, C⁵H, Pyr), 7.37–7.43 (m, 2H, C^{3/5}H, F-Phe), 8.11–8.19 (m, 3H, C^{2/6}H, F-Phe, C⁶H, Pyr) ppm; ¹³C-NMR (DMSO-*d*₆): δ = 43.6 (d, ⁴J_{CF} = 2.8 Hz, CH₂), 110.8 (d, ²J_{CF} = 37.6 Hz, C³H, Pyr), 115.8 (d, ²J_{CF} = 22.0 Hz, C^{3/5}H, F-Phe), 123.8 (d, ⁴J_{CF} = 3.8 Hz, C⁵H, Pyr), 131.3 (d, ³J_{CF} = 9.6 Hz, C^{2/6}H, F-Phe), 132.9 (d, ⁴J_{CF} = 2.7 Hz, C¹, F-Phe), 147.0 (d, ⁵J_{CF} = 15.5 Hz, C⁶H, Pyr), 150.7 (d, ³J_{CF} = 8.5 Hz, C¹, Pyr), 163.1 (d, ¹J_{CF} = 234.3 Hz, C²F, Pyr), 165.2 (d, ¹J_{CF} = 252.0 Hz, C⁴F, F-Phe), 194.6 (CO) ppm; MS (ESI, 70 eV) *m/z* 234 [MH]⁺.

1-(4-Fluorophenyl)-2-(2-fluoropyridin-4-yl)-2-(hydroximino)ethan-1-one (4). NaNO₂ (2.06 g, 29.8 mmol) in 12 mL H₂O was slowly added to a stirred solution of **3** (2.30 g, 9.86 mmol) in 17 mL glacial acetic acid at 10 °C. After stirring at r.t. for 1 h, 30 mL H₂O were added and stirring continued for 3.5 h. The suspension was cooled to 8 °C, filtered, and the residue was washed with H₂O and dried under reduced pressure to afford **4** as colorless solid. Yield 2.46 g (95%); C₁₃H₈F₂N₂O₂ (M_r 262.22); m.p. 185 °C; ¹H-NMR (DMSO-*d*₆): δ = 7.19 (bs, 1H, C³H, Pyr), 7.37–7.46 (m, 3H, C⁵H, Pyr and C^{3/5}H, F-Phe), 7.92–7.98 (m, 2H, C^{2/6}H, F-Phe), 8.30 (d, ³J = 5.3 Hz, 1H, C⁶H, Pyr), 12.67 (s, 1H, OH) ppm; ¹³C-NMR (DMSO-*d*₆): δ = 105.4 (d, ²J_{CF} = 38.9 Hz, C³H, Pyr), 116.7 (d, ²J_{CF} = 22.5 Hz, C^{3/5}H, F-Phe), 118.2 (d, ⁴J_{CF} = 4.2 Hz, C⁵H, Pyr), 130.8 (d, ⁴J_{CF} = 2.7 Hz, C¹, F-Phe), 132.2 (d, ³J_{CF} = 10.1 Hz, C^{2/6}H, F-Phe), 144.3 (d, ³J_{CF} = 8.4 Hz, C⁴, Pyr), 148.8 (d, ⁵J_{CF} = 15.6 Hz, C⁶H, Pyr), 151.9 (d, ⁴J_{CF} = 4.0 Hz, CNOH), 163.5 (d, ¹J_{CF} = 235.6 Hz, C²F, Pyr), 166.0 (d, ¹J_{CF} = 254.8 Hz, C⁴F, F-Phe), 192.04 (CO) ppm; MS (ESI, 70 eV) *m/z* = 263 [MH]⁺.

2-(4-Fluorophenyl)-1-(2-fluoropyridin-4-yl)-2-oxoethan-1-aminium chloride (5). Pd/C 10% (279 mg) was added in one portion under a nitrogen atmosphere to an intensely stirred solution of **4** (1.60 g, 6.10 mmol) in 15 mL 2-propanol and 20 mL HCl sat. 2-propanol and stirring continued for 12 h at r.t. The crude product was obtained by filtration, the residue was resuspended in methanol, filtered again, and the solvent was removed under reduced pressure. Recrystallization from methanol/diethyl ether afforded **5** as beige solid. Yield 1.43 g (82%); C₁₃H₁₁ClF₂N₂O (M_r 284.69); m.p. 216 °C; ¹H-NMR (DMSO-*d*₆): δ = 6.56 (s, 1H, CH), 7.35–7.41 (m, 2H, C^{3/5}H, F-Phe), 7.52–7.54 (m, 2H, C^{3/5}H, Pyr), 8.21 (dd, ³J = 8.4 Hz, ⁴J = 5.6 Hz, 2H, C^{2/6}H, F-Phe), 8.31 (d, ³J = 5.4 Hz, 1H, C⁶H, Pyr), 9.36 (bs, 3H, NH₃⁺) ppm; ¹³C-NMR (DMSO-*d*₆): δ = 56.8 (CNH₃⁺), 110.5 (d, ²J_{CF} = 39.3 Hz, C³H, Pyr), 116.9 (d, ²J_{CF} = 22.1 Hz, C^{3/5}H, F-Phe), 122.3 (d, ⁴J_{CF} = 4.2 Hz, C⁵H, Pyr), 130.0 (d, ⁴J_{CF} = 2.7 Hz, C¹, F-Phe),

132.9 (d, $^3J_{CF} = 9.8$ Hz, $C^{2/6}H$, F-Phe), 147.4 (d, $^3J_{CF} = 8.0$ Hz, C^4 , Pyr), 149.4 (d, $^5J_{CF} = 15.0$ Hz, C^6H , Pyr), 163.5 (d, $^1J_{CF} = 236.7$ Hz, C^2F , Pyr), 166.3 (d, $^1J_{CF} = 255.1$ Hz, C^4F , F-Phe), 191.4 (CO) ppm; MS (ESI, 70 eV) m/z 249 [MCI] $^+$.

2-Fluoro-4-(5-(4-fluorophenyl)-2-(methylthio)-1H-imidazol-4-yl)pyridine (6). A mixture of **5** (4.41 g, 15.5 mmol) and methyl thiocyanate (3.18 mL, 46.5 mmol) was refluxed under a nitrogen atmosphere for 45 min in 140 mL anhyd. DMF and stirred 45 min at r.t. before ice-cold H_2O (400 mL) was added. The suspension was cooled to 8 °C, filtered, the residue was washed with H_2O , and dried under reduced pressure to afford **6** as fine yellow solid. Yield 3.59 g (76%); $C_{15}H_{11}F_2N_3S$ (M_r 303.33); m.p. 205 °C; 1H -NMR (DMSO- d_6): $\delta = 2.63$ (s, 3H, SCH_3), 7.09 (bs, 1H, C^3H , Pyr), 7.26–7.34 (m, 3H, C^5H , Pyr and $C^{3/5}H$, F-Phe), 7.49–7.54 (m, 2H, $C^{2/6}H$, F-Phe), 8.09 (d, $^3J = 5.3$ Hz, 1H, C^6H , Pyr), 12.84 (bs, 1H, NH) ppm; ^{13}C -NMR (DMSO- d_6): $\delta = 14.9$ (SCH_3), 105.0 (d, $^2J_{CF} = 39.5$ Hz, C^3H , Pyr), 115.9 (d, $^2J_{CF} = 21.6$ Hz, $C^{3/5}H$, F-Phe), 118.5 (d, $^4J_{CF} = 2.5$ Hz, C^5H , Pyr), 126.5 (C^1 , F-Phe), 130.9 ($C^{2/6}H$, F-Phe), 132.9 (d, $^3J_{CF} = 8.6$ Hz, C^4 , Pyr), 143.0 (C^2 , Imdz), 147.6 (d, $^3J_{CF} = 16.1$ Hz, C^6H , Pyr), 162.1 (d, $^1J_{CF} = 246.4$ Hz, CF, F-Phe), 163.7 (d, $^1J_{CF} = 233.3$ Hz, CF, Pyr) ppm; MS (ESI, 70 eV) m/z 304 [MH] $^+$.

4-(5-(4-Fluorophenyl)-2-(methylthio)-1H-imidazol-4-yl)pyridin-2-amine (7). A solution of **6** (1.00 g, 3.30 mmol) in 15 mL 32% aq. ammonia solution was heated in a high pressure reactor at 180 °C for 18 h. The reactor was allowed to reach r.t. and H_2O was added. The crude product was obtained by filtration, washed with H_2O and diisopropyl ether and purified by flash chromatography (SiO_2 , 50%–100% ethyl acetate/petrol ether) to afford **7** as beige solid. Yield 852 mg (86%); $C_{15}H_{13}FN_4S$ (M_r 300.36); 1H -NMR (DMSO- d_6): $\delta = 2.60$ (s, 1H, SCH_3), 5.79–5.95 (m, 2H, NH_2), 6.42–6.67 (m, 2H, $C^{3/5}H$, Pyr), 7.17–7.27 (m, 2H, $C^{3/5}H$, F-Phe), 7.48 (bs, 2H, $C^{2/6}H$, F-Phe), 7.74–7.86 (m, 1H, C^6H , Pyr), 12.58 (s, 1H, NH) ppm; ^{13}C -NMR (DMSO- d_6): $\delta = 15.1$ (SCH_3), 105.1 (C^5H , Pyr), 110.0 (C^3H , Pyr), 115.7 (d, $^3J_{CF} = 21.1$ Hz, $C^{3/5}H$, F-Phe), 127.0 (s, C^4/C^5 , Imdz), 129.2 (s, C^1 , F-Phe), 130.5 (d, $^4J_{CF} = 6.6$ Hz, $C^{2/6}H$, F-Phe), 147.5 (C^6H , Pyr), 160.1 (CF) ppm; MS (ESI, 70 eV) m/z 301 [MH] $^+$.

3.2.2. Synthesis of 4-(5-(4-Fluorophenyl)-2-(methylthio)-1H-imidazol-4-yl)pyridin-2-amines and -piperazines **8**, **9**, **10a–i**

3-(2,4-Dimethoxyphenyl)propan-1-ol (8). Under a nitrogen atmosphere a solution of $LiAlH_4$ (120 mg, 3.16 mmol) in 3 mL anhyd. THF was slowly added to 3-(2,4-dimethoxyphenyl)propionic acid (508 mg, 2.42 mmol) in 6 mL anhyd. THF at r.t. with intense stirring that continued for 1 h. After completion, the reaction was cooled down in an ice-bath and quenched by successive addition of H_2O (120 μ L), 15% aq. NaOH solution (120 μ L), and H_2O (360 μ L). The precipitate was filtered off, washed with THF, and the filtrate was concentrated under reduced pressure. The crude product was purified by flash chromatography (SiO_2 , 20%–30% ethyl acetate/petrol ether) to afford **8** as colorless oil. Yield 457 mg (96%); $C_{11}H_{16}O_3$ (M_r 196.25); 1H -NMR ($CDCl_3$): $\delta = 1.78$ –1.83 (m, 2H, $CH_2CH_2CH_2OH$), 2.65 (t, $^3J = 7.3$ Hz, 2H, $CH_2CH_2CH_2OH$), 3.59 (t, $^3J = 6.3$ Hz, 1H, $CH_2CH_2CH_2OH$), 3.78 (s, 1H, OH), 3.79 (s, 3H, C^4OCH_3), 3.81 (s, 3H, C^2OCH_3), 6.42–6.46 (m, 2H, $C^{3/5}H$, $(OCH_3)_2$ -Phe), 7.03 (dd, $^3J = 7.7$ Hz, $^5J = 0.6$ Hz, 1H, C^6H , $(OCH_3)_2$ -Phe) ppm; ^{13}C -NMR ($CDCl_3$): $\delta = 25.4$ ($CH_2CH_2CH_2OH$), 33.2 ($CH_2CH_2CH_2OH$), 55.5 ($C^{2/4}OCH_3$), 62.1 ($CH_2CH_2CH_2OH$), 98.6 (C^3H , $(OCH_3)_2$ -Phe), 104.3 (C^5H , $(OCH_3)_2$ -Phe), 122.4 (C^1 , $(OCH_3)_2$ -Phe), 130.4 (C^6H , $(OCH_3)_2$ -Phe), 158.3 (C^2OCH_3), 159.3 (C^4OCH_3) ppm.

1-(3-Bromopropyl)-2,4-dimethoxybenzene (9). To an ice-cold solution of **8** (260 mg, 1.33 mmol) in 4 mL anhyd. DCM, triphenylphosphine (412 mg, 1.57 mmol) and *N*-bromosuccinimide (263 mg, 1.48 mmol) were added under a nitrogen atmosphere and the reaction was stirred for 2 h. The mixture was washed with H_2O and sat. aq. NaCl solution, dried over anhyd. Na_2SO_4 , and the solvent was removed under reduced pressure. Diethyl ether was added, the precipitate filtered off, and the filtrate was concentrated and purified by flash chromatography (SiO_2 , 2%–10% ethyl acetate/petrol ether) to afford **9** as colorless

oil. Yield 205 mg (60%); $C_{11}H_{15}BrO$ (M_r 259.14); 1H -NMR ($CDCl_3$): δ = 2.11 (quint, 3J = 5.6 Hz, 2H, $CH_2CH_2CH_2Br$), 2.70 (t, 3J = 7.2 Hz, 2H, $CH_2CH_2CH_2Br$), 3.39 (t, 3J = 6.8 Hz, 2H, $CH_2CH_2CH_2Br$), 3.80 (s, 6H, $C^{2/4}OCH_3$), 6.42 (dd, 3J = 8.0 Hz, 4J = 2.5 Hz, 1H, C^5H , $(OCH_3)_2$ -Phe), 6.45 (d, 4J = 2.3 Hz, 1H, C^3H , $(OCH_3)_2$ -Phe), 7.05 (dd, 3J = 8.0 Hz, 5J = 0.5 Hz, 1H, C^6H , $(OCH_3)_2$ -Phe) ppm; ^{13}C -NMR ($CDCl_3$): δ = 28.4 ($CH_2CH_2CH_2Br$), 33.0 ($CH_2CH_2CH_2Br$), 33.9 ($CH_2CH_2CH_2Br$), 55.3 (C^4OCH_3), 55.5 (C^2OCH_3), 98.7 (C^3H , $(OCH_3)_2$ -Phe), 103.9 (C^5H , $(OCH_3)_2$ -Phe), 121.4 (C^1 , $(OCH_3)_2$ -Phe), 130.5 (C^6H , $(OCH_3)_2$ -Phe), 158.5 (C^2OCH_3), 159.6 (C^4OCH_3) ppm.

N-(3-(2,4-Dimethoxyphenyl)propyl)-4-(5-(4-fluorophenyl)-2-(methylthio)-1H-imidazol-4-yl)pyridin-2-amine (**10a**). The synthetic protocol starting from Boc-protected 2-amino-4-methylpyridine and **9** predominantly matches the procedure described for **7** and can be found in the Supporting Information. 1H -NMR ($DMSO-d_6$): δ = 1.67–1.72 (m, 2H, $CH_2CH_2CH_2NH$), 2.48–2.52 (m, 2H, $CH_2CH_2CH_2NH$), 2.60 (s, 3H, SCH_3), 3.13–3.17 (m, 2H, $CH_2CH_2CH_2NH$), 3.72 (s, 3H, C^4OCH_3), 3.74 (s, 3H, C^2OCH_3), 6.41–6.50 (m, 5H, $C^{3/5}H$, Pyr and $C^{3/5}H$, $(OCH_3)_2$ -Phe and $CH_2CH_2CH_2NH$), 7.01 (d, 3J = 8.2 Hz, 1H, C^6H , $(OCH_3)_2$ -Phe), 7.22 (m, 2H, $C^{3/5}H$, F-Phe), 7.48 (m, 2H, $C^{2/6}H$, F-Phe), 7.85 (bs, C^6H , Pyr), 12.58 (bs, 1H, NH) ppm; ^{13}C -NMR ($DMSO-d_6$): δ = 15.1 (SCH_3), 26.6 ($CH_2CH_2CH_2NH$), 29.3 ($CH_2CH_2CH_2NH$), 40.7 ($CH_2CH_2CH_2NH$), 55.1 (C^4OCH_3), 55.2 (C^2OCH_3), 98.3 (C^3H , $(OCH_3)_2$ -Phe), 104.3 (C^5H , $(OCH_3)_2$ -Phe), 104.9 (C^3H , Pyr), 109.7 (C^5H , Pyr), 115.4 ($C^{3/5}H$, F-Phe), 121.8 (C^1 , $(OCH_3)_2$ -Phe), 126.5 (C^4 , Imdz), 127.0 (C^5 , Imdz), 129.7 (C^1 , F-Phe), 129.7 (C^6H , $(OCH_3)_2$ -Phe), 130.1 ($C^{2/6}H$, F-Phe), 142.1 (C^2 , Imdz), 147.5 (C^6H , Pyr), 157.9 (C^2OCH_3), 158.8 (C^4OCH_3), 159.3 (C^2 , Pyr) ppm; MS (ESI, 70 eV) m/z 479 $[MH]^+$; HRMS (EI, 70 eV) m/z $[M]^+$ calcd. for $C_{26}H_{27}FN_4O_2S$, 478.1839; found, 478.1839.

General Procedure for the Preparation Compounds **10b–i**

Compound **6** (1.0 equiv) was suspended in the appropriate amine/piperazine (4.0 to 6.0 equiv) and the intensely stirred mixture was heated to 160 °C. Progress of the reaction was monitored by HPLC control. After complete conversion the mixture was diluted with ethyl acetate, washed with sat. aq. $NaHCO_3$ solution and H_2O , dried over anhyd. Na_2SO_4 , and concentrated under reduced pressure. The crude product was purified by flash chromatography (stationary phase, eluent, and mixing ratio given for each compound, respectively) to afford the particular compound.

N-(2,4-Dimethoxyphenyl)-4-(5-(4-fluorophenyl)-2-(methylthio)-1H-imidazol-4-yl)-pyridin-2-amine (**10b**). Synthesis was performed according to the general procedure from **6** (400 mg, 1.32 mmol) and 2,4-dimethoxyaniline (808 mg, 5.27 mmol). Purification was achieved by flash chromatography (SiO_2 , 20%–90% ethyl acetate/petrol ether) to afford **10b** as greyish crystals. Yield 312 mg (54%); $C_{23}H_{21}FN_4O_2S$ (M_r 436.51); m.p. 206 °C; 1H -NMR ($DMSO-d_6$): δ = 2.60 (s, 3H, SCH_3), 3.75 (s, 6H, 2 OCH_3), 6.39–6.44 (m, 1H, C^5H , $(OCH_3)_2$ -Phe), 6.56–6.58 (m, 1H, C^3H , $(OCH_3)_2$ -Phe), 6.63 (dd, 3J = 5.3 Hz, 4J = 1.2 Hz, 1H, C^5H , Pyr), 6.82 (s, 1H, C^3H , Pyr), 7.18–7.28 (m, 2H, $C^{3/5}H$, F-Phe), 7.41–7.46 (m, 2H, $C^{2/6}H$, F-Phe), 7.52 (d, 3J = 8.7 Hz, 1H, C^6H , $(OCH_3)_2$ -Phe), 7.71 (s, 1H, NH), 7.95 (d, 3J = 5.3 Hz, 1H, C^6H , Pyr), 12.60 (s, 1H, NH , Imdz) ppm; ^{13}C -NMR ($DMSO-d_6$): δ = 15.1 (SCH_3), 55.2 (OCH_3), 55.2 (OCH_3), 99.0 (C^3H , $(OCH_3)_2$ -Phe), 104.0 (C^5H , $(OCH_3)_2$ -Phe), 105.4 (C^3H , Pyr), 111.5 (C^5H , Pyr), 115.4 (dd, $^2J_{CF}$ = 21.8 Hz, $C^{3/5}H$, F-Phe), 122.5 (C, Imdz), 123.6 (C^6H , $(OCH_3)_2$ -Phe), 126.8 (d, $^4J_{CF}$ = 3.1 Hz, C^1 , F-Phe), 130.0 (d, $^3J_{CF}$ = 8.1 Hz, $C^{2/6}H$, F-Phe), 134.9 (C^1 , $(OCH_3)_2$ -Phe), 138.8 (C, Imdz), 141.7 (C^2OCH_3), 142.7 (C^2 , Imdz), 147.6 (C^6H , Pyr), 152.2 (C^4OCH_3), 155.9 (C^4 , Pyr), 157.4 (C^2 , Pyr), 161.8 (d, $^1J_{CF}$ = 245.0 Hz, CF) ppm; MS (ESI, 70 eV) m/z 437 $[MH]^+$.

N-(2-Ethoxyphenyl)-4-(5-(4-fluorophenyl)-2-(methylthio)-1H-imidazol-4-yl)pyridin-2-amine (**10c**). Synthesis was performed according to the general procedure from **6** (1.50 g, 4.95 mmol) and 2-ethoxyaniline (3.88 mL, 29.7 mmol). Purification was achieved by flash chromatography (SiO_2 , 20%–90% ethyl acetate/petrol ether) to afford **10c** as dark red crystals. Yield 1.10 g (52%); $C_{23}H_{21}FN_4OS$ (M_r 420.51); m.p. 179 °C; 1H -NMR ($CDCl_3$): δ = 1.39 (t, 3J = 7.0 Hz, 3H, CH_2CH_3), 2.63 (s, 3H, SCH_3), 4.03 (q, 3J = 7.0 Hz, 2H, CH_2CH_3), 6.76 (t, 3J = 7.7 Hz, 1H, C^5H , EtO-Phe), 6.81–6.84 (m, 2H, C^5H , Pyr and

C^3H , EtO-Phe), 6.91 (t, $^3J = 7.7$ Hz, 1H, C^4H , EtO-Phe), 6.97 (bs, 1H, C^3H , Pyr), 7.00–7.05 (t, $^3J = 8.7$ Hz, 2H, $C^{3/5}H$, F-Phe), 7.21 (bs, 1H, NH), 7.37–7.41 (m, 2H, $C^{2/6}H$, F-Phe), 7.49 (d, $^3J = 7.7$ Hz, 1H, C^6H , EtO-Phe), 8.00 (d, $^3J = 5.5$ Hz, 1H, C^6H , Pyr) ppm; ^{13}C -NMR ($CDCl_3$): $\delta = 15.0$ (CH_3CH_2), 16.6 (SCH_3), 64.3 (CH_2CH_3), 106.5 (C^3H , Pyr), 111.7 (C^3H , EtO-Phe), 112.9 (C^5H , Pyr), 116.0 (d, $^2J_{CF} = 21.7$ Hz, $C^{3/5}H$, F-Phe), 120.0 (C^6H , EtO-Phe), 120.7 (C^5H , EtO-Phe), 122.6 (C^4H , EtO-Phe), 129.4 (C^1 , EtO-Phe), 130.5 (d, $^3J_{CF} = 8.1$ Hz, $C^{2/6}H$, F-Phe), 143.2 (C^2 , Imdz), 146.8 (C^6H , Pyr), 148.7 ($COEt$), 155.5 (C^2 , Pyr), 162.5 (d, $^1J_{CF} = 249.0$ Hz, CF) ppm; MS (ESI, 70 eV) $m/z = 421$ $[MH]^+$.

N-(3,4-Dimethoxyphenethyl)-4-(5-(4-fluorophenyl)-2-(methylthio)-1H-imidazol-4-yl)-pyridin-2-amine (**10d**). Synthesis was performed according to the general procedure from **6** (400 mg, 1.32 mmol) and 3,4-dimethoxyphenethylamine (900 μ L, 5.31 mmol). Purification was achieved by flash chromatography (SiO_2 , 20%–90% ethyl acetate/petrol ether) to afford **10d** as yellow crystals. Yield 550 mg (90%); $C_{25}H_{25}FN_4O_2S$ (M_r 464.56); m.p. 87 °C; 1H -NMR ($CDCl_3$): $\delta = 2.55$ (s, 3H, SCH_3), 2.69 (t, $^3J = 6.9$ Hz, 2H, CH_2CH_2NH), 3.29 (m, 2H, CH_2CH_2NH), 3.74 (s, 3H, C^3OCH_3), 3.75 (s, 3H, C^4OCH_3), 4.86 (bs, 1H, CH_2CH_2NH), 6.51 (d, $^3J = 5.2$ Hz, 1H, C^5H , Pyr), 6.57 (d, $^4J = 2.0$ Hz, 1H, C^3H , Pyr), 6.57–6.70 (m, 3H, $C^{2/5/6}H$, $(OCH_3)_2$ -Phe), 6.91–6.96 (m, 2H, $C^{3/5}H$, F-Phe), 7.32–7.36 (m, 2H, $C^{2/6}H$, F-Phe), 7.74 (d, $^3J = 5.8$ Hz, 1H, C^6H , Pyr), 10.77 (bs, 1H, NH) ppm; ^{13}C -NMR ($CDCl_3$): $\delta = 16.4$ (SCH_3), 35.1 (CH_2CH_2NH), 43.5 (CH_2CH_2NH), 55.9 (C^3OCH_3), 55.9 (C^4OCH_3), 104.1 (C^3H , Pyr), 111.0 (C^5H , Pyr), 111.4 (C^5H , $(OCH_3)_2$ -Phe), 112.1 (C^2H , $(OCH_3)_2$ -Phe), 115.7 (d, $^2J_{CF} = 21.7$ Hz, $C^{3/5}H$, F-Phe), 120.7 (C^6H , $(OCH_3)_2$ -Phe), 130.3 (d, $^3J_{CF} = 8.2$ Hz, $C^{2/6}H$, F-Phe), 131.4 ($C^{4/5}$, Imdz), 142.9 (C^4 , Pyr), 146.7 (C^6H , Pyr), 147.7 (C^4OCH_3), 149.0 (C^3OCH_3), 158.3 (C^2 , Pyr), 162.6 (d, $^1J_{CF} = 248.5$ Hz, CF) ppm; MS (ESI, 70 eV) m/z 465 $[MH]^+$.

N-(2-(1H-Indol-3-yl)-ethyl)-4-(5-(4-fluorophenyl)-2-(methylthio)-1H-imidazol-4-yl)-pyridin-2-amine (**10e**). Synthesis was performed according to the general procedure from **6** (400 mg, 1.32 mmol) and tryptamine (845 mg, 5.27 mmol). Purification was achieved by flash chromatography (SiO_2 , 20%–90% ethyl acetate/petrol ether) to afford **10e** as yellowish-brown crystals. Yield 427 mg (73%); $C_{25}H_{22}FN_5S$ (M_r 443.54); m.p. 122 °C; 1H -NMR ($CDCl_3$): $\delta = 2.61$ (s, 3H, SCH_3), 2.95 (t, $^3J = 6.6$ Hz, 2H, CH_2CH_2NH), 3.39 (t, $^3J = 6.6$ Hz, 2H, CH_2CH_2NH), 6.52 (d, $^3J = 5.7$ Hz, 1H, C^5H , Pyr), 6.52 (bs, 1H, C^2H , Indole), 6.87 (d, $^4J = 2.1$ Hz, 1H, C^3H , Pyr), 6.95–7.01 (m, 2H, $C^{3/5}H$, F-Phe), 7.08 (t, $^3J = 7.8$ Hz, 1H, C^6H , Indole), 7.16 (t, $^3J = 7.9$ Hz, 1H, C^5H , Indole), 7.30 (d, $^3J = 7.9$ Hz, 1H, C^4H , Indole), 7.35–7.39 (m, 2H, $C^{2/6}H$, F-Phe), 7.52 (d, $^3J = 7.7$ Hz, 1H, C^7H , Indole), 7.71 (d, $^3J = 5.7$ Hz, 1H, C^6H , Pyr), 8.38 (s, 1H, NH, Indole) ppm; ^{13}C -NMR ($CDCl_3$): $\delta = 16.4$ (SCH_3), 25.1 (CH_2CH_2NH), 42.2 (CH_2CH_2NH), 104.0 (C^3H , Pyr), 110.6 (C^5H , Pyr), 111.3 (C^4H , Indole), 112.6 (C^3 , Indole), 115.8 (d, $^2J_{CF} = 21.6$ Hz, $C^{3/5}H$, F-Phe), 118.6 (C^7H , Indole), 119.4 (C^6H , Indole), 122.1 (C^5H , Indole), 122.5 (C^2H , Indole), 127.2 (C^{8a} , Indole), 130.3 ($^3J_{CF} = 8.3$ Hz, $C^{2/6}H$, F-Phe), 136.4 (C^{3a} , Indole), 143.3 (C^2 , Imdz), 145.1 (C^6H , Pyr), 158.0 (C^2 , Pyr) ppm; MS (ESI, 70 eV) m/z 444 $[MH]^+$.

N-(4-(5-(4-Fluorophenyl)-2-(methylthio)-1H-imidazol-4-yl)pyridin-2-yl)-*N',N'*-dimethyl-propan-1,3-diamine (**10f**). Synthesis was performed according to the general procedure from **6** (400 mg, 1.32 mmol) and *N*¹,*N*¹-dimethylpropane-1,3-diamine (1.00 mL, 7.93 mmol). Purification was achieved by flash chromatography (SiO_2 , 20%–90% ethyl acetate/petrol ether, then methanol) and subsequent filtration, to afford **10f** as yellow solid. Yield 175 mg (35%); $C_{20}H_{24}FN_5S$ (M_r 385.51); m.p. 129 °C; 1H -NMR ($CDCl_3$): $\delta = 1.61$ (t, $^3J = 6.8$ Hz, 2H, $CH_2CH_2CH_2$), 2.13 (s, 6H, $N(CH_3)_2$), 2.29 (t, $^3J = 6.9$ Hz, 2H, $CH_2N(CH_3)_2$), 2.58 (s, 3H, SCH_3), 3.11 (t, $^3J = 6.7$ Hz, 2H, CH_2NH), 5.22 (bs, 1H, CH_2NH), 6.42–6.46 (m, 2H, $C^{3/5}H$, Pyr), 6.95–7.01 (m, 2H, $C^{3/5}H$, F-Phe), 7.35–7.39 (m, 2H, $C^{2/6}H$, F-Phe), 7.78 (dd, $^3J = 5.4$ Hz, $^5J = 0.6$ Hz, 1H, C^6H , Pyr) ppm; ^{13}C -NMR ($CDCl_3$): $\delta = 16.5$ (SCH_3), 26.7 ($CH_2CH_2CH_2$), 45.2 ($N(CH_3)_2$), 57.6 ($CH_2N(CH_3)_2$), 104.0 (C^3H , Pyr), 111.1 (C^5H , Pyr), 115.5 (d, $^2J_{CF} = 21.5$ Hz, $C^{3/5}H$, F-Phe), 130.2 (d, $^3J_{CF} = 8.1$ Hz, $C^{2/6}H$, F-Phe), 142.7 (C^2 , Imdz), 147.9 (C^6H , Pyr), 159.2 (C^2 , Pyr), 162.4 (d, $^1J_{CF} = 247.7$ Hz, CF) ppm; MS (ESI, 70 eV) m/z 386 $[MH]^+$.

1-(4-(5-(4-Fluorophenyl)-2-(methylthio)-1H-imidazol-4-yl)pyridin-2-yl)-piperazine (10g). Synthesis was performed according to the general procedure from **6** (300 mg, 989 μmol) and piperazine (341 mg, 3.96 mmol). Purification was achieved by flash chromatography (bas. Al_2O_3 , 100% methanol) to afford **10g** as yellow solid. Yield 63.0 mg (17%); $\text{C}_{19}\text{H}_{20}\text{FN}_5\text{S}$ (M_r 369.46); m.p. 146 °C; $^1\text{H-NMR}$ ($\text{DMSO-}d_6$): δ = 2.60 (bs, 3H, SCH_3), 2.73 (t, 3J = 4.5 Hz, 4H, $\text{C}^{2/6}\text{H}_2$, Piperazine), 3.31 (t, 3J = 4.6 Hz, 4H, $\text{C}^{3/5}\text{H}_2$, Piperazine), 6.56 (d, 3J = 5.1 Hz, 1H, C^5H , Pyr), 6.80 (bs, 1H, C^3H , Pyr), 7.20–7.26 (m, 2H, $\text{C}^{3/5}\text{H}$, F-Phe), 7.47–7.51 (m, 2H, $\text{C}^{2/6}\text{H}$, F-Phe), 7.97 (d, 3J = 5.1 Hz, 1H, C^6H , Pyr) ppm; $^{13}\text{C-NMR}$ ($\text{DMSO-}d_6$): δ = 15.1 (SCH_3), 45.3 ($\text{C}^{2/6}\text{H}_2$, Piperazine), 45.8 ($\text{C}^{3/5}\text{H}_2$, Piperazine), 103.8 (C^3H , Pyr), 110.6 (C^5H , Pyr), 115.4 (d, $^2J_{\text{CF}}$ = 21.6 Hz, $\text{C}^{3/5}\text{H}$, F-Phe), 130.3 (d, $^3J_{\text{CF}}$ = 7.6 Hz, $\text{C}^{2/6}\text{H}$, F-Phe), 142.3 (C^2 , Imdz), 147.6 (C^6H , Pyr), 159.6 (C^2 , Pyr), 161.6 (d, $^1J_{\text{CF}}$ = 245.1 Hz, CF) ppm; MS (ESI, 70 eV) m/z 370 $[\text{MH}]^+$.

1-(4-(5-(4-Fluorophenyl)-2-(methylthio)-1H-imidazol-4-yl)pyridin-2-yl)-4-methyl-piperazine (10h). Synthesis was performed according to the general procedure from **6** (400 mg, 1.32 mmol) and *N*-methylpiperazine (600 μL , 5.39 mmol). Purification was achieved by flash chromatography (RP-18, 20%–90% methanol/ H_2O) to afford **10h** as pale yellow solid. Yield 115 mg (23%); $\text{C}_{20}\text{H}_{22}\text{FN}_5\text{S}$ (M_r 383.49); m.p. 111 °C; $^1\text{H-NMR}$ (CDCl_3): δ = 2.28 (s, 3H, CH_3), 2.45 (t, 3J = 4.8 Hz, 4H, $\text{C}^{3/5}\text{H}_2$, Piperazine), 2.57 (s, 3H, SCH_3), 3.40 (t, 3J = 4.8 Hz, 4H, $\text{C}^{2/6}\text{H}_2$, Piperazine), 6.54 (dd, 3J = 5.3 Hz, 4J = 1.1 Hz, 1H, C^5H , Pyr), 6.73 (bs, 1H, C^3H , Pyr), 6.91–6.97 (m, 2H, $\text{C}^{3/5}\text{H}$, F-Phe), 7.32–7.37 (m, 2H, $\text{C}^{2/6}\text{H}$, F-Phe), 7.94 (d, 3J = 5.3 Hz, 1H, C^6H , Pyr) ppm; $^{13}\text{C-NMR}$ (CDCl_3): δ = 16.5 (SCH_3), 44.7 ($\text{C}^{2/6}\text{H}_2$, Piperazine), 45.6 (CH_3), 54.4 ($\text{C}^{3/5}\text{H}_2$, Piperazine), 104.9 (C^3H , Pyr), 111.9 (C^5H , Pyr), 115.7 (d, $^2J_{\text{CF}}$ = 21.6 Hz, $\text{C}^{3/5}\text{H}$, F-Phe), 128.2 (d, $^4J_{\text{CF}}$ = 4.1 Hz, $\text{C}^{\text{C}1}$, F-Phe), 130.2 (d, $^3J_{\text{CF}}$ = 8.1 Hz, $\text{C}^{2/6}\text{H}$, F-Phe), 142.8 (C^2 , Imdz), 147.9 (C^6H , Pyr), 159.6 (C^2 , Pyr), 162.5 (d, $^1J_{\text{CF}}$ = 248.3 Hz, CF) ppm; MS (ESI, 70 eV) m/z 384 $[\text{MH}]^+$.

1-(4-(5-(4-Fluorophenyl)-2-(methylthio)-1H-imidazol-4-yl)pyridin-2-yl)-4-phenyl-piperazine (10i). Synthesis was performed according to the general procedure from **6** (400 mg, 1.32 mmol) and *N*-phenylpiperazine (800 μL , 5.23 mmol). The combined organic phases were extracted with 2 M aq. HCl solution, the aq. layer was neutralized with 2 M aq. KOH solution, and the pale yellow precipitate was collected by filtration, and purified by flash chromatography (SiO_2 , 20%–90% ethyl acetate/petrol ether) to afford **10i** as yellow crystals. Yield 291 mg (50%); $\text{C}_{20}\text{H}_{22}\text{FN}_5\text{S}$ (M_r 445.56); m.p. 101 °C; $^1\text{H-NMR}$ (CDCl_3): δ = 2.64 (s, 3H, SCH_3), 3.19 (t, 3J = 5.1 Hz, 4H, $\text{C}^{2/6}\text{H}_2$, Piperazine), 3.58 (t, 3J = 5.1 Hz, 4H, $\text{C}^{3/5}\text{H}_2$, Piperazine), 6.64 (dd, 3J = 5.4 Hz, 4J = 1.2 Hz, 1H, C^5H , Pyr), 6.93–6.85 (m, 4H, C^3H , Pyr and $\text{C}^{2/4/6}\text{H}$, Phe), 6.99–7.05 (m, 2H, $\text{C}^{3/5}\text{H}$, F-Phe), 7.26 (t, 3J = 8.0 Hz, 2H, $\text{C}^{3/5}\text{H}$, Phe), 7.39–7.44 (m, 2H, $\text{C}^{2/6}\text{H}$, F-Phe), 8.00 (d, 3J = 5.5 Hz, 1H, C^6H , Pyr) ppm; $^{13}\text{C-NMR}$ (CDCl_3): δ = 16.5 (SCH_3), 45.4 ($\text{C}^{2/6}\text{H}_2$, Piperazine), 49.0 ($\text{C}^{3/5}\text{H}_2$, Piperazine), 105.1 (C^3H , Pyr), 111.6 (C^5H , Pyr), 115.8 (d, $^2J_{\text{CF}}$ = 21.7 Hz, $\text{C}^{3/5}\text{H}$, F-Phe), 116.3 ($\text{C}^{2/6}\text{H}$, Phe), 120.2 (C^4H , Phe), 129.2 ($\text{C}^{3/5}\text{H}$, Phe), 130.3 (d, $^3J_{\text{CF}}$ = 8.1 Hz, $\text{C}^{2/6}\text{H}$, F-Phe), 143.0 (C^2 , Imdz), 146.9 (C^6H , Pyr), 151.1 (C^1 , Phe), 159.0 (C^2 , Pyr), 162.6 (d, $^1J_{\text{CF}}$ = 248.5 Hz, CF) ppm; MS (ESI, 70 eV) m/z 446 $[\text{MH}]^+$.

3.2.3. Synthesis of *N*-(4-(5-(4-Fluorophenyl)-2-(methylthio)-1H-imidazol-4-yl)pyridin-2-yl)-3-phenylpropanamides **11a–e**

The appropriate methoxy-substituted 3-phenylpropionic acid and CDI (1.1 equiv) were stirred in 3–4 mL anhyd. DMF until formation of CO_2 was undetectable. **7** was added to the reaction and the mixture was heated at 110 °C under a nitrogen atmosphere for 12 h. The reaction was cooled to rt and ethyl acetate was added. The resulting mixture was washed with H_2O and sat. aq. NaCl solution, dried over anhyd. Na_2SO_4 , and the solvent was removed under reduced pressure. The crude product was purified by flash chromatography (SiO_2 and RP-18, eluent and mixing ratio given for each compound, respectively) to afford the particular compound.

3-(2,4-Dimethoxyphenyl)-*N*-(4-(5-(4-fluorophenyl)-2-(methylthio)-1H-imidazol-4-yl)-pyridin-2-yl)propanamide (11a). Synthesis was performed according to the general procedure from 3-(2,4-dimethoxyphenyl)propionic acid (560 mg, 2.66 mmol) and **7** (400 mg, 1.33 mmol). Purification was achieved by flash chromatography (SiO_2 , 30%–50% ethyl acetate/petrol ether and RP-18, 30%–80% methanol/ H_2O)

to afford **11a** as beige solid. Yield 177 mg (27%); $C_{26}H_{25}FN_4O_3S$ (M_r 492.57); m.p. 90 °C; 1H -NMR (DMSO- d_6): δ = 2.57 (t, 3J = 7.4 Hz, 2H, COCH₂CH₂), 2.62 (s, 3H, SCH₃), 2.75 (t, 3J = 7.5 Hz, 2H, COCH₂CH₂), 3.72 (s, 3H, C²OCH₃), 3.77 (s, 3H, C⁴OCH₃), 6.42 (dd, 3J = 8.3 Hz, 4J = 2.4 Hz, 1H, C⁵H, (OCH₃)₂-Phe), 6.51 (d, 4J = 2.4 Hz, 1H, C³H, (OCH₃)₂-Phe), 6.99 (dd, 3J = 5.3 Hz, 1H, C⁵H, Pyr), 7.03 (d, 3J = 8.3 Hz, 1H, C⁶H, (OCH₃)₂-Phe), 7.28 (bs, 2H, C^{3/5}H, F-Phe), 7.46–7.51 (m, 2H, C^{2/6}H, F-Phe), 8.12 (bs, 1H, C⁶H, Pyr), 8.32 (bs, 1H, C³H, Pyr), 10.29 (bs, 1H, CONH), 12.72 (bs, 1H, NH) ppm; ^{13}C -NMR (DMSO- d_6): δ = 15.1 (SCH₃), 24.7 (COCH₂CH₂), 36.3 (COCH₂CH₂), 55.1 (C²OCH₃), 55.3 (C⁴OCH₃), 98.3 (C³H, (OCH₃)₂-Phe), 104.3 (C⁵H, (OCH₃)₂-Phe), 110.6 (C³H, Pyr), 115.8 (d, $^2J_{CF}$ = 24.1 Hz, C^{3/5}H, F-Phe), 116.4 (C⁵H, Pyr), 120.9 (C¹, (OCH₃)₂-Phe), 126.7 (C¹, F-Phe), 129.8 (C⁶H, (OCH₃)₂-Phe), 130.7 (C⁵, Imdz and C^{2/6}H, F-Phe), 134.5 (C⁴, Imdz), 143.7 (C², Imdz), 147.6 (C⁶H, Pyr), 148.0 (C⁴, Pyr), 152.5 (C², Pyr), 157.9 (C⁴, (OCH₃)₂-Phe), 159.0 (C², (OCH₃)₂-Phe), 161.9 (d, $^1J_{CF}$ = 246.7 Hz, CF), 171.4 (CO) ppm; IR (ATR): ν = 2935, 1670, 1609, 1547, 1505, 1414, 1289, 1262, 1221, 1207, 1153, 1121, 1036, 835 cm⁻¹; MS (ESI, 70 eV) m/z 493 [MH]⁺; HRMS (EI, 70 eV) m/z [M]⁺ calcd. for $C_{26}H_{25}FN_4O_3S$, 492.1631; found, 492.1631.

3-(2,5-Dimethoxyphenyl)-N-(4-(5-(4-fluorophenyl)-2-(methylthio)-1H-imidazol-4-yl)-pyridin-2-yl)-propanamide (**11b**). Synthesis was performed according to the general procedure from 3-(2,5-dimethoxyphenyl) propionic acid (560 mg, 2.66 mmol) and **7** (400 mg, 1.33 mmol). Purification was achieved by flash chromatography (SiO₂, 20%–100% ethyl acetate/petrol ether and RP-18, 20%–100% methanol/H₂O) to afford **11b** as colorless solid. Yield 255 mg (39%); $C_{26}H_{25}FN_4O_3S$ (M_r 492.57); m.p. 91 °C; 1H -NMR (DMSO- d_6): δ = 2.59–2.64 (m, 5H, SCH₃ and COCH₂CH₂), 2.80 (t, 3J = 7.5 Hz, 2H, COCH₂CH₂), 3.66 (s, 3H, C⁵OCH₃), 3.73 (s, 3H, C²OCH₃), 6.72 (dd, 3J = 8.8 Hz, 4J = 3.1 Hz, 1H, C⁴H, (OCH₃)₂-Phe), 6.78 (d, 4J = 3.0 Hz, 1H, C⁶H, (OCH₃)₂-Phe), 6.86 (d, 3J = 8.8 Hz, 1H, C³H, (OCH₃)₂-Phe), 6.99 (dd, 3J = 5.2 Hz, 4J = 1.6 Hz, 1H, C⁵H, Pyr), 7.26 (bs, 2H, C^{3/5}H, F-Phe), 7.46–7.51 (m, 2H, C^{2/6}H, F-Phe), 8.13 (bs, 1H, C⁶H, Pyr), 8.32 (bs, 1H, C³H, Pyr), 10.34 (bs, 1H, CONH), 12.72 (bs, 1H, NH) ppm; ^{13}C -NMR (DMSO- d_6): δ = 15.1 (SCH₃), 25.3 (COCH₂CH₂), 36.0 (COCH₂CH₂), 55.2 (C⁵OCH₃), 55.8 (C²OCH₃), 110.6 (C³H, Pyr), 111.2 (C⁴H, (OCH₃)₂-Phe), 111.5 (C³H, (OCH₃)₂-Phe), 115.6 (C^{3/5}H, F-Phe), 115.9 (C⁶H, (OCH₃)₂-Phe), 116.5 (C⁵H, Pyr), 126.7 (C¹, F-Phe), 130.0 (C¹, (OCH₃)₂-Phe), 130.6 (C⁵, Imdz and C^{2/6}H, F-Phe), 134.5 (C⁴, Imdz), 142.3 (C², Imdz), 147.7 (C⁴ and C⁶H, Pyr), 151.2 (C², (OCH₃)₂-Phe), 152.5 (C², Pyr), 153.0 (C⁵, (OCH₃)₂-Phe), 161.9 (d, $^1J_{CF}$ = 247.3, CF), 171.3 (CO) ppm; MS (ESI, 70 eV) m/z 494 [MH]⁺; HRMS (EI, 70 eV) m/z [M]⁺ calcd. for $C_{26}H_{25}FN_4O_3S$, 492.1631; found, 492.1631. The compound was demonstrated to have the desired structure by small molecule X-ray structure determination (Figure 6). For further details see CCDC and Supporting Information.

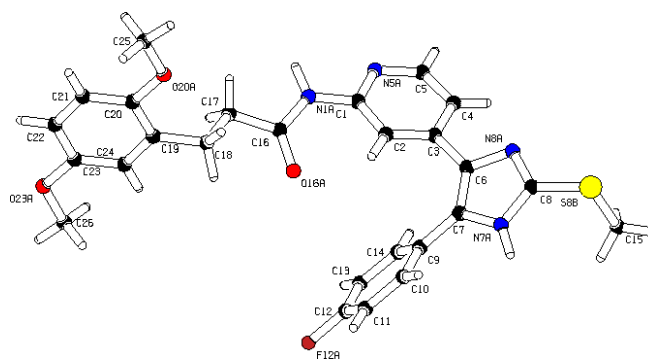


Figure 6. Small molecule X-ray crystal structure determination of compound **11b**.

3-(2,3-Dimethoxyphenyl)-N-(4-(5-(4-fluorophenyl)-2-(methylthio)-1H-imidazol-4-yl)-pyridin-2-yl)-propanamide (**11c**). Synthesis was performed according to the general procedure from 3-(2,3-dimethoxyphenyl) propionic acid (700 mg, 3.33 mmol) and **7** (500 mg, 1.67 mmol). Purification was achieved by flash chromatography (SiO₂, 30%–100% ethyl acetate/petrol ether and RP-18, 50%–100% methanol/H₂O) to

afford **11c** as colorless solid. Yield 515 mg (63%); $C_{26}H_{25}FN_4O_3S$ (M_r 492.57); 1H -NMR (DMSO- d_6): δ = 2.62 (s, 3H, SCH₃), 2.59–2.66 (m, 2H, COCH₂CH₂), 2.84 (t, 3J = 7.7 Hz, 2H, COCH₂CH₂), 3.73 (s, 3H, C²OCH₃), 3.78 (s, 3H, C³OCH₃), 6.79 (dd, 3J = 7.5 Hz, 4J = 1.6 Hz, 1H, C⁶H, (OCH₃)₂-Phe), 6.88 (dd, 3J = 8.1 Hz, 4J = 1.2 Hz, 1H, C⁴H, (OCH₃)₂-Phe), 6.97 (t, 3J = 7.8 Hz, 1H, C⁵H, (OCH₃)₂-Phe), 7.01 (dd, 3J = 5.3 Hz, 4J = 1.5 Hz, 1H, C⁵H, Pyr), 7.26–7.32 (m, 2H, C^{3/5}H, F-Phe), 7.45–7.51 (m, 2H, C^{2/6}H, F-Phe), 8.11 (d, 3J = 5.3 Hz, 1H, C⁶H, Pyr), 8.34 (bs, 1H, C³H, Pyr), 10.35 (s, 1H, CONH), 12.70 (s, 1H, NH) ppm; ^{13}C -NMR (DMSO- d_6): δ = 15.1 (SCH₃), 24.8 (COCH₂CH₂), 36.8 (COCH₂CH₂), 55.3 (C³OCH₃), 60.0 (C²OCH₃), 110.6 (C³H, Pyr), 110.9 (C⁴H, (OCH₃)₂-Phe), 115.8 (d, $^2J_{CF}$ = 21.8 Hz, C^{3/5}H, F-Phe), 116.4 (C⁵H, Pyr), 121.4 (C⁶H, (OCH₃)₂-Phe), 123.7 (C⁵H, (OCH₃)₂-Phe), 126.6 (d, $^4J_{CF}$ = 3.1 Hz, C¹, F-Phe), 130.1 (C⁵, Imdz), 130.7 (d, $^3J_{CF}$ = 8.4 Hz, C^{2/6}H, F-Phe), 134.4 (C¹, (OCH₃)₂-Phe), 134.5 (C⁴, Imdz), 142.2 (C², Imdz), 143.8 (C⁴, Pyr), 146.6 (C²OCH₃), 147.6 (C⁶H, Pyr), 152.4 (C³OCH₃), 152.5 (C², Pyr), 162.0 (d, $^1J_{CF}$ = 244.7 Hz, CF), 171.1 (CO) ppm; MS (ESI, 70 eV) m/z 493 [MH]⁺.

3-(3,4-Dimethoxyphenyl)-N-(4-(5-(4-fluorophenyl)-2-(methylthio)-1H-imidazol-4-yl)-pyridin-2-yl)-propanamide (**11d**). Synthesis was performed according to the general procedure from 3-(3,4-dimethoxyphenyl) propionic acid (700 mg, 3.33 mmol) and **7** (500 mg, 1.67 mmol). Purification was achieved by flash chromatography (SiO₂, 30%–100% ethyl acetate/petrol ether and RP-18, 50%–100% methanol/H₂O) to afford **11d** as colorless solid. Yield 468 mg (57%); 1H -NMR (DMSO- d_6): δ = 2.62 (s, 3H, SCH₃), 2.62–2.67 (m, 2H, COCH₂CH₂), 2.81 (t, 3J = 7.4 Hz, 2H, COCH₂CH₂), 3.70 (s, 3H, C⁴OCH₃), 3.72 (s, 3H, C³OCH₃), 6.73 (dd, 3J = 8.2 Hz, 4J = 1.9 Hz, 1H, C⁶H, (OCH₃)₂-Phe), 6.84 (d, 3J = 8.3 Hz, 1H, C⁵H, (OCH₃)₂-Phe), 6.85 (bs, 1H, C²H, (OCH₃)₂-Phe), 7.00 (dd, 3J = 5.2 Hz, 4J = 1.5 Hz, 1H, C⁵H, Pyr), 7.26–7.31 (m, 2H, C^{3/5}H, F-Phe), 7.46–7.50 (m, 2H, C^{2/6}H, F-Phe), 8.10–8.34 (m, 2H, C^{3/6}H Pyr), 10.33 (s, 1H, CONH), 12.71 (s, 1H, NH) ppm; ^{13}C -NMR (DMSO- d_6): δ = 15.1 (SCH₃), 30.4 (COCH₂CH₂), 38.0 (COCH₂CH₂), 55.4 (C⁴OCH₃), 55.5 (C³OCH₃), 110.6 (C³H, Pyr), 111.9 (C⁵H, (OCH₃)₂-Phe), 112.3 (C²H, (OCH₃)₂-Phe), 115.8 (d, $^2J_{CF}$ = 22.5 Hz, C^{3/5}H, F-Phe), 116.4 (C⁵H, Pyr), 120.0 (C⁶H, (OCH₃)₂-Phe), 130.6 (C^{2/6}H, F-Phe), 133.5 (C¹, (OCH₃)₂-Phe), 147.1 (C⁴OCH₃), 147.6 (C⁶H, Pyr), 148.6 (C³OCH₃), 152.5 (C², Pyr), 165.8 (d, $^1J_{CF}$ = 242.6 Hz, CF), 171.2 (CO) ppm; MS (ESI, 70 eV) m/z 493 [MH]⁺.

3-(3,4,5-Trimethoxyphenyl)-N-(4-(5-(4-fluorophenyl)-2-(methylthio)-1H-imidazol-4-yl)-pyridin-2-yl)-propanamide (**11e**). Synthesis was performed according to the general procedure from 3-(3,4,5-dimethoxyphenyl) propionic acid (800 mg, 3.33 mmol) and **7** (500 mg, 1.67 mmol). Purification was achieved by flash chromatography (SiO₂, 20%–100% ethyl acetate/petrol ether and RP-18, 50%–100% methanol/H₂O) to afford **11e** as pale yellowish solid. Yield 422 mg (49%); $C_{27}H_{27}FN_4O_4S$ (M_r 522.60); 1H -NMR (DMSO- d_6): δ = 2.62 (s, 3H, SCH₃), 2.62–2.69 (m, 2H, COCH₂CH₂), 2.80–2.85 (m, 2H, COCH₂CH₂), 3.61 (s, 3H, C⁴OCH₃), 3.74 (bs, 6H, C^{3/5}OCH₃), 6.56 (s, 2H, C^{2/6}H, (OCH₃)₃-Phe), 7.01 (dd, 3J = 5.3 Hz, 4J = 1.6 Hz, 1H, C⁵H, Pyr), 7.26–7.32 (m, 2H, C^{3/5}H, F-Phe), 7.46–7.51 (m, 2H, C^{2/6}H, F-Phe), 8.11 (dd, 3J = 5.3 Hz, 5J = 0.5 Hz, 1H, C⁶H, Pyr), 8.36 (bs, 1H, C³H, Pyr), 10.36 (s, 1H, CONH), 12.70 (s, 1H, NH) ppm; ^{13}C -NMR (DMSO- d_6): δ = 15.1 (SCH₃), 31.3 (COCH₂CH₂), 37.9 (COCH₂CH₂), 55.7 (C^{3/5}OCH₃), 59.9 (C⁴OCH₃), 105.5 (C^{2/6}H, (OCH₃)₃-Phe), 110.6 (C³H, Pyr), 115.8 (d, $^2J_{CF}$ = 21.7 Hz, C^{3/5}H, F-Phe), 116.4 (C⁵H, Pyr), 126.6 (d, $^4J_{CF}$ = 3.3 Hz, C¹, F-Phe), 130.1 (C⁵, Imdz), 130.7 (d, $^3J_{CF}$ = 8.4 Hz, C^{2/6}H, F-Phe), 134.5 (C⁴, Imdz), 135.7 (C⁴OCH₃), 136.8 (C¹, (OCH₃)₃-Phe), 142.2 (C², Imdz), 143.8 (C⁴, Pyr), 147.6 (C⁶H, Pyr), 152.5 (C², Pyr), 152.7 (C^{3/5}OCH₃), 162.0 (d, $^1J_{CF}$ = 245.4 Hz, CF), 171.2 (CO) ppm; MS (ESI, 70 eV) m/z 523 [MH]⁺.

3.2.4. Synthesis of 4-(5-(4-Fluorophenyl)-2-(methylthio)-1H-imidazol-4-yl)pyridin-2-carbamides **12a–g**

A solution of **7** (1.0 equiv), the appropriate isocyanate (1.1 equiv) and DIPEA (1.2 equiv) in 5 mL anhyd. DMF was stirred under a nitrogen atmosphere at rt for 12 h. The solvent was removed under reduced pressure, the residue resuspended in ethyl acetate, and washed with 0.1 M aq. HCl, sat. aq. NaHCO₃ solution, and sat. aq. NaCl solution, dried over anhyd. Na₂SO₄, and concentrated under reduced pressure. The crude product was purified by flash chromatography (SiO₂ and RP-18, eluent and mixing ratio given for each compound, respectively) to afford the particular compound.

1-(2,4-Dimethoxyphenyl)-3-(4-(5-(4-fluorophenyl)-2-(methylthio)-1H-imidazol-4-yl)-pyridin-2-yl)carbamide (12a). Synthesis was performed according to the general procedure from 2,4-dimethoxyphenyl isocyanate (262 mg, 1.47 mmol). Purification was achieved by flash chromatography (SiO₂, 0%–10% methanol/DCM and RP-18, 50%–100% methanol/H₂O) to afford **12a** as colorless solid. Yield 135 mg (21%); C₂₄H₂₂FN₅O₃S (M_r 479.53); m.p. 214 °C; ¹H-NMR (DMSO-*d*₆): δ = 2.63 (s, 3H, SCH₃), 3.74 (s, 3H, C⁴OCH₃), 3.88 (s, 3H, C²OCH₃), 6.48 (dd, ³J = 8.9 Hz, ⁴J = 2.7 Hz, 1H, C⁵H, (OCH₃)₂-Phe), 6.62 (d, ⁴J = 2.7 Hz, 1H, C³H, (OCH₃)₂-Phe), 6.92 (dd, ³J = 5.4 Hz, ⁴J = 1.5 Hz, 1H, C⁵H, Pyr), 7.30–7.51 (m, 5H, C^{3/5}H, F-Phe and C³H, Pyr and C^{2/6}H, F-Phe), 8.03 (d, ³J = 8.9 Hz, 1H, C⁶H, (OCH₃)₂-Phe), 8.12 (bs, 1H, C⁶H, Pyr), 9.64 (bs, 1H, NH), 10.89–11.26 (m, 1H, NH), 12.74 (bs, 1H, NH, Imdz) ppm; ¹³C-NMR (DMSO-*d*₆): δ = 15.1 (SCH₃), 55.3 (C⁴OCH₃), 56.0 (C²OCH₃), 98.8 (C³H, (OCH₃)₂-Phe), 104.1 (C⁵H, (OCH₃)₂-Phe), 108.6 (C³H, Pyr), 114.6 (C⁵H, Pyr), 115.7 (C^{2/6}H, F-Phe), 119.7 (C⁶H, (OCH₃)₂-Phe), 121.9 (C¹, (OCH₃)₂-Phe), 130.7 (C^{3/5}H, F-Phe), 134.2 (C⁴, Pyr), 142.3 (C², Imdz), 146.1 (C⁶H, Pyr), 149.4 (C², (OCH₃)₂-Phe), 152.2 (CO), 153.6 (C², Pyr), 155.2 (C⁴, (OCH₃)₂-Phe), 161.8 (d, ¹J_{CF} = 241.6 Hz, CF) ppm; MS (ESI, 70 eV) *m/z* 480 [MH]⁺.

1-(2,5-Dimethoxyphenyl)-3-(4-(5-(4-fluorophenyl)-2-(methylthio)-1H-imidazol-4-yl)-pyridin-2-yl)carbamide (12b). Synthesis was performed according to the general procedure from 2,5-dimethoxyphenyl isocyanate (300 mg, 1.67 mmol). Purification was achieved by flash chromatography (SiO₂, 20%–100% ethyl acetate/petrol ether) to afford **12b** as pale yellowish solid. Yield 79.9 mg (15%); C₂₄H₂₂FN₅O₃S (M_r 479.53); m.p. 184 °C; ¹H-NMR (DMSO-*d*₆): δ = 2.63 (s, 3H, SCH₃), 3.70 (s, 3H, C⁵OCH₃), 3.84 (s, 3H, C²OCH₃), 6.52 (dd, ³J = 8.8 Hz, ⁴J = 2.9 Hz, 1H, C⁴H, (OCH₃)₂-Phe), 6.91–6.96 (m, 1H, C³H, (OCH₃)₂-Phe), 6.95 (dd, ³J = 5.5 Hz, ⁴J = 1.4 Hz, 1H, C⁵H, Pyr), 7.28–7.38 (m, 2H, C^{3/5}H, F-Phe), 7.47–7.51 (m, 3H, C^{2/6}H, F-Phe and C³H, Pyr), 7.92 (d, ⁴J = 2.9 Hz, 1H, C⁶H, (OCH₃)₂-Phe), 8.13 (d, ³J = 5.4 Hz, 1H, C⁶H, Pyr), 9.76 (bs, 1H, NH), 11.52 (vbs, 1H, NH), 12.74 (bs, 1H, NH, Imdz) ppm; ¹³C-NMR (DMSO-*d*₆): δ = 15.1 (SCH₃), 55.3 (C⁵OCH₃), 55.6 (C²OCH₃), 105.6 (C⁶H, (OCH₃)₂-Phe), 105.8 (C⁴H, (OCH₃)₂-Phe), 108.5 (C³H, Pyr), 111.7 (C³H, (OCH₃)₂-Phe), 114.7 (C⁵H, Pyr), 115.9 (d, ²J_{CF} = 22.0 Hz, C^{3/5}H, F-Phe), 126.5 (d, ⁴J_{CF} = 3.3 Hz, C¹, F-Phe), 129.6 (C¹, (OCH₃)₂-Phe), 130.4 (C⁵, Imdz), 130.8 (d, ³J_{CF} = 8.4 Hz, C^{2/6}H, F-Phe), 134.1 (C⁴, Imdz), 142.3 (C², Imdz), 142.4 (C²OCH₃), 144.2 (C⁴, Pyr), 146.1 (C⁶H, Pyr), 152.2 (CO), 153.4 (C⁵OCH₃), 153.4 (C², Pyr), 162.1 (d, ¹J_{CF} = 245.9 Hz, CF) ppm; MS (ESI, 70 eV) *m/z* 480 [MH]⁺.

1-(4-(5-(4-Fluorophenyl)-2-(methylthio)-1H-imidazol-4-yl)pyridin-2-yl)-3-(4-methoxy-phenyl)carbamide (12c). Synthesis was performed according to the general procedure from 4-methoxyphenyl isocyanate (165 μL, 1.27 mmol). Purification was achieved by flash chromatography (SiO₂, 50%–100% ethyl acetate/petrol ether and RP-18, 60%–100% methanol/H₂O) to afford **12c** as pale yellow solid. Yield 137 mg (26%); C₂₃H₂₀FN₅O₂S (M_r 449.50); m.p. 201 °C; ¹H-NMR (DMSO-*d*₆): δ = 2.62 (s, 3H, SCH₃), 3.72 (s, 3H, OCH₃), 6.86–6.90 (m, 2H, C^{3/5}H, H₃CO-Phe), 6.92 (dd, ³J = 5.4 Hz, ⁴J = 1.5 Hz, 1H, C⁵H, Pyr), 7.30 (bs, 2H, C^{3/5}H, F-Phe), 7.39–7.44 (m, 2H, C^{2/6}H, H₃CO-Phe), 7.47–7.51 (m, 2H, C^{2/6}H, F-Phe), 7.58 (bs, 1H, C³H, Pyr), 8.11 (bs, 1H, C⁶H, Pyr), 9.40 (bs, 1H, NH), 10.35–10.71 (m, 1H, NH), 12.74 (s, 1H, NH, Imdz) ppm; ¹³C-NMR (DMSO-*d*₆): δ = 15.1 (SCH₃), 55.2 (OCH₃), 105.3 (C⁴, Pyr), 108.7 (C³H, Pyr), 114.0 (C^{3/5}H, H₃CO-Phe), 114.6 (C⁵H, Pyr), 115.8 (d, ²J_{CF} = 22.0 Hz, C^{3/5}H, F-Phe), 120.6 (C^{2/6}H, H₃CO-Phe), 130.6–130.8 (C^{2/6}H, F-Phe), 132.0 (C¹, H₃CO-Phe), 142.3 (C², Imdz), 146.4 (C⁶H, Pyr), 152.3 (CO), 153.5 (C², Pyr), 154.9 (C⁴, H₃CO-Phe), 162.1 (d, ¹J_{CF} = 252.6 Hz, CF) ppm; MS (ESI, 70 eV) *m/z* 450 [MH]⁺.

1-(4-(5-(4-Fluorophenyl)-2-(methylthio)-1H-imidazol-4-yl)pyridin-2-yl)-3-(*m*-tolyl)-carbamide (12d). Synthesis was performed according to the general procedure from 3-methylphenyl isocyanate (284 μL, 2.20 mmol). Purification was achieved by flash chromatography (SiO₂, 30%–100% ethyl acetate/petrol ether and RP-18, 60%–80% methanol/H₂O) to afford **12d** as colorless solid. Yield 241 mg (28%); C₂₃H₂₀FN₅OS (M_r 433.51); m.p. 211 °C; ¹H-NMR (DMSO-*d*₆): δ = 2.29 (s, 3H, CH₃), 2.63 (s, 3H, SCH₃), 6.83 (d, ³J = 7.4 Hz, 1H, C⁴H, Tol), 6.95 (dd, ³J = 5.4 Hz, ⁴J = 1.5 Hz, 1H, C⁵H, Pyr), 7.15–7.35 (m, 2H, C^{3/5}H, F-Phe), 7.17 (t, ³J = 7.6 Hz, 1H, C⁵H, Tol), 7.31 (d, ³J = 8.0 Hz, 1H, C⁶H, Tol), 7.35 (s, 1H, C²H, Tol), 7.47–7.52 (m, 2H, C^{2/6}H, F-Phe), 7.61 (bs, 1H, C³H, Pyr), 8.13 (bs, 1H, C⁶H, Pyr), 9.44 (s, 1H, NH),

10.42–10.78 (m, 1H, NH), 12.74 (bs, 1H, NH, Imdz) ppm; ^{13}C -NMR (DMSO- d_6): δ = 15.1 (SCH₃), 21.2 (CH₃), 108.7 (C³H, Pyr), 114.8 (C⁵H, Pyr), 115.8 (d, $^2J_{\text{CF}}$ = 22.3 Hz, C^{3/5}H, F-Phe), 116.0 (C⁶H, Tol), 119.3 (C²H, Tol), 123.2 (C⁴H, Tol), 126.6 (d, $^4J_{\text{CF}}$ = 2.6 Hz, C¹, F-Phe), 128.7 (C⁵H, Tol), 129.7 (C⁵, Imdz), 130.8 (C^{2/6}H, F-Phe), 134.2 (C⁴, Imdz), 138.1 (C³, Tol), 139.0 (C¹, Tol), 142.4 (C², Imdz), 144.3 (C⁴, Pyr), 146.4 (C⁶H, Pyr), 152.1 (CO), 153.4 (C², Pyr), 162.0 (d, $^1J_{\text{CF}}$ = 243.0 Hz, CF) ppm; MS (ESI, 70 eV) m/z 434 [MH]⁺.

1-(3-Chloro-4-methylphenyl)-3-(4-(5-(4-fluorophenyl)-2-(methylthio)-1H-imidazol-4-yl)-pyridin-2-yl)-carbamide (12e). Synthesis was performed according to the general procedure from 3-chloro-4-methylphenyl isocyanate (205 μL , 1.47 mmol). Purification was achieved by flash chromatography (SiO₂, 0%–10% methanol/DCM and RP-18, 70%–100% methanol/H₂O and SiO₂, 20%–100% ethyl acetate/petrol ether) to afford **12e** as colorless solid. Yield 210 mg (34%); C₂₃H₁₉ClFN₅OS (M_r 467.95); m.p. 210 °C; ^1H -NMR (DMSO- d_6): δ = 2.27 (s, 3H, CH₃), 2.63 (s, 3H, SCH₃), 6.96 (dd, 3J = 5.5 Hz, 4J = 1.4 Hz, 1H, C⁵H, Pyr), 7.26 (m, 2H, C^{5/6}H, Cl-Tol), 7.28–7.34 (m, 2H, C^{3/5}H, F-Phe), 7.46–7.50 (m, 2H, C^{2/6}H, F-Phe), 7.59 (bs, 1H, C³H, Pyr), 7.77 (s, 1H, C²H, Cl-Tol), 8.12 (d, 3J = 5.4 Hz, 1H, C⁶H, Pyr), 9.51 (s, 1H, NH), 10.99 (s, 1H, NH), 12.73 (s, 1H, NH, Imdz) ppm; ^{13}C -NMR (DMSO- d_6): δ = 15.1 (SCH₃), 18.8 (CH₃), 108.7 (C³H, Pyr), 114.8 (C⁵H, Pyr), 115.9 (d, $^2J_{\text{CF}}$ = 21.7 Hz, C^{3/5}H, F-Phe), 117.6 (C⁶H, Cl-Tol), 118.7 (C²H, Cl-Tol), 126.5 (d, $^4J_{\text{CF}}$ = 3.1 Hz, C¹, F-Phe), 128.9 (C⁴, Cl-Tol), 130.4 (C⁵, Imdz), 130.8 (d, $^3J_{\text{CF}}$ = 8.3 Hz, C^{2/6}H, F-Phe), 131.2 (C⁵H, Cl-Tol), 133.2 (C³, Cl-Tol), 134.1 (C⁴, Imdz), 138.2 (C¹, Cl-Tol), 142.3 (C², Imdz), 144.3 (C⁴, Pyr), 146.4 (C⁶H, Pyr), 152.2 (CO), 153.2 (C², Pyr), 162.1 (d, $^1J_{\text{CF}}$ = 245.5 Hz, CF) ppm; MS (ESI, 70 eV) m/z 468 [MH]⁺.

1-(4-(5-(4-Fluorophenyl)-2-(methylthio)-1H-imidazol-4-yl)pyridin-2-yl)-3-(3-(trifluoromethyl)phenyl)-carbamide (12f). Synthesis was performed according to the general procedure from 3-(trifluoromethyl)phenyl isocyanate (300 μL , 2.20 mmol). Purification was achieved by flash chromatography (SiO₂, 40% methanol/DCM) and subsequent filtration to afford **12f** as colorless solid. Yield 255 mg (26%); C₂₃H₁₇FN₅OS (M_r 487.48); m.p. 234 °C; ^1H -NMR (DMSO- d_6): δ = 2.63 (s, 3H, SCH₃), 6.99 (dd, 3J = 5.6 Hz, 4J = 1.2 Hz, 1H, C⁵H, Pyr), 7.28–7.37 (m, 3H, C^{3/5}H, F-Phe and C⁴H, F₃C-Phe), 7.46–7.66 (m, 5H, C³H, Pyr and C^{2/6}H, F-Phe and C^{5/6}H, F₃C-Phe), 8.08 (bs, 1H, C²H, F₃C-Phe), 8.14 (d, 3J = 5.5 Hz, 1H, C⁶H, Pyr), 9.56 (s, 1H, NH), 11.12 (s, 1H, NH), 12.74 (s, 1H, NH, Imdz) ppm; ^{13}C -NMR (DMSO- d_6): δ = 15.1 (SCH₃), 108.7 (C³H, Pyr), 114.7 (C²H, F₃C-Phe), 115.0 (C⁵H, Pyr), 115.9 (d, $^2J_{\text{CF}}$ = 21.8 Hz, C^{3/5}H, F-Phe), 118.7 (C⁴H, F₃C-Phe), 122.5 (C⁶H, F₃C-Phe), 124.2 (q, $^1J_{\text{CF}}$ = 272.1 Hz, CF₃, F₃C-Phe), 126.5 (d, $^4J_{\text{CF}}$ = 2.9 Hz, C¹, F-Phe), 129.6 (q, $^2J_{\text{CF}}$ = 31.3 Hz, C³, F₃C-Phe), 130.0 (C⁵H, F₃C-Phe), 130.5 (C⁵, Imdz), 130.8 (d, $^3J_{\text{CF}}$ = 8.3 Hz, C^{2/6}H, F-Phe), 134.0 (C⁴, Imdz), 139.9 (C¹, F₃C-Phe), 142.3 (C², Imdz), 144.3 (C⁴, Pyr), 146.6 (C⁶H, Pyr), 152.2 (CO), 153.0 (C², Pyr), 162.0 (d, $^1J_{\text{CF}}$ = 245.2 Hz, CF) ppm; MS (ESI, 70 eV) m/z 488 [MH]⁺; HRMS (EI, 70 eV) m/z [M]⁺ calcd. for C₂₃H₁₇FN₅OS, 487.1090; found 487.1090.

1-(4-(5-(4-Fluorophenyl)-2-(methylthio)-1H-imidazol-4-yl)pyridin-2-yl)-3-(naphthalen-1-yl)carbamide (12g). Synthesis was performed according to the general procedure from naphthyl isocyanate (211 μL , 1.47 mmol). Purification was achieved by flash chromatography (SiO₂, 0%–10% methanol/DCM and SiO₂, 30%–100% ethyl acetate/petrol ether and RP-18, 50%–100% methanol/H₂O) to afford **12g** as pale yellow solid. Yield 257 mg (41%); C₂₆H₂₀FN₅OS (M_r 469.54); m.p. 249 °C; ^1H -NMR (DMSO- d_6): δ = 2.64 (s, 3H, SCH₃), 7.01 (dd, 3J = 5.5 Hz, 4J = 1.4 Hz, 1H, C⁵H, Pyr), 7.30–7.36 (m, 2H, C^{3/5}H, F-Phe), 7.42–7.59 (m, 5H, C³H, Pyr and C^{2/6}H, F-Phe and C^{3/6}H, Naph), 7.63–7.68 (m, 2H, C^{4/7}H, Naph), 7.95 (d, 3J = 8.1 Hz, 1H, C⁵H, Naph), 8.16–8.22 (m, 2H, C^{2/8}H, Naph), 8.27 (d, 3J = 5.5 Hz, 1H, C⁶H, Pyr), 9.87 (s, 1H, NH), 11.86 (bs, 1H, NH), 12.77 (s, 1H, NH, Imdz) ppm; ^{13}C -NMR (DMSO- d_6): δ = 15.1 (SCH₃), 108.7 (C³H, Pyr), 114.7 (C⁵H, Pyr), 115.9 (d, $^2J_{\text{CF}}$ = 21.7 Hz, C^{3/5}H, F-Phe), 116.7 (C²H, Naph), 120.9 (C⁸H, Naph), 123.0 (C⁴H, Naph), 125.4 (C¹, Naph), 126.0 (C^{3/6}H, Naph), 126.3 (C⁷H, Naph), 126.5 (d, $^4J_{\text{CF}}$ = 3.2 Hz, C¹, F-Phe), 128.6 (C⁵H, Naph), 130.6 (C⁵, Imdz), 130.8 (d, $^3J_{\text{CF}}$ = 8.3 Hz, C^{2/6}H, F-Phe), 133.7 (C^{4a}, Naph), 134.0 (C^{8a}, Naph), 134.2 (C⁴, Imdz), 142.4 (C², Imdz), 144.5 (C⁴, Pyr), 146.1 (C⁶H, Pyr), 152.6 (CO), 153.5 (C², Pyr), 162.1 (d, $^1J_{\text{CF}}$ = 246.2 Hz, CF) ppm; MS (ESI, 70 eV) m/z 471 [MH]⁺.

3.2.5. Synthesis of *N*-(4-(5-(4-Fluorophenyl)-2-(methylthio)-1*H*-imidazol-4-yl)pyridin-2-yl)-1-methyl-4-phenyl-1*H*-pyrrole-2-carboxamides **13**, **14a–b**, **15a–b**, **16a–b**

Ethyl 4-bromo-1-methyl-1H-pyrrole-2-carboxylate (13). NaH (240 mg 60% dispersion in mineral oil, 6.05 mmol) was added in one portion to a solution of 4-bromo-1*H*-pyrrole-2-carboxylate (1.17 g, 5.34 mmol) in 15 mL anhyd. DMF at 0 °C under a nitrogen atmosphere. The suspension was stirred for 20 min at the same temp. before methyl iodide (400 µL, 6.43 mmol) was carefully added and stirring continued at 0 °C for 15 min and another 2.5 h at r.t. The reaction was quenched with H₂O and extracted with ethyl acetate. The combined organic phases were washed with H₂O and sat. aq. NaCl solution, dried over anhyd. Na₂SO₄, and the solvent was removed under reduced pressure. Purification was achieved by flash chromatography (SiO₂, 2%–10% ethyl acetate/petrol ether) to afford **13** as clear colorless oil that crystallized on standing as colorless needles. Yield 1.22 g (98%); C₈H₁₀BrNO₂ (M_r 232.08); m.p. 43 °C; ¹H-NMR (DMSO-*d*₆): δ = 1.26 (t, ³J = 7.1 Hz, 3H, COOCH₂CH₃), 3.83 (d, *J* = 0.2 Hz, 3H, CH₃), 4.21 (q, ³J = 7.1 Hz, 2H, COOCH₂CH₃), 6.84 (d, ⁴J = 2.0 Hz, 1H, C³H, Pyrrole), 7.28 (d, ⁴J = 1.7 Hz, 1H, C⁵H, Pyrrole) ppm; ¹³C-NMR (DMSO-*d*₆): δ = 14.2 (COOCH₂CH₃), 36.6 (CH₃), 59.8 (COOCH₂CH₃), 93.8 (CBr), 118.1 (C³H, Pyrrole), 122.7 (C², Pyrrole), 129.5 (C⁵H, Pyrrole), 159.5 (COOCH₂CH₃) ppm.

Ethyl 4-(2,4-dimethoxyphenyl)-1-methyl-1H-pyrrole-2-carboxylate (14a). 27 mL 2 M aq. Na₂CO₃ solution were added to a stirred solution of **13** (1.22 g, 5.26 mmol), 2,4-dimethoxyphenyl boronic acid (2.89 g, 15.9 mmol), and Pd(PPh₃)₄ (306 mg, 265 µmol) in 80 mL DMF. Stirring continued for 4 h under reflux and 12 h at r.t. H₂O was added and the mixture was extracted with ethyl acetate. The combined organic phases were washed with H₂O and sat. aq. NaCl solution, dried over anhyd. Na₂SO₄, and the solvent was removed under reduced pressure. The crude product was purified by flash chromatography (SiO₂, 5%–10% ethyl acetate/petrol ether and RP-18, 50%–70% methanol/H₂O) to afford **14a** as colorless solid. Yield 1.02 g (67%); C₁₆H₁₉NO₄ (M_r 289.33); ¹H-NMR (DMSO-*d*₆): δ = 1.29 (t, ³J = 7.1 Hz, 3H, COOCH₂CH₃), 3.77 (s, 3H, C⁴OCH₃), 3.84 (s, 3H, C²OCH₃), 3.87 (s, 3H, CH₃), 4.23 (q, ³J = 7.1 Hz, 2H, COOCH₂CH₃), 6.53 (dd, ³J = 8.5 Hz, ⁴J = 2.5 Hz, 1H, C⁵H, (OCH₃)₂-Phe), 6.60 (d, ⁴J = 2.5 Hz, 1H, C³H, (OCH₃)₂-Phe), 7.17 (d, ⁴J = 2.0 Hz, 1H, C³H, Pyrrole), 7.44 (d, ³J = 8.5 Hz, 1H, C⁶H, (OCH₃)₂-Phe), 7.46 (dd, ⁴J = 2.0 Hz, ⁵J = 0.4 Hz, 1H, C⁵H, Pyrrole) ppm; ¹³C-NMR (DMSO-*d*₆): δ = 14.4 (COOCH₂CH₃), 36.4 (CH₃), 55.2 (C⁴OCH₃), 55.4 (C²OCH₃), 59.4 (CH₂), 98.8 (C³H, (OCH₃)₂-Phe), 105.2 (C⁵H, (OCH₃)₂-Phe), 115.4 (C³H, Pyrrole), 115.5 (C¹, (OCH₃)₂-Phe), 119.0 (C⁴, Pyrrole), 121.3 (C², Pyrrole), 127.7 (C⁶H, (OCH₃)₂-Phe), 129.0 (C⁵H, Pyrrole), 156.7 (C⁴OCH₃), 158.74 (C²OCH₃), 160.5 (COOCH₂CH₃) ppm; MS (ESI, 70 eV) *m/z* 290 [MH]⁺.

Ethyl 4-(2,5-dimethoxyphenyl)-1-methyl-1H-pyrrole-2-carboxylate (14b). Synthesis was performed according to the procedure described for **14a** starting from **13** (1.11 g, 4.78 mmol), 2,5-dimethoxyphenyl boronic acid (2.65 g, 14.6 mmol), Pd(PPh₃)₄ (289 mg, 250 µmol) in 80 mL DMF, and 25 mL 2 M aq. Na₂CO₃ solution. Purification was achieved by flash chromatography (SiO₂, 2%–10% ethyl acetate/petrol ether and RP-18, 65% methanol/H₂O) to afford **14b** as colorless solid. Yield 984 mg (71%); C₁₆H₁₉NO₄ (M_r 289.33); ¹H-NMR (DMSO-*d*₆): δ = 1.30 (t, ³J = 7.1 Hz, 3H, COOCH₂CH₃), 3.74 (s, 3H, C⁵OCH₃), 3.79 (s, 3H, C²OCH₃), 3.89 (s, 3H, CH₃), 4.24 (q, ³J = 7.1 Hz, 2H, COOCH₂CH₃), 6.74 (dd, ³J = 8.9 Hz, ⁴J = 3.1 Hz, 1H, C⁴H, (OCH₃)₂-Phe), 6.96 (d, ³J = 8.9 Hz, 1H, C³H, (OCH₃)₂-Phe), 7.09 (d, ⁴J = 3.1 Hz, 1H, C⁶H, (OCH₃)₂-Phe), 7.28 (d, ⁴J = 2.0 Hz, 1H, C³H, Pyrrole), 7.60 (dd, ⁴J = 2.0 Hz, ⁵J = 0.4 Hz, 1H, C⁵H, Pyrrole) ppm; ¹³C-NMR (DMSO-*d*₆): δ = 14.3 (COOCH₂CH₃), 36.5 (CH₃), 55.4 (C⁵OCH₃), 55.9 (C²OCH₃), 59.4 (COOCH₂CH₃), 111.7 (C⁴H, (OCH₃)₂-Phe), 112.5 (C⁶H, (OCH₃)₂-Phe), 112.9 (C³H, (OCH₃)₂-Phe), 116.1 (C³H, Pyrrole), 118.9 (C⁴, Pyrrole), 121.6 (C¹, Pyrrole), 123.4 (C¹, (OCH₃)₂-Phe), 130.0 (C⁵H, Pyrrole), 150.0 (C²OCH₃), 153.4 (C⁵OCH₃), 160.5 (COOCH₂CH₃) ppm; MS (ESI, 70 eV) *m/z* 290 [MH]⁺.

4-(2,4-Dimethoxyphenyl)-1-methyl-1H-pyrrole-2-carboxylic acid (15a). 7 mL 4 M aq. NaOH were added to a solution of **14a** (990 mg, 3.42 mmol) in 18 mL THF and 9 mL methanol and the mixture was stirred

at 50 °C for 5 h and then 12 h at r.t. H₂O was added to the reaction, the pH was adjusted to 3 using 1 M aq. HCl, and the mixture was extracted with ethyl acetate. The combined organic phases were washed with H₂O and sat. aq. NaCl solution, the organic phase was dried over anhyd. Na₂SO₄, and the solvent was removed under reduced pressure to afford **15a** as brown solid. Yield 894 mg (quant.); C₁₄H₁₅NO₄ (M_r 261.28); m.p. 164 °C; ¹H-NMR (DMSO-*d*₆): δ = 3.76 (s, 3H, C⁴OCH₃), 3.83 (s, 3H, C²OCH₃), 3.86 (s, 3H, CH₃), 6.53 (dd, ³J = 8.5 Hz, ⁴J = 2.4 Hz, 1H, C⁵H, (OCH₃)₂-Phe), 6.59 (d, ⁴J = 2.4 Hz, 1H, C³H, (OCH₃)₂-Phe), 7.14 (d, ⁴J = 2.0 Hz, 1H, C³H, Pyrrole), 7.41 (d, ⁴J = 2.0 Hz, 1H, C⁵H, Pyrrole), 7.42 (d, ³J = 8.4 Hz, 1H, C⁶H, (OCH₃)₂-Phe), 12.17 (bs, 1H, COOH) ppm; ¹³C-NMR (DMSO-*d*₆): δ = 36.3 (CH₃), 55.2 (C⁴OCH₃), 55.4 (C²OCH₃), 98.8 (C³H, (OCH₃)₂-Phe), 105.2 (C⁵H, (OCH₃)₂-Phe), 115.7 (C³H, Pyrrole), 115.7 (C¹, (OCH₃)₂-Phe), 118.8 (C⁴, Pyrrole), 122.0 (C², Pyrrole), 127.6 (C⁶H, (OCH₃)₂-Phe), 128.6 (C⁵H, Pyrrole), 156.7 (C²OCH₃), 158.7 (C⁴OCH₃), 162.1 (COOH) ppm; MS (ESI, 70 eV) *m/z* 262 [MH]⁺.

4-(2,5-Dimethoxyphenyl)-1-methyl-1H-pyrrole-2-carboxylic acid (15b). Synthesis was performed according to the procedure described for **15a** starting from **14b** (980 mg, 3.39 mmol) in 19 mL THF and 10 mL methanol, and 7 mL 4 M aq. NaOH to afford **15b** as brown solid. Yield 885 mg (quant.); C₁₄H₁₅NO₄ (M_r 261.28); m.p. 149 °C; ¹H-NMR (DMSO-*d*₆): δ = 3.74 (s, 3H, C²OCH₃), 3.79 (s, 3H, C⁵OCH₃), 3.88 (CH₃), 6.72 (dd, ³J = 8.9 Hz, ⁴J = 3.1 Hz, 1H, C⁴H, (OCH₃)₂-Phe), 6.95 (d, ³J = 8.9 Hz, 1H, C³H, (OCH₃)₂-Phe), 7.08 (d, ⁴J = 3.1 Hz, 1H, C⁶H, (OCH₃)₂-Phe), 7.25 (d, ⁴J = 2.0 Hz, 1H, C³H, Pyrrole), 7.55 (d, ⁴J = 2.0 Hz, 1H, C⁵H, Pyrrole), 12.15 (bs, 1H, COOH) ppm; ¹³C-NMR (DMSO-*d*₆): δ = 36.4 (CH₃), 55.4 (C²OCH₃), 55.9 (C⁵OCH₃), 111.5 (C⁴H, (OCH₃)₂-Phe), 112.5 (C⁶H, (OCH₃)₂-Phe), 112.9 (C³H, (OCH₃)₂-Phe), 116.2 (C³H, Pyrrole), 118.7 (C⁴, Pyrrole), 122.4 (C², Pyrrole), 123.6 (C¹, (OCH₃)₂-Phe), 129.6 (C⁵H, Pyrrole), 150.1 (C⁵OCH₃), 153.4 (C²OCH₃), 162.1 (COOH) ppm; MS (ESI, 70 eV) *m/z* 262 [MH]⁺.

4-(2,4-Dimethoxyphenyl)-N-(4-(5-(4-fluorophenyl)-2-(methylthio)-1H-imidazol-4-yl)-pyridin-2-yl)-1-methyl-1H-pyrrole-2-carboxamide (16a). A solution of **15a** (1.01 g, 4.07 mmol), PyBOP (2.54 g, 4.88 mmol), and DIPEA (2.15 mL, 12.3 mmol) was stirred in 14 mL anhyd. DMF under a nitrogen atmosphere for 30 min at r.t. **7** (1.60 g, 5.31 mmol) was added in one portion and the mixture was stirred for 12 h at 110 °C. The reaction was quenched with H₂O and extracted with ethyl acetate. The combined organic phases were washed with H₂O and sat. aq. NaCl solution, dried over anhyd. Na₂SO₄, and the solvent was removed under reduced pressure. The crude product was purified by flash chromatography (SiO₂, 30%–100% ethyl acetate/petrol ether and RP-18, 50%–100% methanol/H₂O) to afford **16a** as beige solid. Yield 303 mg (24%); C₂₉H₂₆FN₅O₃S (M_r 543.62); m.p. 236 °C; ¹H-NMR (DMSO-*d*₆): δ = 2.64 (s, 3H, SCH₃), 3.78 (s, 3H, C²OCH₃), 3.86 (s, 3H, C⁴OCH₃), 3.90 (s, 3H, CH₃), 6.57 (dd, ³J = 8.5 Hz, ⁴J = 2.3 Hz, 1H, C⁵H, (OCH₃)₂-Phe), 6.61 (d, ⁴J = 2.3 Hz, 1H, C³H, (OCH₃)₂-Phe), 7.06 (dd, ³J = 5.3 Hz, ⁴J = 1.2 Hz, 1H, C⁵H, Pyr), 7.28–7.34 (m, 2H, C^{3/5}H, F-Phe), 7.41 (d, ⁴J = 1.3 Hz, 1H, C³H, Pyrrole), 7.46 (d, ³J = 8.4 Hz, 1H, C⁶H, (OCH₃)₂-Phe), 7.49–7.54 (m, 2H, C^{2/6}H, F-Phe), 7.66 (d, ⁴J = 1.4 Hz, 1H, C⁵H, Pyrrole), 8.18 (d, ³J = 5.2 Hz, 1H, C⁶H, Pyr), 8.38 (bs, 1H, C³H, Pyr), 10.10 (bs, 1H, CONH), 12.73 (bs, 1H, NH) ppm; ¹³C-NMR (DMSO-*d*₆): δ = 15.3 (SCH₃), 36.5 (CH₃), 55.2 (C²OCH₃), 55.5 (C⁴OCH₃), 98.8 (C³H, (OCH₃)₂-Phe), 105.2 (C⁵H, (OCH₃)₂-Phe), 111.3 (C³H, Pyr), 113.2 (C⁵H, Pyrrole), 115.9 (d, ²J_{CF} = 21.9 Hz, C^{3/5}H, F-Phe), 115.9 (C¹, (OCH₃)₂-Phe), 116.3 (C⁵H, Pyr), 118.5 (C⁴, Pyrrole), 124.1 (C², Pyrrole), 126.7 (d, ⁴J_{CF} = 3.5 Hz, C¹, F-Phe), 127.5 (C⁶H, (OCH₃)₂-Phe), 128.5 (C³H, Pyrrole), 130.8 (d, ³J_{CF} = 8.4 Hz, C^{2/6}H, F-Phe), 134.5 (C⁵, Imdz), 142.1 (C², Imdz), 143.6 (C⁴, Imdz), 147.6 (C⁶H, Pyr), 152.7 (C², Pyr), 156.7 (C⁴OCH₃), 158.6 (C²OCH₃), 159.8 (CONH), 162.0 (d, ¹J_{CF} = 245.6 Hz, CF) ppm; MS (ESI, 70 eV) *m/z* 544 [MH]⁺; HRMS (EI, 70 eV) *m/z* [M]⁺ calcd. for C₂₉H₂₆FN₅O₃S, 543.1740; found, 543.1740.

4-(2,5-Dimethoxyphenyl)-N-(4-(5-(4-fluorophenyl)-2-(methylthio)-1H-imidazol-4-yl)-pyridin-2-yl)-1-methyl-1H-pyrrole-2-carboxamide (16b). Synthesis was performed according to the procedure described for **16a** starting from **15b** (604 mg, 2.31 mmol), PyBOP (1.45 g, 2.79 mmol), DIPEA (1.20 mL, 6.87 mmol), and **7** (904 mg, 3.01 mmol) in 12 mL anhyd. DMF. The crude product was purified by flash chromatography

(SiO₂, 30%–100% ethyl acetate/petrol ether and RP-18, 50%–100% methanol/H₂O) to afford **16b** as pale yellowish solid. Yield 255 mg (20%); m.p. 127 °C; ¹H-NMR (DMSO-*d*₆): δ = 2.64 (s, 3H, SCH₃), 3.76 (s, 3H, C⁵OCH₃), 3.81 (s, 3H, C²OCH₃), 3.92 (s, 3H, CH₃), 6.73 (dd, ³J = 8.9 Hz, ⁴J = 3.1 Hz, 1H, C⁴H, (OCH₃)₂-Phe), 6.96 (d, ³J = 9.0 Hz, 1H, C³H, (OCH₃)₂-Phe), 7.06 (dd, ³J = 5.3 Hz, ⁴J = 1.6 Hz, 1H, C⁵H, Pyr), 7.17 (d, ⁴J = 3.1 Hz, 1H, C⁶H, (OCH₃)₂-Phe), 7.24–7.30 (m, 2H, C^{3/5}H, F-Phe), 7.50–7.55 (m, 2H, C^{2/6}H, F-Phe), 7.56 (d, ⁴J = 1.7 Hz, 1H, C⁵H, Pyrrole), 7.80 (d, ⁴J = 1.8 Hz, 1H, C³H, Pyrrole), 8.22 (d, ³J = 5.2 Hz, 1H, C⁶H, Pyr), 8.35 (bs, 1H, C³H, Pyr), 10.15 (bs, 1H, CONH), 12.77 (vbs, 1H, NH) ppm; ¹³C-NMR (DMSO-*d*₆): δ = 15.2 (SCH₃), 36.7 (CH₃), 55.4 (C⁵OCH₃), 55.9 (C²OCH₃), 111.3 (C⁴H, (OCH₃)₂-Phe and C³H, Pyr), 112.5 (C⁶H, (OCH₃)₂-Phe), 112.8 (C³H, (OCH₃)₂-Phe), 113.6 (C³H, Pyrrole), 115.7 (d, ²J_{CF} = 21.5 Hz, C^{3/5}H, F-Phe), 116.5 (C⁵H, Pyr), 118.3 (C⁴, Pyrrole), 123.8 (C¹, (OCH₃)₂-Phe), 124.3 (C², Pyrrole), 129.7 (C⁵H, Pyrrole), 130.42 (C^{2/6}H, F-Phe), 142.5 (C², Imdz and C⁴, Pyr), 147.7 (C⁶H, Pyr), 150.1 (C²OCH₃), 152.7 (C¹, Pyr), 153.4 (C⁵OCH₃), 159.8 (CONH), 161.9 (d, ¹J_{CF} = 247.7 Hz, CF) ppm; MS (ESI, 70 eV) *m/z* 544 [MH]⁺; HRMS (EI, 70 eV) *m/z* [M]⁺ calcd. for C₂₉H₂₆FN₅O₃S, 543.1740; found, 543.1740.

3.2.6. Synthesis of Sulfoxides **10j–k**, **11f–g**, **12h–m**, **16c**

The sulfide (1.0 equiv) was dissolved in THF and H₂O was added (approx. 3:1). The mixture was stirred at 0 °C for 10 min before an ice-cold aq. solution of potassium peroxomonosulfate (Oxone[®], 0.6 equiv) was added and stirring continued for 0.5–2 h at the same temp. After completion of the reaction sat. aq. NaHCO₃ solution, H₂O, and ethyl acetate were added and the phases were separated. The organic layer was washed with H₂O and sat. aq. NaCl solution, dried over anhyd. Na₂SO₄, and the solvent was removed under reduced pressure. Purification of the crude products was achieved by crystallization from ethyl acetate or flash chromatography (SiO₂ and RP-18, eluent and mixing ratio given for each compound) to afford the appropriate compound.

N-(2-Ethoxyphenyl)-4-(5-(4-fluorophenyl)-2-(methylsulfinyl)-1H-imidazol-4-yl)pyridin-2-amine (**10j**). Synthesis was performed according to the general procedure for sulfoxidation starting from **10c** (300 mg, 713 μmol) in 5 mL THF and 2 mL H₂O. Flash chromatography (RP-18, 20%–90% methanol/H₂O) afforded **10j** as voluminous yellow solid. Yield 255 mg (82%); C₂₃H₂₁FN₄O₂S (M_r 436.51); m.p. 152 °C; ¹H-NMR (CDCl₃): δ = 1.42 (t, ³J = 7.0 Hz, 3H, CH₃), 3.03 (s, 3H, SCH₃), 4.07 (q, ³J = 7.0 Hz, 2H, CH₂), 6.94–6.78 (m, 4H, C^{4–6}H, EtO-Phe and C⁵H, Pyr), 7.03 (dd, ⁴J = 1.4 Hz, ⁵J = 0.7 Hz, 1H, C³H, Pyr), 7.07–7.13 (m, 3H, C^{3/5}H, F-Phe and NH), 7.46–7.50 (m, 2H, C^{2/6}H, F-Phe), 7.62 (dd, ³J = 7.8 Hz, ⁴J = 1.5 Hz, 1H, C³H, EtO-Phe), 8.14 (dd, ³J = 5.3 Hz, ⁵J = 0.7 Hz, 1H, C⁶H, Pyr) ppm; ¹³C-NMR (CDCl₃): δ = 14.9 (CH₃), 40.8 (SCH₃), 64.1 (CH₂), 106.9 (C³H, Pyr), 111.5 (C³H, EtO-Phe), 113.3 (C⁵H, Pyr), 116.0 (d, ²J_{CF} = 21.7 Hz, C^{3/5}H, F-Phe), 118.2 (C⁶H, EtO-Phe), 120.6 (C⁵H, EtO-Phe), 121.9 (C⁴H, EtO-Phe), 129.9 (C¹, EtO-Phe), 130.6 (d, ³J_{CF} = 8.2 Hz, C^{2/6}H, F-Phe), 146.7 (C², Imdz), 148.2 (C², EtO-Phe), 148.5 (C⁶H, Pyr), 156.0 (C², Pyr), 162.9 (d, ¹J_{CF} = 248.8 Hz, CF) ppm; MS (ESI, 70 eV) *m/z* 437 [MH]⁺.

N-(3,4-Dimethoxyphenethyl)-4-(5-(4-fluorophenyl)-2-(methylsulfinyl)-1H-imidazol-4-yl)-pyridin-2-amine (**10k**). Synthesis was performed according to the general procedure for sulfoxidation starting from **10d** (500 mg, 1.08 mmol) in 5 mL H₂O in 9 mL THF and 3 mL H₂O. Flash chromatography (RP-18, 20%–90% methanol/H₂O) afforded **10k** as pale yellow solid. Yield 208 mg (39%); C₂₅H₂₅FN₄O₃S (M_r 480.56); m.p. 183 °C; ¹H-NMR (CDCl₃): δ = 2.74 (t, ³J = 6.8 Hz, 1H, CH₂CH₂NH), 2.97 (s, 3H, SCH₃), 3.36 (m, 2H, CH₂CH₂NH), 3.76 (s, 6H, 2 OCH₃), 5.00 (bs, 1H, CH₂CH₂NH), 6.49 (bs, 1H, C³H, Pyr), 6.52 (dd, ³J = 5.4 Hz, ⁴J = 1.3 Hz, 1H, C⁵H, Pyr), 6.60–6.63 (m, 2H, C^{2/6}H, (OCH₃)₂-Phe), 6.71 (d, ³J = 8.7 Hz, 1H, C⁵H, (OCH₃)₂-Phe), 6.96–7.02 (m, 2H, C^{3/5}H, F-Phe), 7.36–7.41 (m, 2H, C^{2/6}H, F-Phe), 7.80 (d, ³J = 5.5 Hz, 1H, C⁶H, Pyr) ppm; ¹³C-NMR (CDCl₃): δ = 35.1 (CH₂CH₂NH), 40.7 (SCH₃), 43.3 (CH₂CH₂NH), 55.9 (C³OCH₃), 55.9 (C⁴OCH₃), 104.6 (C³H, Pyr), 111.2 (C⁵H, Pyr), 111.4 (C⁵H, (OCH₃)₂-Phe), 112.1 (C²H, (OCH₃)₂-Phe), 115.9 (d, ²J_{CF} = 21.7 Hz, C^{3/5}H, F-Phe), 120.7 (C⁶H, (OCH₃)₂-Phe), 127.2 (C¹, F-Phe), 130.5 (d, ³J_{CF} = 8.2 Hz, C^{2/6}H, F-Phe), 131.5 (C¹, (OCH₃)₂-Phe), 135.3

(C^{4/5}, Imdz), 141.6 (C⁴, Pyr), 146.8 (C², Imdz), 147.4 (C⁶H, Pyr), 147.7 (C⁴OCH₃), 149.0 (C³OCH₃), 158.6 (C², Pyr), 162.9 (d, ¹J_{CF} = 249.2 Hz, CF) ppm; MS (ESI, 70 eV) *m/z* 481 [MH]⁺.

3-(2,4-Dimethoxyphenyl)-N-(4-(5-(4-fluorophenyl)-2-(methylsulfinyl)-1H-imidazol-4-yl)-pyridin-2-yl)-propanamide (11f). Synthesis was performed according to the general procedure for sulfoxidation starting from **11a** (100 mg, 203 μmol) in 2 mL THF and 0.6 mL H₂O. Flash chromatography (SiO₂, 40%–100% ethyl acetate/petrol ether) afforded **11f** as colorless solid. Yield 96.1 mg (93%); C₂₆H₂₅FN₄O₄S (M_r 508.57); m.p. 209 °C; ¹H-NMR (DMSO-*d*₆): δ = 2.58 (t, ³J = 7.5 Hz, 2H, CH₂CH₂CO), 2.75 (t, ³J = 7.4 Hz, 2H, CH₂CH₂CO), 3.08 (s, 3H, SCH₃), 3.72 (s, 3H, C²OCH₃), 3.77 (s, 3H, C⁴OCH₃), 6.42 (dd, ³J = 8.3 Hz, ⁴J = 2.4 Hz, 1H, C⁵H, (OCH₃)₂-Phe), 6.51 (d, ⁴J = 2.4 Hz, 1H, C³H, (OCH₃)₂-Phe), 7.01–7.05 (m, 2H, C⁵H, Pyr and C⁶H, (OCH₃)₂-Phe), 7.26–7.32 (m, 2H, C^{3/5}H, F-Phe), 7.51–7.55 (m, 2H, C^{2/6}H, F-Phe), 8.19 (d, ³J = 5.2 Hz, 1H, C⁶H, Pyr), 8.34 (bs, 1H, C³H, Pyr), 10.40 (s, 1H, CONH), 13.89 (bs, NH) ppm; ¹³C-NMR (DMSO-*d*₆): δ = 24.7 (CH₂CH₂CO), 36.3 (CH₂CH₂CO), 39.1 (SCH₃), 55.1 (C²OCH₃), 55.3 (C⁴OCH₃), 98.3 (C³H, (OCH₃)₂-Phe), 104.3 (C⁵H, (OCH₃)₂-Phe), 111.1 (C³H, Pyr), 115.8 (d, ²J_{CF} = 21.7 Hz, C^{3/5}H, F-Phe), 117.0 (C⁵H, Pyr), 120.9 (C¹, (OCH₃)₂-Phe), 127.3 (C¹, F-Phe), 129.8 (C⁶H, (OCH₃)₂-Phe), 130.8 (d, ³J_{CF} = 8.2 Hz, C^{2/6}H, F-Phe), 133.4 (C⁴, Imdz), 133.9 (C⁵, Imdz), 142.2 (C⁴, Pyr), 147.9 (C⁶H, Pyr), 148.9 (C², Imdz), 152.6 (C², Pyr), 157.9 (C⁴OCH₃), 159.0 (C²OCH₃), 162.1 (d, ¹J_{CF} = 245.5 Hz, CF), 171.54 (CO) ppm; MS (ESI, 70 eV) *m/z* 509 [MH]⁺; HRMS (EI, 70 eV) *m/z* [M]⁺ calcd. for C₂₆H₂₅FN₄O₄S, 508.1581; found, 508.1581.

3-(2,5-Dimethoxyphenyl)-N-(4-(5-(4-fluorophenyl)-2-(methylsulfinyl)-1H-imidazol-4-yl)-pyridin-2-yl)propanamide (11g). Synthesis was performed according to the general procedure for sulfoxidation starting from **11b** (100 mg, 203 μmol) in 2 mL THF and 0.6 mL H₂O. Crystallization from ethyl acetate afforded **11g** as colorless solid. Yield 26.6 mg (26%); m.p. 204 °C; ¹H-NMR (DMSO-*d*₆): δ = 2.62 (t, ³J = 7.7 Hz, 2H, CH₂CH₂CO), 2.80 (t, ³J = 7.5 Hz, 2H, CH₂CH₂CO), 3.09 (s, 3H, SCH₃), 3.66 (s, 3H, C⁵OCH₃), 3.72 (s, 3H, C²OCH₃), 6.72 (dd, ³J = 8.8 Hz, ⁴J = 3.1 Hz, 1H, C⁴H, (OCH₃)₂-Phe), 6.77 (d, ⁴J = 3.0 Hz, 1H, C⁶H, (OCH₃)₂-Phe), 6.86 (d, ³J = 8.8 Hz, 1H, C³H, (OCH₃)₂-Phe), 7.02 (dd, ³J = 5.2 Hz, ⁴J = 1.5 Hz, 1H, C⁵H, Pyr), 7.25–7.31 (m, 2H, C^{3/5}H, F-Phe), 7.51–7.55 (m, 2H, C^{2/6}H, F-Phe), 8.19 (d, ³J = 5.0 Hz, 1H, C⁶H, Pyr), 8.33 (s, 1H, C³H, Pyr), 10.45 (s, 1H, CONH), 14.00 (bs, 1H, NH) ppm; ¹³C-NMR (DMSO-*d*₆): δ = 25.3 (CH₂CH₂CO), 36.0 (CH₂CH₂CO), 39.0 (SCH₃), 55.2 (C⁵OCH₃), 55.8 (C²OCH₃), 111.2 (C⁴H, (OCH₃)₂-Phe), 111.3 (C³H, Pyr), 111.5 (C³H, (OCH₃)₂-Phe), 115.8 (d, ²J_{CF} = 21.3 Hz, C^{3/5}H, F-Phe), 115.9 (C⁶H, (OCH₃)₂-Phe), 126.5 (C¹, F-Phe), 130.8 (d, ³J_{CF} = 8.3 Hz, C^{2/6}H, F-Phe), 142.1 (C⁴, Pyr), 148.0 (C⁶H, Pyr), 148.8 (C², Imdz), 151.2 (C²OCH₃), 152.58 (C², Pyr), 153.0 (C⁵OCH₃), 162.1 (d, ¹J_{CF} = 245.6 Hz, CF), 171.42 (CO) ppm; MS (ESI, 70 eV) *m/z* 509 [MH]⁺.

1-(2,4-Dimethoxyphenyl)-3-(4-(5-(4-fluorophenyl)-2-(methylsulfinyl)-1H-imidazol-4-yl)-pyridin-2-yl)-carbamide (12h). Synthesis was performed according to the general procedure for sulfoxidation starting from **12a** (85.0 mg, 177 μmol) in 3.4 mL THF and 1 mL H₂O. Flash chromatography (SiO₂, 35%–100% ethyl acetate/petrol ether and RP-18, 55%–100% methanol/H₂O) afforded **12h** as colorless solid. Yield 18.9 mg (22%); C₂₄H₂₂FN₅O₄S (M_r 495.53); m.p. 227 °C; ¹H-NMR (DMSO-*d*₆): δ = 3.08 (s, 3H, SCH₃), 3.74 (s, 3H, C⁴OCH₃), 3.88 (s, 3H, C²OCH₃), 6.48 (dd, ³J = 8.9 Hz, ⁴J = 2.7 Hz, 1H, C⁵H, (OCH₃)₂-Phe), 6.62 (d, ⁴J = 2.7 Hz, 1H, C³H, (OCH₃)₂-Phe), 6.95 (dd, ³J = 5.4 Hz, ⁴J = 1.5 Hz, 1H, C⁵H, Pyr), 7.27–7.33 (m, 2H, C^{3/5}H, F-Phe), 7.46 (bs, 1H, C³H, Pyr), 7.51–7.56 (m, 2H, C^{2/6}H, F-Phe), 8.02 (d, ³J = 8.9 Hz, 1H, C⁶H, (OCH₃)₂-Phe), 8.19 (d, ³J = 5.3 Hz, 1H, C⁶H, Pyr), 9.70 (s, 1H, NH), 11.07 (bs, 1H, NH), 13.87 (bs, 1H, NH, Imdz) ppm; ¹³C-NMR (DMSO-*d*₆): δ = 39.1 (SCH₃), 55.3 (C²OCH₃), 56.0 (C⁴OCH₃), 98.8 (C³H, (OCH₃)₂-Phe), 104.1 (C⁵H, (OCH₃)₂-Phe), 109.2 (C³H, Pyr), 115.1 (C⁵H, Pyr), 115.8 (d, ²J_{CF} = 21.7 Hz, C^{3/5}H, F-Phe), 119.8 (C⁶H, (OCH₃)₂-Phe), 121.8 (C¹, (OCH₃)₂-Phe), 127.2 (C¹, F-Phe), 130.8 (d, ³J_{CF} = 8.4 Hz, C^{2/6}H, F-Phe), 132.7 (C⁴, Imdz), 134.1 (C⁵, Imdz), 142.8 (C⁴, Pyr), 146.5 (C⁶H, Pyr), 149.1 (C², Imdz), 149.4 (C²OCH₃), 152.2 (CO), 153.6 (C², Pyr), 155.2 (C⁴OCH₃), 162.14 (d, ¹J_{CF} = 244.6 Hz, CF) ppm; MS (ESI, 70 eV) *m/z* 496 [MH]⁺.

1-(4-(5-(4-Fluorophenyl)-2-(methylsulfinyl)-1H-imidazol-4-yl)pyridin-2-yl)-3-(4-methoxyphenyl)carbamide (**12i**). Synthesis was performed according to the general procedure for sulfoxidation starting from **12c** (100 mg, 225 μmol) in 2 mL THF and 0.6 mL H_2O . Flash chromatography (RP-18, 50%–70% methanol/ H_2O) afforded **12i** as colorless solid. Yield 62.6 mg (61%); $\text{C}_{23}\text{H}_{20}\text{FN}_5\text{O}_3\text{S}$ (M_r 465.50); m.p. 233 $^\circ\text{C}$; $^1\text{H-NMR}$ ($\text{DMSO-}d_6$): δ = 3.09 (s, 3H, SCH_3), 3.73 (s, 3H, C^4OCH_3), 6.89 (d, 3J = 9.1 Hz, 2H, $\text{C}^{3/5}\text{H}$, $\text{H}_3\text{CO-Phe}$), 6.95 (dd, 3J = 5.4 Hz, 4J = 1.5 Hz, 1H, C^5H , Pyr), 7.28–7.34 (m, 2H, $\text{C}^{3/5}\text{H}$, F-Phe), 7.41 (d, 3J = 9.1 Hz, 2H, $\text{C}^{2/6}\text{H}$, $\text{H}_3\text{CO-Phe}$), 7.51–7.56 (m, 2H, $\text{C}^{2/6}\text{H}$, F-Phe), 7.65 (bs, 1H, C^3H , Pyr), 8.18 (d, 3J = 5.4 Hz, 1H, C^6H , Pyr), 9.43 (s, 1H, NH), 10.47 (bs, 1H, NH), 13.92 (bs, 1H, NH, Imdz) ppm; $^{13}\text{C-NMR}$ ($\text{DMSO-}d_6$): δ = 39.1 (SCH_3), 55.2 (C^4OCH_3), 109.4 (C^3H , Pyr), 114.0 ($\text{C}^{3/5}\text{H}$, $\text{H}_3\text{CO-Phe}$), 115.2 (C^5H , Pyr), 115.9 (d, $^2J_{\text{CF}}$ = 21.7 Hz, $\text{C}^{3/5}\text{H}$, F-Phe), 120.6 ($\text{C}^{2/6}\text{H}$, $\text{H}_3\text{CO-Phe}$), 127.5 (C^1 , F-Phe), 130.9 (d, $^3J_{\text{CF}}$ = 8.7 Hz, $\text{C}^{2/6}\text{H}$, F-Phe), 132.0 (C^1 , $\text{H}_3\text{CO-Phe}$), 146.9 (C^6H , Pyr), 148.8 (C^2 , Imdz), 152.2 (CO), 153.5 (C^2 , Pyr), 154.9 (C^4OCH_3), 162.2 (d, $^1J_{\text{CF}}$ = 246.7 Hz, CF) ppm; MS (ESI, 70 eV) m/z 466 $[\text{MH}]^+$.

1-(4-(5-(4-Fluorophenyl)-2-(methylsulfinyl)-1H-imidazol-4-yl)pyridin-2-yl)-3-(*m*-tolyl)-carbamide (**12j**). Synthesis was performed according to the general procedure for sulfoxidation starting from **12d** (100 mg, 231 μmol) in 2 mL THF and 0.6 mL H_2O . Flash chromatography (SiO_2 , 20%–100% ethyl acetate/petrol ether) afforded **12j** as colorless solid. Yield 74.8 mg (72%); $\text{C}_{23}\text{H}_{20}\text{FN}_5\text{O}_2\text{S}$ (M_r 449.50); m.p. 235 $^\circ\text{C}$; $^1\text{H-NMR}$ ($\text{DMSO-}d_6$): δ = 2.29 (s, 3H, CH_3), 3.09 (s, 3H, SCH_3), 6.83 (d, 3J = 7.4 Hz, 1H, C^4H , Tol), 6.97 (dd, 3J = 5.4 Hz, 4J = 1.4 Hz, 1H, C^5H , Pyr), 7.18 (t, 3J = 7.7 Hz, 1H, C^5H , Tol), 7.29–7.35 (m, 4H, $\text{C}^{3/5}\text{H}$, F-Phe and $\text{C}^{2/6}\text{H}$, Tol), 7.52–7.57 (m, 2H, $\text{C}^{2/6}\text{H}$, F-Phe), 7.69 (s, 1H, C^3H , Pyr), 8.19 (d, 3J = 5.1 Hz, 1H, C^6H , Pyr), 9.48 (s, 1H, NH), 10.54 (bs, 1H, NH), 13.92 (bs, 1H, NH, Imdz) ppm; $^{13}\text{C-NMR}$ (75 MHz, $\text{DMSO-}d_6$): δ = 21.2 (CH_3), 39.1 (SCH_3), 109.3 (C^3H , Pyr), 115.3 (C^5H , Pyr), 115.9 (d, $^2J_{\text{CF}}$ = 21.5 Hz, $\text{C}^{3/5}\text{H}$, F-Phe), 116.0 (C^6H , Tol), 119.3 (C^2H , Tol), 123.2 (C^4H , Tol), 128.7 (C^5H , Tol), 130.9 ($\text{C}^{2/6}\text{H}$, F-Phe), 138.1 (C^3 , Tol), 138.9 (C^1 , Tol), 143.1 (C^4 , Pyr), 147.0 (C^6H , Pyr), 148.7 (C^2 , Imdz), 152.1 (CO), 153.4 (C^2 , Pyr), 162.2 (d, $^1J_{\text{CF}}$ = 244.0 Hz, CF) ppm; MS (ESI, 70 eV) m/z 450 $[\text{MH}]^+$.

1-(3-Chloro-4-methylphenyl)-3-(4-(5-(4-fluorophenyl)-2-(methylsulfinyl)-1H-imidazol-4-yl)pyridin-2-yl)-carbamide (**12k**). Synthesis was performed according to the general procedure for sulfoxidation starting from **12e** (100 mg, 214 μmol) in 4 mL THF and 1 mL H_2O . Flash chromatography (SiO_2 , 20%–100% ethyl acetate/petrol ether and RP-18, 50%–100% methanol/ H_2O) afforded **12k** as beige solid. Yield 78.0 mg (75%); $\text{C}_{23}\text{H}_{19}\text{ClFN}_5\text{O}_2\text{S}$ (M_r 483.95); $^1\text{H-NMR}$ ($\text{DMSO-}d_6$): δ = 2.27 (s, 3H, CH_3), 3.09 (s, 3H, SCH_3), 6.99 (dd, 3J = 5.4 Hz, 4J = 1.3 Hz, 1H, C^5H , Pyr), 7.26 (s, 1H, C^5H , Cl-Tol), 7.26 (s, 1H, C^6H , Cl-Tol), 7.29–7.35 (m, 2H, $\text{C}^{3/5}\text{H}$, F-Phe), 7.52–7.56 (m, 2H, $\text{C}^{2/6}\text{H}$, F-Phe), 7.65 (bs, 1H, C^3H , Pyr), 7.76 (bs, 1H, C^2H , Cl-Tol), 9.55 (s, 1H, NH), 10.77 (bs, 1H, NH), 13.93 (bs, 1H, NH, Imdz) ppm; $^{13}\text{C-NMR}$ ($\text{DMSO-}d_6$): δ = 18.8 (CH_3), 39.1 (SCH_3), 109.2 (C^3H , Pyr), 115.4 (C^5H , Pyr), 115.9 (d, $^2J_{\text{CF}}$ = 21.5 Hz, $\text{C}^{3/5}\text{H}$, F-Phe), 117.5 (C^6H , Cl-Tol), 118.7 (C^2H , Cl-Tol), 129.0 (C^4 , Cl-Tol), 131.1 ($\text{C}^{2/6}\text{H}$, F-Phe), 131.2 (C^5 , Imdz and C^5H , Cl-Tol), 133.2 (C^3 , Cl-Tol), 134.6 (C^4 , Imdz), 138.2 (C^1 , Cl-Tol), 147.0 (C^6H , Pyr), 148.7 (C^2 , Imdz), 152.1 (CO), 153.2 (C^2 , Pyr), 162.3 (d, $^1J_{\text{CF}}$ = 249.9 Hz, CF) ppm; MS (ESI, 70 eV) m/z 484 $[\text{MH}]^+$.

1-(4-(5-(4-Fluorophenyl)-2-(methylsulfinyl)-1H-imidazol-4-yl)pyridin-2-yl)-3-(3-(trifluoromethyl)phenyl)carbamide (**12l**). Synthesis was performed according to the general procedure for sulfoxidation starting from **12f** (20.0 mg, 41.0 μmol) in 0.4 mL THF and 0.1 mL water. Flash chromatography (SiO_2 , 40%–100% ethyl acetate/petrol ether) afforded **12l** as a colorless solid. Yield 15.1 mg (73%); m.p. 235 $^\circ\text{C}$; $^1\text{H-NMR}$ ($\text{DMSO-}d_6$): δ = 3.10 (s, 3H, SCH_3), 7.02 (dd, 3J = 5.4 Hz, 4J = 1.4 Hz, 1H, C^5H , Pyr), 7.30–7.37 (m, 2H, $\text{C}^{3/5}\text{H}$, F-Phe), 7.36 (d, 3J = 7.7 Hz, 1H, C^4H , $\text{F}_3\text{C-Phe}$), 7.51–7.57 (m, 3H, $\text{C}^{2/6}\text{H}$, F-Phe and C^5H , $\text{F}_3\text{C-Phe}$), 7.65 (d, 3J = 8.3 Hz, 1H, C^6H , $\text{F}_3\text{C-Phe}$), 7.71 (s, 1H, C^2H , $\text{F}_3\text{C-Phe}$), 8.08 (bs, 1H, C^3H , Pyr), 8.22 (bs, 1H, C^6H , Pyr), 9.59 (s, 1H, NH), 10.90 (bs, 1H, NH), 13.93 (bs, 1H, NH, Imdz) ppm; $^{13}\text{C-NMR}$ ($\text{DMSO-}d_6$): δ = 39.1 (SCH_3), 109.3 (C^2H , $\text{F}_3\text{C-Phe}$), 114.7 (q, $^3J_{\text{CF}}$ = 2.5 Hz, C^3H , Pyr), 115.5 (C^5H , Pyr), 115.9 (d, $^3J_{\text{CF}}$ = 21.9 Hz, $\text{C}^{3/5}\text{H}$, F-Phe), 118.7 (q, $^3J_{\text{CF}}$ = 2.1 Hz, C^4H , $\text{F}_3\text{C-Phe}$), 122.5 (C^6H , $\text{F}_3\text{C-Phe}$), 124.2 (q, $^1J_{\text{CF}}$ = 272.2 Hz, CF_3), 125.9 (d, $^4J_{\text{CF}}$ = 3.2 Hz, C^1 , F-Phe), 129.6 (q, $^2J_{\text{CF}}$ = 31.4 Hz, C^3 , $\text{F}_3\text{C-Phe}$), 130.0 (C^5H , $\text{F}_3\text{C-Phe}$), 130.8 (C^5 , Imdz), 131.1 (d, $^4J_{\text{CF}}$ = 11.4 Hz, $\text{C}^{2/6}\text{H}$, F-Phe), 134.5 (C^4 , Imdz), 139.9

(C¹, F₃C-Phe), 143.4 (C⁴, Pyr), 147.1 (C⁶H, Pyr), 148.7 (C², Imdz), 152.2 (CO), 162.4 (d, ¹J_{CF} = 242.12 Hz, CF) ppm; MS (ESI, 70 eV) *m/z* 504 [MH]⁺.

1-(4-(5-(4-Fluorophenyl)-2-(methylthio)-1H-imidazol-4-yl)pyridin-2-yl)-3-(naphthalen-1-yl)carbamide (**12m**). Synthesis was performed according to the general procedure for sulfoxidation starting from **12g** (51.0 mg, 109 μmol) in 5 mL THF and 1.5 mL H₂O. Flash chromatography (SiO₂, 20%–100% ethyl acetate/petrol ether) afforded **12m** as colorless solid. Yield 37.0 mg (70%); C₂₆H₂₀FN₅O₂S (M_r 485.54); m.p. 244 °C; ¹H-NMR (DMSO-*d*₆): δ = 3.10 (s, 3H, SCH₃), 7.04 (dd, ³J = 5.4 Hz, ⁴J = 1.4 Hz, 1H, C⁵H, Pyr), 7.31–7.36 (m, 2H, C^{3/5}H, F-Phe), 7.49 (t, ³J = 7.9 Hz, 1H, C³H, Naph), 7.54–7.59 (m, 4H, C³H, Pyr and C^{2/6}H, F-Phe and C⁶H, Naph), 7.63–7.68 (m, 2H, C^{4/7}H, Naph), 7.96 (dd, ³J = 8.1 Hz, ⁴J = 0.8 Hz, 1H, C⁵H, Naph), 8.16–8.20 (m, 2H, C^{2/8}H, Naph), 8.34 (d, ³J = 5.4 Hz, 1H, C⁶H, Pyr), 8.93 (s, 1H, NH), 11.58 (bs, 1H, NH), 13.95 (bs, 1H, NH, Imdz) ppm; ¹³C-NMR (DMSO-*d*₆): δ = 39.1 (SCH₃), 109.4 (C³H, Pyr), 115.3 (C⁵H, Pyr), 115.9 (d, ²J_{CF} = 21.8 Hz, C^{3/5}H, F-Phe), 116.9 (C²H, Naph), 120.9 (C⁸H, Naph), 123.1 (C⁴H, Naph), 125.5 (C¹, Naph), 126.0 (C⁶H, Naph), 126.0 (C³H, Naph), 126.3 (C⁷H, Naph), 128.6 (C⁵H, Naph), 130.7 (C⁵, Imdz), 130.9 (C^{2/6}H, F-Phe), 133.7 (C^{4a}, Naph), 134.1 (C^{8a}, Naph), 143.5 (C⁴, Pyr), 146.7 (C⁶H, Pyr), 148.9 (C², Imdz), 152.6 (CO), 153.6 (C², Pyr), 162.3 (d, ¹J_{CF} = 246.9 Hz, CF) ppm; MS (ESI, 70 eV) *m/z* 486 [MH]⁺.

4-(2,4-Dimethoxyphenyl)-N-(4-(5-(4-fluorophenyl)-2-(methylsulfinyl)-1H-imidazol-4-yl)-pyridin-2-yl)-1-methyl-1H-pyrrol-2-carboxamide (**16c**). Synthesis was performed according to the general procedure for sulfoxidation starting from **16a** (196 mg, 368 μmol) in 4 mL THF and 1 mL H₂O. Flash chromatography (SiO₂, 40%–100% ethyl acetate/petrol ether) afforded **16c** as yellow solid. Yield 182 mg (88%); C₂₉H₂₆FN₅O₄S (M_r 559.62); m.p. 136 °C; ¹H-NMR (DMSO-*d*₆): δ = 3.11 (s, 3H, SCH₃), 3.78 (s, 3H, C²OCH₃), 3.86 (s, 3H, C⁴OCH₃), 3.90 (s, 3H, CH₃), 6.57 (dd, ³J = 8.5 Hz, ⁴J = 2.4 Hz, 1H, C⁵H, (OCH₃)₂-Phe), 6.61 (d, ⁴J = 2.3 Hz, 1H, C³H, (OCH₃)₂-Phe), 7.07 (d, ³J = 4.8 Hz, 1H, C⁵H, Pyr), 7.23–7.38 (m, 2H, C^{3/5}H, F-Phe), 7.42 (bs, 1H, C³H, Pyrrole), 7.46 (d, ³J = 8.4 Hz, 1H, C⁶H, (OCH₃)₂-Phe), 7.54–7.59 (m, 2H, C^{2/6}H, F-Phe), 7.68 (bs, 1H, C⁵H, Pyrrole), 8.22 (d, ³J = 4.5 Hz, 1H, C⁶H, Pyr), 8.42 (s, 1H, C³H, Pyr), 10.17 (s, 1H, CONH), 13.89 (s, 1H, NH) ppm; ¹³C-NMR (DMSO-*d*₆): δ = 36.6 (CH₃), 39.2 (SCH₃), 55.2 (C²OCH₃), 55.4 (C⁴OCH₃), 98.8 (C³H, (OCH₃)₂-Phe), 105.2 (C⁵H, (OCH₃)₂-Phe), 111.8 (C³H, Pyr), 113.3 (C⁵H, Pyrrole), 115.9 (C¹, (OCH₃)₂-Phe), 116.0 (d, ²J_{CF} = 22.4 Hz, C^{3/5}H, F-Phe), 116.1 (C⁵H, Pyr), 118.5 (C⁴, Pyrrole), 124.0 (C², Pyrrole), 125.8 (d, ⁴J_{CF} = 3.3 Hz, C¹, F-Phe), 127.5 (C⁶H, (OCH₃)₂-Phe), 128.6 (C³H, Pyrrole), 131.3 (d, ³J_{CF} = 8.3 Hz, C^{2/6}H, F-Phe), 131.9 (C⁴, Imdz), 135.1 (C⁵, Imdz), 143.0 (C⁴, Pyr), 147.8 (C⁶H, Pyr), 148.5 (C², Imdz), 152.9 (C², Pyr), 156.7 (C⁴OCH₃), 158.6 (C²OCH₃), 159.9 (CO), 162.4 (d, ¹J_{CF} = 244.3 Hz, CF) ppm; MS (ESI, 70 eV) *m/z* 560 [MH]⁺.

3.3. Kinase Assays and IC₅₀ Determination

In vitro kinase assays using 2 μCi 32P-γ-ATP per reaction as co-factor were carried out in kinase buffer containing 25 mM Tris-HCl [pH 7.5], 10 mM MgCl₂, 100 μM EDTA, and 10 μM ATP. Potential inhibitor compounds were used in a dilution series ranging from 10 μM to 5 nM final reaction concentration which was prepared by serial dilution in DMSO. Recombinant human CK1δ transcription variant 1 (expressed and purified as GST fusion protein as described earlier [60]) and human GST-CK1ε (Invitrogen) were used as sources of enzyme while α-casein (C6780; Sigma-Aldrich) was used as substrate. Kinase reactions were incubated for 30 min at 30 °C. Subsequently, reactions were separated by SDS-PAGE and phosphorylated protein bands were visualized on dried gels by autoradiography. The phosphorylated substrate protein bands were excised and phosphorylation was quantified by Cherenkov counting. Dose-response analyses and calculation of IC₅₀ values were carried out using GraphPad Prism 6 statistical software (San Diego, CA, USA).

3.4. Cell Culture

3.4.1. Cell Lines

The human pancreatic cancer cell lines Colo357 [61], Panc-1 [62], and MiaPaCa-2 [63] were grown in Dulbecco's modified Eagle's medium (DMEM). Panc89 [64] was grown in DMEM:RPMI-1640 medium in ratio 1:1. The human colon adenocarcinoma cell line HT-29 [65] was grown in McCoy's 5A medium. All media were supplemented with 10% fetal calf serum (FCS), 100 units·mL⁻¹ penicillin, 100 µg·mL⁻¹ streptomycin and 2 mM glutamine. All cells were grown at 37 °C in a humidified 5% carbon dioxide atmosphere.

3.4.2. Cell Assays and EC₅₀ Determination

In order to determine the cytotoxic effects of investigated inhibitors conventional MTT assay were used. 1×10^4 cells·well⁻¹ were seeded in 96-well cell culture plates and cultivated for 24 h. Cell lines were exposed to increasing concentrations of the indicated inhibitor compounds, with untreated and DMSO-treated cells serving as control. After an incubation period of 48 h 10 µL of MTT solution (5 mg·mL⁻¹ in PBS) were added and cells were incubated for 4 h. MTT-containing medium was carefully removed and 100 µL acidic isopropanol (0.04 N HCl in isopropanol) per well were added. For dissolution of formazan crystals plates were shaken for 30 min on an orbital shaker in the dark. Finally, dissolved crystals were measured spectrophotometrically at 570 nm. All experiments were performed in triplicate with four technical replicates per assay. Results were normalized considering the mean optical density value of control wells as 100%. GraphPad Prism 6 (La Jolla, CA, USA) software was used to calculate EC₅₀ values.

3.5. X-ray Crystallography

3.5.1. Protein Expression, Purification, and Crystallisation of CK1δ

BL21 (DE3) TaKaRa 2 cells (Clontech) were transformed with the plasmid pET28a-tCK1δ which contains a codon-optimized construct of CK1δ spanning residues 1–294 in a pET28a vector (NdeI and XhoI restriction sites) and streaked out on LB agar plates containing 50 µg·mL⁻¹ kanamycin and 20 µg·mL⁻¹ chloramphenicol as selective antibiotics. A pre-culture was prepared by inoculating cells from a single colony in LB medium supplemented with selective antibiotics and 4 mg·mL⁻¹ L-arabinose and overnight cultivation at 37 °C. Expression cultures were prepared by diluting a fresh pre-culture with LB medium (plus selective antibiotics and 4 mg·mL⁻¹ L-arabinose) to an optical density of 0.1 at 600 nm (OD600). Expression cultures were cultivated at 37 °C until an OD600 of 0.6 was reached, then cultivation temperature was reduced to 20 °C and tCK1δ expression was induced by adding 0.5 mM IPTG (isopropyl-β-D-1-thiogalactopyranoside). 16 h after IPTG addition, cells were harvested by centrifugation (4000× g, 20 min 4 °C), washed with TBS (20 mM Tris pH 7.5, 300 mM NaCl), and stored at –80 °C until purification.

Cells were thawed and resuspended (4 mL·g⁻¹ wet cell pellet) in TBS plus 0.5 mM TCEP and subsequently lysed on ice by sonication (Vibra-Cell VCX500, Sonics, Newtown, CT, USA). The resultant lysate was clarified by ultracentrifugation (165,000× g at 4 °C for 30 min) and supplemented with 5 mM imidazole pH 7.5 before loading it on 2 mL TALON® (Clontech Takara Bio Europe SAS, Saint-Germain-en-Laye, France) resin. After a wash step with TBS containing 10 mM imidazole, tCK1δ was eluted with TBS and 120 mM imidazole, concentrated, and applied to a Superdex S200 16/600 size exclusion chromatography column using TBS as chromatography buffer. Fractions containing monomeric tCK1δ were pooled and concentrated to 10 mg/mL and stored at –80 °C.

For co-crystallization of tCK1δ with **16b**, protein stock solution (10 mg·mL⁻¹) was mixed 30:1 with 10 mM **16b** (solubilized in DMSO) and incubated for 30 min at room temperature. Sitting drop crystallization trials were set up at 4 °C with drop ratios of 3 µL protein/inhibitor solution to 2 µL precipitant solution. Crystals appeared after three to four days in drops containing 0.1 M Hepes pH

7.0, 0.7 M NaH₂PO₄, and 0.7 M KH₂PO₄. For data collection, these crystals were cryo-protected by swiping them through reservoir solution supplemented with sucrose (60% saturation) and 0.3 mM **16b** and subsequently flash frozen.

Diffraction data was collected at beamLine X06DA at the Swiss Light Source, Paul-Scherrer-Institute, Villigen, Switzerland and processed using XDS [66]. The structure was solved by molecular replacement using the program PHASER [67] with a truncated crystal structure of CK1δ (pdb 4TWC [25]) as search model. Between iterative cycles of refinement using phenix.refine [68] missing loops as well as **16b** were manually built with Coot [69]. Restraints of **16b** were calculated using phenix.elbow [70].

3.5.2. Protein Expression, Purification, and Crystallization of p38α MAPK

The expression and purification of inactive, non-phosphorylated p38α wt MAPK was done as previously reported [71]. Briefly, an N-terminal His₆-p38α wt construct was transformed into *E. coli* BL21 (DE3) and expressed overnight at 18 °C. The protein was purified by Ni²⁺-NTA-affinity chromatography, followed by anion exchange and size exclusion chromatography after removal of the His-tag by proteolytic cleavage. The pure protein was subsequently concentrated to 10–30 mg·mL⁻¹, aliquoted, flash frozen in liquid N₂, and stored at –80 °C.

11b was co-crystallized with p38α wt using conditions similar to those as described previously [72]. Briefly, protein-ligand complexes were prepared by mixing 20 μL p38α wt (10 mg·mL⁻¹) with 0.2 μL compound (50 mM in DMSO) that were subsequently incubated for 60 min on ice. The samples were centrifuged at 13,000 rpm for 10 min to remove excess ligand. Crystals were grown in 24-well crystallisation plates (EasyXtal Tool, Qiagen, Hilden, Germany) using the hanging drop vapor diffusion method and by mixing 1.5 μL protein-ligand solution with 0.5 μL reservoir (100 mM MES pH 5.6–6.2, 20%–30% PEG4000 and 50 mM β-gluco-D-pyranoside). The crystals were protected using 25% PEG400 before they were flash frozen in liquid N₂. Diffraction data of the p38α-ligand complexes were collected at the PX II beam line of the Swiss Light Source (Paul-Scherrer-Institute, Villigen, Switzerland) using wavelengths close to 1 Å. The datasets were integrated with XDS and scaled using XSCALE [73]. The complex structures were solved by molecular replacement with PHASER [67] using the published p38α structure (pdb 4DLI [74]) as template. Molecules in the asymmetric unit were manually modified using the program COOT [75]. The final refinement was performed with REFMAC [76]. Inhibitor topology files were generated using the Dundee PRODRG server [77]. Refined structures were validated by Ramachandran plot analysis with RAMPAGE [78]. Data collection, structure refinement statistics, and the Ramachandran plot results are shown in Supplementary Table S6.

4. Conclusions

Deriving from hit compounds **1** and **2** we report on design and synthesis of novel sets of highly potent and specific ATP-competitive inhibitors of CK1δ thereby confirming modeled binding modes by X-ray analysis in CK1δ and also in comparison to p38α. Especially **11b** (CK1δ IC₅₀ ≤ 3–4 nM, CK1ε IC₅₀ = 25 nM, p38α IC₅₀ = 10 nM) has been identified as promising agent with IC₅₀ values in the single-digit nanomolar range and is therefore among the most potent inhibitors of CK1δ reported so far. Interestingly, X-ray analysis of ligand-protein complexes demonstrated a binding mode for **11b** deviating from typical type I within the active site of p38α, thereby stabilizing the kinase in an intermediate conformation between DFG-in and DFG-out (*DFG-in-between*). CK1δ, however, is addressed by conventional type I inhibition in a DFG-in conformation as confirmed by co-crystallization with **16b**. In addition, at 100 nM **11b** is rather selective for CK1δ/ε hitting only six off-targets from a panel of 321 protein kinases, among them p38α. Compound **11b** further exhibited single-digit micromolar efficacy in MTT viability assays in pancreatic Colo357 and Panc89 carcinoma cell lines. Protein kinase CK1δ, however, executes diverse physiological and pathophysiological functions and specific inhibitors might therefore strongly depend on tissue and

cellular background [2,19,28,79]. Consequently, additional experiments using cellular systems as well as optimization of physicochemical properties might prove beneficial. Nevertheless, the implied hit structure has to be considered inept in order to achieve complete CK1 isoform selectivity regarding CK1 δ and CK1 ϵ , although moderate discrimination of CK1 α and significant selectivity against CK1 γ 1-3 have been successfully achieved. Based on the current results, additional optimization cycles might therefore focus on decreased fitting into the active site of p38 α . Reducing the acrylamide moiety of **1** proved beneficial as the obtained propionic amide **11b** does not show a *Michael* acceptor moiety. All synthesized inhibitors were stable in DMSO solution at room temperature over a period of 72 h. In fact, the compound is among the most potent and stable inhibitors of CK1 δ published to date with good selectivity regarding a screen comprising 321 protein kinases and suitable efficacy in different human cancer cell lines. Fortunately, sulfoxidation, which is believed to be the predominant metabolic pathway of this inhibitor class [44], did not abrogate activity. Co-crystallization of compounds with CK1 δ and related p38 α confirmed our postulated binding modes within these kinases. Taken together, small molecule kinase inhibitor **11b** can be suggested for the use as a pharmacological tool to further investigate the significance of CK1 δ in signaling pathways, especially linked to proliferative and neurodegenerative diseases.

Supplementary Materials: Supplementary materials are available online.

Acknowledgments: We gratefully acknowledge the help of Dieter Schollmeyer, University of Mainz, Institute for Organic Chemistry, Germany, for X-ray analysis of compound **11b**. Chiara Ianes is financially supported by a grant of the medical faculty of Ulm University (“Bausteinprogramm”) awarded to Joachim Bischof. We acknowledge financial support by Land Schleswig-Holstein within the funding program Open Access Publikationsfonds.

Author Contributions: J.H., L.W., C.I., M.K., M.B., D.R., C.P., E.B., A.L., U.B., U.K., J.B. and C.P. conceived and designed the experiments; J.H. and L.W. performed synthesis; C.I. and M.K. performed the biological evaluation in vitro; M.B., C.P. and E.B. performed crystallization experiments. J.H. and C.I. analyzed the data; J.H. wrote the paper.

Conflicts of Interest: The authors declare no competing financial interest.

Abbreviations

The following abbreviations are used in this manuscript:

AD	Alzheimer’s disease
ALS	amyotrophic lateral sclerosis
ATP	adenosine triphosphate
B-Raf	rapidly accelerated fibrosarcoma B
Boc	<i>tert</i> -butyloxycarbonyl
CDI	<i>N,N'</i> -carbonyldiimidazole
CK1	protein kinase CK1, formerly known as casein kinase 1
DCM	dichloromethane
DFG-in/out	sequence motif of aspartic acid (D), phenylalanine (F), and glycine (G) within the activation loop of the kinase domain
DIPEA	<i>N,N</i> -diisopropylethylamine
DMEM	Dulbecco’s modified Eagle’s medium
DMF	<i>N,N</i> -dimethylformamide
DMSO	dimethyl sulfoxide
EDTA	ethylenediaminetetraacetic acid
FASPS	familial advanced sleep phase syndrome
FCS	fetal calf serum
GST	glutathione S-transferase
HPI	hydrophobic pocket I
HRII	hydrophobic region II
JNK	c-Jun N-terminal kinase
LB	lysogeny broth

LCK	lymphocyte-specific protein tyrosine kinase
MAPK	mitogen-activated protein kinase
MTT	3-(4,5-dimethylthiazol-2-yl)-2,5-diphenyltetrazolium bromide
NaHMDS	sodium bis(trimethylsilyl)amide
NBS	N-bromosuccinimide
NTA	nitrilotriacetic acid
PBS	phosphate-buffered saline
Pd/C	palladium on activated charcoal
pdb	Research Collaboratory for Structural Bioinformatics (RCSB) protein data bank
PEG	polyethylene glycol
PPh ₃	triphenylphosphine
PyBOP	(Benzotriazol-1-yloxy)tripyrrolidinophosphonium hexafluorophosphate
rt	room temperature
RIPK	receptor-interacting Ser/Thr-protein kinase
RPMI	Roswell Park Memorial Institute medium
SAR	structure-activity relationship
SDS-PAGE	sodium dodecyl sulfate polyacrylamide gel electrophoresis
TBS	Tris-buffered saline
TCEP	tris(2-carboxyethyl)phosphine
THF	tetrahydrofuran
Tris	tris(hydroxymethyl)aminomethane
TTBK	tau tubulin kinase
VRK	vaccinia-related kinase

References

- Venerando, A.; Ruzzene, M.; Pinna, L.A. Casein kinase: The triple meaning of a misnomer. *Biochem. J.* **2014**, *460*, 141–156. [[CrossRef](#)] [[PubMed](#)]
- Knippschild, U.; Kruger, M.; Richter, J.; Xu, P.; Garcia-Reyes, B.; Peifer, C.; Halekotte, J.; Bakulev, V.; Bischof, J. The CK1 Family: Contribution to Cellular Stress Response and Its Role in Carcinogenesis. *Front. Oncol.* **2014**, *4*, 96. [[CrossRef](#)] [[PubMed](#)]
- Gross, S.D.; Anderson, R.A. Casein Kinase I: Spatial Organization and Positioning of a Multifunctional Protein Kinase Family. *Cell. Signal.* **1998**, *10*, 699–711. [[CrossRef](#)]
- Knippschild, U.; Wolff, S.; Giamas, G.; Brockschmidt, C.; Wittau, M.; Wurl, P.U.; Eismann, T.; Stoter, M. The role of the casein kinase 1 (CK1) family in different signaling pathways linked to cancer development. *Onkologie* **2005**, *28*, 508–514. [[CrossRef](#)] [[PubMed](#)]
- Knippschild, U.; Gocht, A.; Wolff, S.; Huber, N.; Lohler, J.; Stoter, M. The casein kinase 1 family: Participation in multiple cellular processes in eukaryotes. *Cell. Signal.* **2005**, *17*, 675–689. [[CrossRef](#)] [[PubMed](#)]
- Li, G.; Yin, H.; Kuret, J. Casein kinase 1 δ phosphorylates tau and disrupts its binding to microtubules. *J. Biol. Chem.* **2004**, *279*, 15938–15945. [[CrossRef](#)] [[PubMed](#)]
- Ghoshal, N.; Smiley, J.F.; DeMaggio, A.J.; Hoekstra, M.F.; Cochran, E.J.; Binder, L.I.; Kuret, J. A New Molecular Link between the Fibrillar and Granulovacuolar Lesions of Alzheimer's Disease. *Am. J. Pathol.* **1999**, *155*, 1163–1172. [[CrossRef](#)]
- Yasojima, K.; Kuret, J.; DeMaggio, A.J.; McGeer, E.; McGeer, P.L. Casein kinase 1 δ mRNA is upregulated in Alzheimer disease brain. *Brain Res.* **2000**, *865*, 116–120. [[CrossRef](#)]
- Salado, I.G.; Redondo, M.; Bello, M.L.; Perez, C.; Liachko, N.F.; Kraemer, B.C.; Miguel, L.; Lecourtois, M.; Gil, C.; Martinez, A.; et al. Protein kinase CK-1 inhibitors as new potential drugs for amyotrophic lateral sclerosis. *J. Med. Chem.* **2014**, *57*, 2755–2772. [[CrossRef](#)] [[PubMed](#)]
- Xu, Y.; Padiath, Q.S.; Shapiro, R.E.; Jones, C.R.; Wu, S.C.; Saigoh, N.; Saigoh, K.; Ptacek, L.J.; Fu, Y.-H. Functional consequences of a CK1 δ mutation causing familial advanced sleep phase syndrome. *Nature* **2005**, *434*, 640–644. [[CrossRef](#)] [[PubMed](#)]
- Tsai, I.-C.; Woolf, M.; Neklason, D.W.; Branford, W.W.; Yost, H.J.; Burt, R.W.; Virshup, D.M. Disease-associated casein kinase I δ mutation may promote adenomatous polyps formation via a Wnt/ β -catenin independent mechanism. *Int. J. Cancer* **2007**, *120*, 1005–1012. [[CrossRef](#)] [[PubMed](#)]

12. Richter, J.; Ullah, K.; Xu, P.; Alscher, V.; Blatz, A.; Peifer, C.; Halekotte, J.; Leban, J.; Vitt, D.; Holzmann, K.; et al. Effects of altered expression and activity levels of CK1 δ and varepsilon on tumor growth and survival of colorectal cancer patients. *Int. J. Cancer* **2015**, *136*, 2799–2810. [[CrossRef](#)] [[PubMed](#)]
13. Kumar, A.; Rajendran, V.; Sethumadhavan, R.; Purohit, R. Relationship between a point mutation S97C in CK1 δ protein and its affect on ATP-binding affinity. *J. Biomol. Struct. Dyn.* **2013**, *32*, 394–405. [[CrossRef](#)] [[PubMed](#)]
14. Schitteck, B.; Sinnberg, T. Biological functions of casein kinase 1 isoforms and putative roles in tumorigenesis. *Mol. Cancer* **2014**, *13*, 231. [[CrossRef](#)] [[PubMed](#)]
15. Richter, J.; Rudeck, S.; Kretz, A.-L.; Kramer, K.; Just, S.; Henne-Bruns, D.; Hillenbrand, A.; Leithäuser, F.; Lemke, J.; Knippschild, U. Decreased CK1 δ expression predicts prolonged survival in colorectal cancer patients. *Tumor Biol.* **2016**, *37*, 8731–8739. [[CrossRef](#)] [[PubMed](#)]
16. Brockschmidt, C.; Hirner, H.; Huber, N.; Eismann, T.; Hillenbrand, A.; Giamas, G.; Radunsky, B.; Ammerpohl, O.; Bohm, B.; Henne-Bruns, D.; et al. Anti-apoptotic and growth-stimulatory functions of CK1 δ and epsilon in ductal adenocarcinoma of the pancreas are inhibited by IC261 in vitro and in vivo. *Gut* **2008**, *57*, 799–806. [[CrossRef](#)] [[PubMed](#)]
17. Winkler, B.S.; Oltmer, F.; Richter, J.; Bischof, J.; Xu, P.; Burster, T.; Leithäuser, F.; Knippschild, U. CK1 δ in lymphoma: Gene expression and mutation analyses and validation of CK1 δ kinase activity for therapeutic application. *Front. Cell Dev. Biol.* **2015**, *3*, 9. [[CrossRef](#)] [[PubMed](#)]
18. Rosenberg, L.H.; Lafitte, M.; Quereda, V.; Grant, W.; Chen, W.; Bibian, M.; Noguchi, Y.; Fallahi, M.; Yang, C.; Chang, J.C.; et al. Therapeutic targeting of casein kinase 1 δ in breast cancer. *Sci. Transl. Med.* **2015**, *7*, 318ra202. [[CrossRef](#)] [[PubMed](#)]
19. Stöter, M.; Bamberger, A.-M.; Aslan, B.; Kurth, M.; Speidel, D.; Löning, T.; Frank, H.-G.; Kaufmann, P.; Löhler, J.; Henne-Bruns, D.; et al. Inhibition of casein kinase I δ alters mitotic spindle formation and induces apoptosis in trophoblast cells. *Oncogene* **2005**, *24*, 7964–7975. [[CrossRef](#)] [[PubMed](#)]
20. Cozza, G.; Pinna, L.A. Casein kinases as potential therapeutic targets. *Expert Opin. Ther. Targets* **2015**, *20*, 319–340. [[CrossRef](#)] [[PubMed](#)]
21. Mashhoon, N.; DeMaggio, A.J.; Tereshko, V.; Bergmeier, S.C.; Egli, M.; Hoekstra, M.F.; Kuret, J. Crystal Structure of a Conformation-selective Casein Kinase-1 Inhibitor. *J. Biol. Chem.* **2000**, *275*, 20052–20060. [[CrossRef](#)] [[PubMed](#)]
22. Cheong, J.K.; Hung, N.T.; Wang, H.; Tan, P.; Voorhoeve, P.M.; Lee, S.H.; Virshup, D.M. IC261 induces cell cycle arrest and apoptosis of human cancer cells via CK1 δ/ϵ and Wnt/ β -catenin independent inhibition of mitotic spindle formation. *Oncogene* **2011**, *30*, 2558–2569. [[CrossRef](#)] [[PubMed](#)]
23. Kruger, M.; Kalbacher, H.; Kastritis, P.L.; Bischof, J.; Barth, H.; Henne-Bruns, D.; Vorgias, C.; Sarno, S.; Pinna, L.A.; Knippschild, U. New potential peptide therapeutics perturbing CK1 δ/α -tubulin interaction. *Cancer Lett.* **2016**, *375*, 375–383. [[CrossRef](#)] [[PubMed](#)]
24. Föhr, K.J.; Knippschild, U.; Herkommer, A.; Fauler, M.; Peifer, C.; Georgieff, M.; Adolph, O. State-dependent block of voltage-gated sodium channels by the casein-kinase 1 inhibitor IC261. *Investig. New Drugs* **2017**. [[CrossRef](#)] [[PubMed](#)]
25. Bischof, J.; Leban, J.; Zaja, M.; Grothey, A.; Radunsky, B.; Othersen, O.; Strobl, S.; Vitt, D.; Knippschild, U. 2-Benzamido-N-(1H-benzo[d]imidazol-2-yl)thiazole-4-carboxamide derivatives as potent inhibitors of CK1 δ/ϵ . *Amino Acids* **2012**, *43*, 1577–1591. [[CrossRef](#)] [[PubMed](#)]
26. Richter, J.; Bischof, J.; Zaja, M.; Kohlhof, H.; Othersen, O.; Vitt, D.; Alscher, V.; Pospiech, I.; Garcia-Reyes, B.; Berg, S.; et al. Difluoro-dioxolo-benzoimidazol-benzamides as potent inhibitors of CK1 δ and epsilon with nanomolar inhibitory activity on cancer cell proliferation. *J. Med. Chem.* **2014**, *57*, 7933–7946. [[CrossRef](#)] [[PubMed](#)]
27. Fischer, S.; Koeberle, S.C.; Laufer, S.A. p38 α mitogen-activated protein kinase inhibitors, a patent review (2005–2011). *Expert Opin. Ther. Pat.* **2011**, *21*, 1843–1866. [[CrossRef](#)] [[PubMed](#)]
28. Peifer, C.; Abadleh, M.; Bischof, J.; Hauser, D.; Schattel, V.; Hirner, H.; Knippschild, U.; Laufer, S. 3,4-Diaryl-isoxazoles and -imidazoles as Potent Dual Inhibitors of p38 α Mitogen Activated Protein Kinase and Casein Kinase 1 δ . *J. Med. Chem.* **2009**, *52*, 7618–7630. [[CrossRef](#)] [[PubMed](#)]
29. Bissantz, C.; Kuhn, B.; Stahl, M. A Medicinal Chemist's Guide to Molecular Interactions. *J. Med. Chem.* **2010**, *53*, 5061–5084. [[CrossRef](#)] [[PubMed](#)]

30. Ferreira, L.; Dos Santos, R.; Oliva, G.; Andricopulo, A. Molecular Docking and Structure-Based Drug Design Strategies. *Molecules* **2015**, *20*, 13384–13421. [[CrossRef](#)] [[PubMed](#)]
31. Long, A.; Zhao, H.; Huang, X. Structural Basis for the Interaction between Casein Kinase 1 δ and a Potent and Selective Inhibitor. *J. Med. Chem.* **2012**, *55*, 956–960. [[CrossRef](#)] [[PubMed](#)]
32. Laufer, S.A.; Hauser, D.R.J.; Domeyer, D.M.; Kinkel, K.; Liedtke, A.J. Design, Synthesis, and Biological Evaluation of Novel Tri- and Tetrasubstituted Imidazoles as Highly Potent and Specific ATP-Mimetic Inhibitors of p38 MAP Kinase: Focus on Optimized Interactions with the Enzyme's Surface-Exposed Front Region. *J. Med. Chem.* **2008**, *51*, 4122–4149. [[CrossRef](#)] [[PubMed](#)]
33. Wang, Z.; Canagarajah, B.J.; Boehm, J.C.; Kassisa, S.; Cobb, M.H.; Young, P.R.; Abdel-Meguid, S.; Adams, J.L.; Goldsmith, E.J. Structural basis of inhibitor selectivity in MAP kinases. *Structure* **1998**, *6*, 1117–1128. [[CrossRef](#)]
34. Traxler, P.; Furet, P. Strategies toward the Design of Novel and Selective Protein Tyrosine Kinase Inhibitors. *Pharmacol. Ther.* **1999**, *82*, 195–206. [[CrossRef](#)]
35. Mente, S.; Arnold, E.; Butler, T.; Chakrapani, S.; Chandrasekaran, R.; Cherry, K.; DiRico, K.; Doran, A.; Fisher, K.; Galatsis, P.; et al. Ligand–Protein Interactions of Selective Casein Kinase 1 δ Inhibitors. *J. Med. Chem.* **2013**, *56*, 6819–6828. [[CrossRef](#)] [[PubMed](#)]
36. Peifer, C.; Kinkel, K.; Abadleh, M.; Schollmeyer, D.; Laufer, S. From five- to six-membered rings: 3,4-diarylquinolinone as lead for novel p38MAP kinase inhibitors. *J. Med. Chem.* **2007**, *50*, 1213–1221. [[CrossRef](#)] [[PubMed](#)]
37. Thompson, J.E.; Cubbon, R.M.; Cummings, R.T.; Wicker, L.S.; Frankshun, R.; Cunningham, B.R.; Cameron, P.M.; Meinke, P.T.; Liverton, N.; Weng, Y.; et al. Photochemical Preparation of a Pyridone Containing Tetracycle: A Jak Protein Kinase Inhibitor. *Bioorg. Med. Chem. Lett.* **2002**, *12*, 1219–1223. [[CrossRef](#)]
38. Laufer, S.A.; Liedtke, A.J. A concise and optimized four-step approach toward 2-(aryl)-alkylsulfanyl-, 4(5)-aryl-, 5(4)-heteroaryl-substituted imidazoles using alkyl- or arylalkyl thiocyanates. *Tetrahedron Lett.* **2006**, *47*, 7199–7203. [[CrossRef](#)]
39. Lal, K.; Ghosh, S.; Salomon, R.G. Hydroxyl-Directed Regioselective Monodemethylation of Polymethoxyarenes. *J. Org. Chem.* **1987**, *52*, 1072–1078. [[CrossRef](#)]
40. Kiuchi, M.; Marukawa, K.; Hamada, M.; Sugahara, K. Amine Compound and Pharmaceutical Use Thereof. Patent WO2008153159 A1, 18 December 2008.
41. Engen, W.; O'Brien, T.E.; Kelly, B.; Do, J.; Rillera, L.; Stapleton, L.K.; Youngren, J.F.; Anderson, M.O. Synthesis of Aryl-Heteroaryl Ureas (AHUs) Based on 4-Aminoquinoline and Their Evaluation Against the Insulin-Like Growth Factor Receptor (IGF-1R). *Bioorg. Med. Chem.* **2010**, *18*, 5995–6005. [[CrossRef](#)] [[PubMed](#)]
42. Handy, S.T.; Zhang, Y.; Bregman, H. A Modular Synthesis of the Lamellarins: Total Synthesis of Lamellarin G Trimethyl Ether. *J. Org. Chem.* **2004**, *69*, 2362–2366. [[CrossRef](#)] [[PubMed](#)]
43. Buhler, S.; Goettert, M.; Schollmeyer, D.; Albrecht, W.; Laufer, S.A. Chiral sulfoxides as metabolites of 2-thioimidazole-based p38 α mitogen-activated protein kinase inhibitors: Enantioselective synthesis and biological evaluation. *J. Med. Chem.* **2011**, *54*, 3283–3297. [[CrossRef](#)] [[PubMed](#)]
44. Ziegler, K.; Hauser, D.R.J.; Unger, A.; Albrecht, W.; Laufer, S.A. 2-Acylaminopyridin-4-ylimidazoles as p38 MAP Kinase Inhibitors: Design, Synthesis, and Biological and Metabolic Evaluations. *ChemMedChem* **2009**, *4*, 1939–1948. [[CrossRef](#)] [[PubMed](#)]
45. Kornev, A.P.; Taylor, S.S.; Eyck, L.F.; Ten Eyck, L.F. A helix scaffold for the assembly of active protein kinases. *Proc. Natl. Acad. Sci. USA* **2008**, *105*, 14377–14382. [[CrossRef](#)] [[PubMed](#)]
46. Meharena, H.S.; Chang, P.; Keshwani, M.M.; Oruganty, K.; Nene, A.K.; Kannan, N.; Taylor, S.S.; Kornev, A.P. Deciphering the structural basis of eukaryotic protein kinase regulation. *PLoS Biol.* **2013**, *11*, e1001680. [[CrossRef](#)] [[PubMed](#)]
47. Bukhtiyarova, M.; Karpusas, M.; Northrop, K.; Namboodiri, H.V.M.; Springman, E.B. Mutagenesis of p38 α MAP kinase establishes key roles of Phe169 in function and structural dynamics and reveals a novel DFG-OUT state. *Biochemistry* **2007**, *46*, 5687–5696. [[CrossRef](#)] [[PubMed](#)]
48. Simard, J.R.; Grutter, C.; Pawar, V.; Aust, B.; Wolf, A.; Rabiller, M.; Wulfert, S.; Robubi, A.; Kluter, S.; Ottmann, C.; et al. High-throughput screening to identify inhibitors which stabilize inactive kinase conformations in p38 α . *J. Am. Chem. Soc.* **2009**, *131*, 18478–18488. [[CrossRef](#)] [[PubMed](#)]

49. Fischer, S.; Wentsch, H.K.; Mayer-Wrangowski, S.C.; Zimmermann, M.; Bauer, S.M.; Storch, K.; Niess, R.; Koeberle, S.C.; Grütter, C.; Boeckler, F.M.; et al. Dibenzosuberones as p38 Mitogen-Activated Protein Kinase Inhibitors with Low ATP Competitiveness and Outstanding Whole Blood Activity. *J. Med. Chem.* **2013**, *56*, 241–253. [[CrossRef](#)] [[PubMed](#)]
50. Fabbro, D. 25 years of small molecular weight kinase inhibitors: Potentials and limitations. *Mol. Pharmacol.* **2015**, *87*, 766–775. [[CrossRef](#)] [[PubMed](#)]
51. Laufer, S.; Hauser, D.; Stegmiller, T.; Bracht, C.; Ruff, K.; Schattel, V.; Albrecht, W.; Koch, P. Tri- and tetrasubstituted imidazoles as p38 α mitogen-activated protein kinase inhibitors. *Bioorg. Med. Chem. Lett.* **2010**, *20*, 6671–6675. [[CrossRef](#)] [[PubMed](#)]
52. Gill, A.L.; Frederickson, M.; Cleasby, A.; Woodhead, S.J.; Carr, M.G.; Woodhead, A.J.; Walker, M.T.; Congreve, M.S.; Devine, L.A.; Tisi, D.; et al. Identification of Novel p38 α MAP Kinase Inhibitors Using Fragment-Based Lead Generation. *J. Med. Chem.* **2005**, *48*, 414–426. [[CrossRef](#)] [[PubMed](#)]
53. Karaman, M.W.; Herrgard, S.; Treiber, D.K.; Gallant, P.; Atteridge, C.E.; Campbell, B.T.; Chan, K.W.; Ciceri, P.; Davis, M.I.; Edeen, P.T.; et al. A quantitative analysis of kinase inhibitor selectivity. *Nat. Biotechnol.* **2008**, *26*, 127–132. [[CrossRef](#)] [[PubMed](#)]
54. Rena, G.; Bain, J.; Elliott, M.; Cohen, P. D4476, a cell-permeant inhibitor of CK1, suppresses the site-specific phosphorylation and nuclear exclusion of FOXO1a. *EMBO Rep.* **2004**, *5*, 60–65. [[CrossRef](#)] [[PubMed](#)]
55. Sastry, G.M.; Adzhigirey, M.; Day, T.; Annabhimoju, R.; Sherman, W. Protein and ligand preparation: Parameters, protocols, and influence on virtual screening enrichments. *J. Comput. Aided Mol. Des.* **2013**, *27*, 221–234. [[CrossRef](#)] [[PubMed](#)]
56. Greenwood, J.R.; Calkins, D.; Sullivan, A.P.; Shelley, J.C. Towards the comprehensive, rapid, and accurate prediction of the favorable tautomeric states of drug-like molecules in aqueous solution. *J. Comput. Aided Mol. Des.* **2010**, *24*, 591–604. [[CrossRef](#)] [[PubMed](#)]
57. Jacobson, M.P.; Pincus, D.L.; Rapp, C.S.; Day, T.J.F.; Honig, B.; Shaw, D.E.; Friesner, R.A. A Hierarchical Approach to All-Atom Protein Loop Prediction. *Proteins* **2004**, *55*, 351–367. [[CrossRef](#)] [[PubMed](#)]
58. Watts, K.S.; Dalal, P.; Murphy, R.B.; Sherman, W.; Friesner, R.A.; Shelley, J.C. ConfGen: A Conformational Search Method for Efficient Generation of Bioactive Conformers. *J. Chem. Inf. Model.* **2010**, *50*, 534–546. [[CrossRef](#)] [[PubMed](#)]
59. Friesner, R.A.; Murphy, R.B.; Repasky, M.P.; Frye, L.L.; Greenwood, J.R.; Halgren, T.A.; Sanschagrin, P.C.; Mainz, D.T. Extra Precision Glide: Docking and Scoring Incorporating a Model of Hydrophobic Enclosure for Protein-Ligand Complexes. *J. Med. Chem.* **2006**, *49*, 6177–6196. [[CrossRef](#)] [[PubMed](#)]
60. Wolff, S.; Xiao, Z.; Wittau, M.; Sussner, N.; Stoter, M.; Knippschild, U. Interaction of casein kinase 1 δ (CK1 δ) with the light chain LC2 of microtubule associated protein 1A (MAP1A). *Biochim. Biophys. Acta* **2005**, *1745*, 196–206. [[CrossRef](#)] [[PubMed](#)]
61. Morgan, R.T.; Woods, L.K.; Moore, G.E.; Quinn, L.A.; McGavran, L.; Gordon, S.G. Human cell line (COLO 357) of metastatic pancreatic adenocarcinoma. *Int. J. Cancer* **1980**, *25*, 591–598. [[CrossRef](#)] [[PubMed](#)]
62. Lieber, M.; Mazzetta, J.; Nelson-Rees, W.; Kaplan, M.; Todaro, G. Establishment of a continuous tumor-cell line (panc-1) from a human carcinoma of the exocrine pancreas. *Int. J. Cancer* **1975**, *15*, 741–747. [[CrossRef](#)] [[PubMed](#)]
63. Yunis, A.A.; Arimura, G.K.; Russin, D.J. Human pancreatic carcinoma (MIA PaCa-2) in continuous culture: Sensitivity to asparaginase. *Int. J. Cancer* **1977**, *19*, 128–135. [[CrossRef](#)] [[PubMed](#)]
64. Okabe, T.; Yamaguchi, N.; Ohsawa, N. Establishment and characterization of a carcinoembryonic antigen (CEA)-producing cell line from a human carcinoma of the exocrine pancreas. *Cancer* **1983**, *51*, 662–668. [[CrossRef](#)]
65. Fogh, J.; Trempe, G. New Human Tumor Cell Lines. In *Human Tumor Cells In Vitro*; Fogh, J., Ed.; Springer: Boston, MA, USA, 1975; pp. 115–159.
66. Kabsch, W. XDS. *Acta Crystallogr. Sect. D Biol. Crystallogr.* **2010**, *66*, 125–132. [[CrossRef](#)] [[PubMed](#)]
67. Read, R.J. Pushing the boundaries of molecular replacement with maximum likelihood. *Acta Crystallogr. Sect. D Biol. Crystallogr.* **2001**, *57*, 1373–1382. [[CrossRef](#)]
68. Afonine, P.V.; Grosse-Kunstleve, R.W.; Echols, N.; Headd, J.J.; Moriarty, N.W.; Mustyakimov, M.; Terwilliger, T.C.; Urzhumtsev, A.; Zwart, P.H.; Adams, P.D. Towards automated crystallographic structure refinement with phenix. *Acta Crystallogr. Sect. D Biol. Crystallogr.* **2012**, *68*, 352–367. [[CrossRef](#)] [[PubMed](#)]

69. Emsley, P.; Lohkamp, B.; Scott, W.G.; Cowtan, K. Features and development of Coot. *Acta Crystallogr. Sect. D Biol. Crystallogr.* **2010**, *66*, 486–501. [[CrossRef](#)] [[PubMed](#)]
70. Moriarty, N.W.; Grosse-Kunstleve, R.W.; Adams, P.D. electronic Ligand Builder and Optimization Workbench (eLBOW): A tool for ligand coordinate and restraint generation. *Acta Crystallogr. Sect. D Biol. Crystallogr.* **2009**, *65*, 1074–1080. [[CrossRef](#)] [[PubMed](#)]
71. Simard, J.R.; Getlik, M.; Grutter, C.; Pawar, V.; Wulfert, S.; Rabiller, M.; Rauh, D. Development of a fluorescent-tagged kinase assay system for the detection and characterization of allosteric kinase inhibitors. *J. Am. Chem. Soc.* **2009**, *131*, 13286–13296. [[CrossRef](#)] [[PubMed](#)]
72. Bukhtiyarova, M.; Northrop, K.; Chai, X.; Casper, D.; Karpusas, M.; Springman, E. Improved expression, purification, and crystallization of p38 α MAP kinase. *Protein Expr. Purif.* **2004**, *37*, 154–161. [[CrossRef](#)] [[PubMed](#)]
73. Kabsch, W. Automatic processing of rotation diffraction data from crystals of initially unknown symmetry and cell constants. *J. Appl. Crystallogr.* **1993**, *26*, 795–800. [[CrossRef](#)]
74. Getlik, M.; Simard, J.R.; Termathe, M.; Grutter, C.; Rabiller, M.; van Otterlo, W.A.L.; Rauh, D. Fluorophore labeled kinase detects ligands that bind within the MAPK insert of p38 α kinase. *PLoS ONE* **2012**, *7*, e39713. [[CrossRef](#)] [[PubMed](#)]
75. Emsley, P.; Cowtan, K. Coot: Model-building tools for molecular graphics. *Acta Crystallogr. Sect. D Biol. Crystallogr.* **2004**, *60*, 2126–2132. [[CrossRef](#)] [[PubMed](#)]
76. Murshudov, G.N.; Vagin, A.A.; Dodson, E.J. Refinement of macromolecular structures by the maximum-likelihood method. *Acta Crystallogr. Sect. D Biol. Crystallogr.* **1997**, *53*, 240–255. [[CrossRef](#)] [[PubMed](#)]
77. Schuttelkopf, A.W.; van Aalten, D.M.F. PRODRG: A tool for high-throughput crystallography of protein-ligand complexes. *Acta Crystallogr. Sect. D Biol. Crystallogr.* **2004**, *60*, 1355–1363. [[CrossRef](#)] [[PubMed](#)]
78. Lovell, S.C.; Davis, I.W.; Arendall, W.B.; de Bakker, P.I.W.; Word, J.M.; Prisant, M.G.; Richardson, J.S.; Richardson, D.C. Structure validation by C α geometry: Phi, psi and C β deviation. *Proteins* **2003**, *50*, 437–450. [[CrossRef](#)] [[PubMed](#)]
79. Löhler, J.; Hirner, H.; Schmidt, B.; Kramer, K.; Fischer, D.; Thal, D.R.; Leithäuser, F.; Knippschild, U. Immunohistochemical Characterisation of Cell-Type Specific Expression of CK1 δ in Various Tissues of Young Adult BALB/c Mice. *PLoS ONE* **2009**, *4*, e4174. [[CrossRef](#)] [[PubMed](#)]

Sample Availability: Samples of the compounds **1**, **3**, **4** and **5** are available from the authors.



© 2017 by the authors. Licensee MDPI, Basel, Switzerland. This article is an open access article distributed under the terms and conditions of the Creative Commons Attribution (CC BY) license (<http://creativecommons.org/licenses/by/4.0/>).